2005-09-20

Regulation of Cell Growth and Differentiation within the Context of Nuclear Architecture by the Runx2 Transcription Factor: a Dissertation

Daniel W. Young
University of Massachusetts Medical School

A Dissertation Presented

By

Daniel W. Young

Submitted to the Faculty of the

Graduate School of Biomedical Sciences

University of Massachusetts Medical School

In partial fulfillment of the requirements for the degree of

DOCTOR OF PHILOSOPHY

IN

BIOMEDICAL SCIENCE

SEPTEMBER 20, 2005

REGULATION OF CELL GROWTH AND DIFFERENTIATION WITHIN THE CONTEXT OF NUCLEAR ARCHITECTURE BY THE RUNX2 TRANSCRIPTION FACTOR

A Dissertation Presented
By

Daniel W. Young

Approved as to content and style by:

Anthony N. Imbalzano, Ph.D., Chair of the Committee

Kendall Knight, Ph.D., Member of the Committee

Jeanne B. Lawrence, Ph.D., Member of the Committee

Jeffrey A. Nickerson, Ph.D., Member of the Committee

Arthur B. Pardee, Ph.D., Member of the Committee

Jane B. Lian, Ph.D., Thesis Co-Advisor

Gary S. Stein, Ph.D., Thesis Co-Advisor

Anthony Carruthers, Ph.D.,
Dean of the Graduate School of Biomedical Sciences

Program in Cell Biology

September 20, 2005

COPYRIGHT

Portions of this thesis have been appeared in:

Daniel W. Young, Jitesh Pratap, Amjad Javed, Brian Wiener, Yasuyuki Ohkawa, Andre J. van Wijnen, Gary S. Stein, Janet L. Stein, Anthony N. Imbalzano and Jane B. Lian; The SWI/SNF Chromatin Remodeling Complex is Obligatory for BMP2 Induced, Runx2-Dependent Skeletal Gene Expression that Controls Osteoblast Differentiation, Journal of Cellular Biochemistry 2005 Mar 1;94(4):720-30. *Journal Cover Image*

Daniel W. Young, Sayyed K. Zaidi, Andre J. van Wijnen, Janet L. Stein, Jane B. Lian, and Gary S. Stein; Quantitative Signature for Architectural Organization of Regulatory Factors using Intranuclear Informatics, Journal of Cell Science, (2004) 117 4889-4896 *Accompanied by Cover Reference and Editorial Commentary JCS 2004 117: 2102*

Sayyed K. Zaidi*, Daniel W. Young*, Amjad Javed, Janet L. Stein, Jane B. Lian, Andre J. van Wijnen, Gary S. Stein; Mitotic Partitioning and Subnuclear Reorganization of Tissue Specific Transcription Factors in Progeny Cells, Proceedings of the National Academy of Sciences, U S A. 2003 Dec 9;100(25):14852-7 (* authors contributed equally)

Daniel W. Young, Xiaoqing Yang, Mario Galindo, Amjad Javed, Sayyed K Zaidi, Jane B. Lian, Janet L. Stein, Andre J. van Wijnen and Gary S. Stein; Mitotic Retention of Phenotype by the Cell-Fate Determining Transcription Factor Runx2, *Manuscript In Review*

Daniel W. Young, Mario Galindo, Xiaoqing Yang, Jitesh Pratap, Jean Underwood, Jeffrey Nickerson, Sheldon Penman, Janet L. Stein, Jane B. Lian, Andre J. van Wijnen, and Gary S. Stein; Mitotic occupancy and lineage-specific transcriptional control of ribosomal RNA genes by the RUNX2 transcription factor, *Manuscript in Review*

Gary S. Stein, Daniel W. Young, et al., Quantitative Assessment of Biological Function Based on the Temporal and Spatial Organization of Subnuclear Protein Domains (U.S. Patent Pending #60/608,846)

ACKNOWLEDGEMENTS

Although in reflection I believe that I always knew I was molded for science, this thesis is the culmination of a goal that was formally born in my mind sometime in 1998 when I worked as a mechanical engineer at FMGlobal Research. There I was inspired to pursue a career in science and to obtain a PhD degree by my interactions with Dr. Praveen Malhotra, a genuine scientist and good friend who in many ways I view as my first research mentor. My next step in this process was a move to full-time graduate student at WPI in the Dept. of Biomedical Engineering. During this transition I was fortunate to receive support and encouragement from many individuals to whom I am grateful: Tony Braga, Paul Senseny, Roger Allard, Al Boucher, Kavi Devraj, Chris Wilson, Jill Rulfs, Chris Sotak, George Pins, Satya Shivkumar, and Ross Shonat. In particular I would like to thank Sean Kohles, my advisor at WPI, who was a champion for me at WPI and in my transition to the PhD program at UMass Medical School.

I would also like to recognize Massachusetts Maritime Academy and the faculty of the Marine Engineering Department not only for my academic foundation, but also for providing an environment for me to discover the value of discipline and the joy of success. These key pieces have been fundamental to my successful pursuit of this PhD degree.

During my graduate work at WPI I had the opportunity to meet Jane Lian at an ORS meeting in San Francisco. I noticed her name tag in a glance as she was running down the hall to catch a poster session where we ultimately met and talked about possible doctoral research opportunities. The energy I saw in her that day drew me to the lab and motivated the development of my relationships with a team of advisors that also include Gary Stein, Janet Stein, and Andre van Wijnen. I thank Gary for posing the basic question to me that ultimately became the basis for many exciting discoveries and the core of this thesis. I am grateful to Gary, Jane, Janet, and Andre for their support and encouragement and for providing me with endless opportunities to develop my scientific thinking, to appreciate the business of academic science, to communicate my work in writing and at 'the podium', and to explore the complexities of nuclear structure and gene expression with outside-of-the-box thinking and, at times, brute force execution.

Coming to the laboratory with a non-traditional background I drew on the expertise of many talented biochemists, developmental, molecular and cell biologists that comprise our group, and I am grateful to you all for your support and on-the-job instruction. I thank Kaleem Zaidi and Jitesh Pratap my first rotation mentors, as well as Mohammed Hassan, Amjad Javed, Soraya Gutierrez all of whom taught me how to 'crawl' and then 'walk' in the lab and who over the years have become good friends. I also thank Shirwin Pockwinse, Mario Galindo, Hayk Hovhannisyan, Chris Lengner, Tripti Gaur, Laura Saltman, Angela Miele, Nadiya Teplyuk, Ricardo Medina, Arun

Rajgopal, Partha Mitra, Ronglin Xie, Corey Braastad, Klaus Becker and others who over the years have helped fine tune my scientific thoughts and have been great people with whom to work. A special thanks to Shirwin whose energy, endurance, and enthusiasm have been a silent motivation to me over the years. I thank Betsy Brontsein and Judy Rask for their openness to help and support my work. I thank my thesis committee for their encouragement and for helping me to stay on track. I thank Tony Imbalzano and Jeff Nickerson who have been my mentors outside the lab and who have been significant supporters in my transition to the next phase of my career. To Art Pardee, I thank you for serving on my dissertation committee and for providing insightful comments on my thesis and manuscripts.

To my family and friends…I share this achievement with you all.

I have endless thanks to my parents who have constantly encouraged me, and when necessary pushed me, to learn and to challenge myself. I am grateful for their love and for the sacrifices that they have made over the years, financial and emotional, to provide me with the opportunity to experience life and to discover the person and the scientist within me. I thank my sister, Kim and her husband Pat for their continual support and encouragement in this endeavor and for sharing their life's successes. I am particularly thankful to my second parents, the Devereaux's, who have been incredibly supportive of this goal, and especially for providing a loving home for our daughters during the day. I am grateful to Marc and Jeton for opening up their home

to us on day one to help this mission get off the ground, for providing a second home to our children, and for always helping us stay focused on the goal. To Marc, I thank you for your friendship and dependability over the years. I thank Loren for constant encouragement, for always being there to help with the kids, and for genuine enthusiasm in sharing this accomplishment. I thank Erik for helping me to determine that a transition to the biological sciences was the right move for me. For Rob and Mary, I extend many thanks for your support and kind thoughts over the years. I am also grateful to my extended family and friends whose support and good wishes have always helped me to stay on track. In particular, I thank our friends John and Andrea who have helped us through this process in many ways.

Most of all I thank my wife and best friend, Leigh. Your love and support has been the foundation on which this goal has become a reality. This achievement is ours, and I am grateful that we can share it together with our two beautiful daughters Madeline and Paige who everyday are a reflection your love and devotion to our family. I Love You.

For my little girls, Madeline and Paige...

We shall not cease from exploration
And the end of all our exploring
Will be to arrive where we started
And know the place for the first time.
- T.S. Elliot

ABSTRACT

The Runx family of transcription factors performs an essential role in animal development by controlling gene expression programs that mediate cell proliferation, growth and differentiation. The work described in this thesis is concerned with understanding mechanisms by which Runx proteins support this program of gene expression within the architectural context of the mammalian cell nucleus. Multiple aspects of nuclear architecture are influenced by Runx2 proteins including sequence-specific DNA binding at gene regulatory regions, organization of promoter chromatin structure, and higher-order compartmentalization of proteins in nuclear foci. This work provides evidence for several functional activities of Runx2 in relation to architectural parameters of gene expression for the control of cell growth and differentiation. First, the coordination of SWI/SNF mediated chromatin alterations by Runx2 proteins is found to be a critical component of osteoblast differentiation for skeletal development. Several chromatin modifying enzymes and signaling factors interact with the developmentally essential Runx2 C-terminus. A patent-pending microscopic image analysis strategy invented as part of this thesis work – called intranuclear informatics – has contributed to defining the C-terminal portion of Runx2 as a molecular determinant for the nuclear organization of Runx2 foci and directly links Runx2 function with its organization in the nucleus. Intranuclear informatics also led to the discovery that nuclear organization of Runx2 foci is equivalently restored in progeny cells following mitotic division – a natural perturbation in nuclear structure and function. Additional microscopic studies

revealed the sequential and selective reorganization of transcriptional regulators and RNA processing factors during progression of cell division to render progeny cells equivalently competent to support Runx2 mediated gene expression. Molecular studies provide evidence that the Runx proteins have an active role in retaining phenotype by interacting with target gene promoters through sequence-specific DNA binding during cell division to support lineage-specific control of transcriptional programs in progeny cells. Immunolocalization of Runx2 foci on mitotic chromosome spreads revealed several large foci with pairwise symmetry on sister chromatids; these foci co-localize with the RNA polymerase I transcription factor, Upstream Binding Factor (UBF1) at nucleolar organizing regions. A series of experiments were carried out to reveal that Runx2 interacts directly with ribosomal DNA loci in a cell cycle dependent manner; that Runx2 is localized to UBF foci within nucleoli during interphase; that Runx2 attenuates rRNA synthesis; and that this repression of ribosomal gene expression by Runx2 is associated with cell growth inhibition and induction of osteoblast-specific gene expression. This thesis has identified multiple novel mechanisms by which Runx2 proteins function within the hierarchy of nuclear architecture to control cell proliferation, growth and differentiation.

TABLE OF CONTENTS

LIST OF FIGURES AND TABLES

CHAPTER I:

Embryonic development entails a complex process of spatially ordered cell proliferation, growth, and differentiation that is established through a program of gene expression, which is determined at both genetic and epigenetic levels. Critical aspects of these events are controlled by master transcriptional regulators that are essential for the formation of tissue-specific properties of the organism. Throughout the development and life of the organism there is an intimate connection between structure and function. This coupling of form with function exists at all levels, from the composition and construction of load bearing tissues such as bone, to the precise arrangement of the macromolecular protein-RNA complexes that comprise the protein translational machinery. Perturbations in both structure and function are observed at all levels in genetic disorders and are hallmarks of cancer. Elucidating structure-function relationships in the context of development and disease is fundamental to understanding the mechanisms underlying these processes.

The work described in this thesis is concerned with mechanisms controlling cell cycle progression, growth and differentiation, and has been pursued with the objective of understanding the nuclear organization of the gene regulatory machinery that is central to these processes. *The working hypothesis addressed by this study is that components of nuclear architecture, including chromatin structure and the higher-order spatial organization of genes and cognate regulatory proteins, support the program of gene expression for cell proliferation and differentiation.* The Runx family of proteins, established as cell fate determining transcription factors, is studied as a model system to

address several aspects of this hypothesis, including: (i) the requirements for chromatin remodeling during differentiation, (ii) the molecular determinants for nuclear organization of transcription factor domains (i.e., localized concentrations of protein) in relationship to competency for differentiation, (iii) the partitioning and domain organization of cell fate determining transcription factors during mitotic division, (iv) the maintenance of lineage-specific gene regulation in progeny following cell division, and (v) the delineation of heritable cell growth properties as a component of establishing cell identity at the transcriptional level. These concepts have been studied with the central goal of revealing connections between nuclear structure and regulation of gene expression.

Runx Family of Transcription Factors: A Model for Gene Expression in the context of Nuclear Architecture for Cell Growth and Differentiation:

The Runx family of proteins is a class of transcription factors that control lineage-commitment and phenotypic gene expression, as well as control proliferative potential of committed progenitors (Pratap et al., 2003; Lian et al., 2004; Galindo et al., 2005). The roles of the mammalian Runx proteins in establishing the identity of cells have been determined in mouse gene ablation studies which reveal essential contributions to hematopoiesis (Runx1), osteogenesis (Runx2), or neuronal and gastro-intestinal development (Runx3) (Choi et al., 2001; Li et al., 2002; Komori, 2002; Inoue et al., 2002). Furthermore, Runx exhibits properties of both tumor suppressors and oncoproteins; and the deregulation of these factors in specific cellular

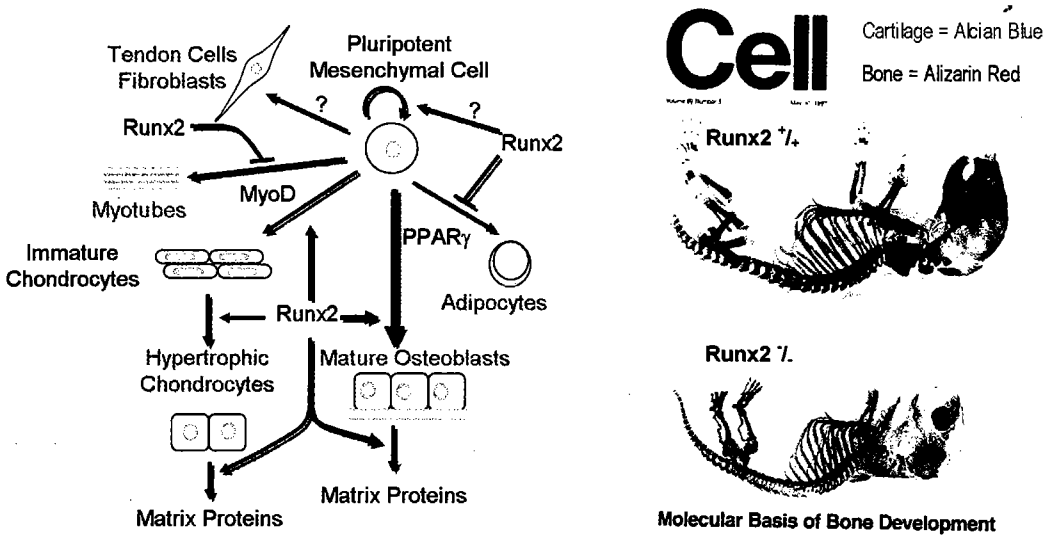

Figure 1.1: Regulation of Osteogenic Cell Fate and Skeletal Development by the Runx2 transcription factor

Left Panel: Runx2 transcription factor controls the fate of pluripotent mesenchymal stem cells with both positive and negative modes of regulation. Runx2 has inhibitory effects on myogenesis and adipogenesis and promotes multiple stages of chrondrogenesis and osteogenesis. **Right Panel:** Gene ablation studies have revealed that Runx2 has an essential role in skeletal development through the control of osteoblast cell maturation. In 1997, Komori and colleagues demonstrated that mice homozygous for the Runx2 null allele have an embryonic lethal phenotype that is characterized by the complete absence of a mineralized skeleton. The results of this study were featured on the cover of Cell.

contexts has been associated with oncogenesis and metastases (Blyth et al., 2005). Runx1 is frequently rearranged in acute myelogenous leukemia, Runx2 is implicated in metastatic breast cancer and T-cell lymphomas and Runx3 is associated with gastric cancer. Runx2 normally attenuates osteoblast proliferation and promotes the development of the mature bone cell phenotype (Figure 1.1).

Runx factors are scaffolding proteins that integrate cell signaling pathways (e.g., TGF-Beta/BMP and Yes/Src) and recruit chromatin modifying enzymes (e.g., HDACs, HATs, SWI/SNF, SUV39H1) to modulate promoter accessibility within a nucleosomal context (Figure 1.2, (Zaidi et al., 2001a; Zaidi et al., 2003; Taniuchi and Littman, 2004; Vradii et al., 2005; Young et al., 2005; Sierra et al., 2003b; Westendorf and Hiebert, 1999). At gene regulatory regions Runx proteins function as scaffolds that organize the machinery for the activation or suppression of gene expression within punctate subnuclear domains (Zaidi et al., 2005; Young et al., 2004). Pathological perturbations in the organization of these domains are linked with altered development and tumorigenesis (Westendorf and Hiebert, 1999; Javed et al., 2005; Barnes et al., 2003; Barnes et al., 2004; Blyth et al., 2001; Brubaker et al., 2003; Cameron and Neil, 2004; Ito, 2004; Neil et al., 1999; Vaillant et al., 1999; Otto et al., 2002; Ito, 2004).

Mammalian Nuclear Architecture:

Spatial Aspects of Genome Organization: During interphase the human cell organizes 46 chromosomes that collectively comprise roughly 3 gigabases of genome DNA encoding an estimated 24000 protein coding genes within the confines of a

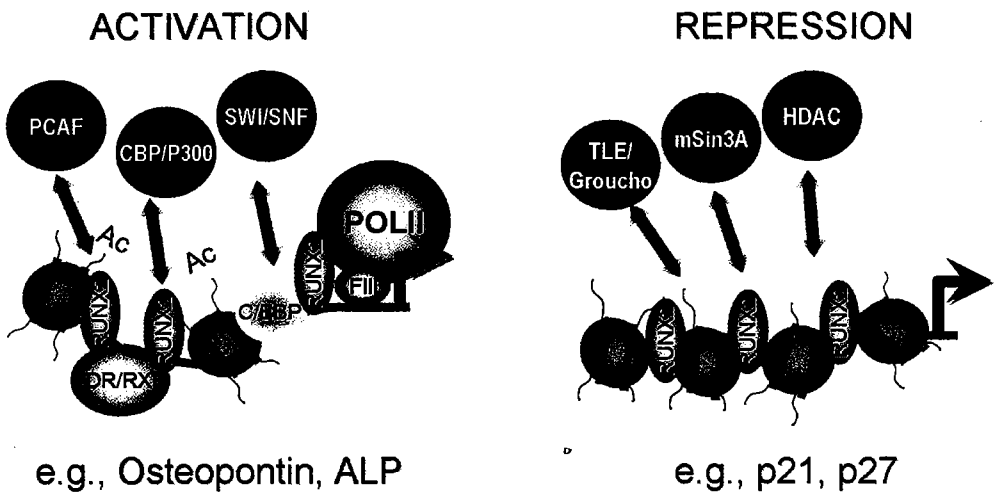

Figure 1.2 Activation and Repression of Transcription by Runx2: Runx2 associates with DNA in a sequence-specific manner at promoter regions of target genes and interacts with co-regulator proteins, such as hormone receptors and C/EBP transcription factors. These events facilitate the recruitment of chromatin modifying enzymes that alter chromatin architecture at gene promoters in manner that either promotes, or inhibits, gene transcription. Runx2 target genes include both tissue-specific proteins, such as osteopontin and alkaline phosphatase (ALP), and cell cycle regulatory proteins, such as p21 and p27.

1000 μm^3 nuclear volume. Compaction of DNA within this nuclear volume is accomplished through a hierarchy of histone-mediated molecular interactions. A histone protein octamer (two each of histones H2A, H2B, H3, and H4) wraps ~150bp of DNA into the basic chromatin unit called nucleosomes (reviewed in (Horn and Peterson, 2002)). Nucleosome-nucleosome interactions mediated through histone tails, and also linker histones, develop secondary levels of compaction in the form of a 30nm chromatin fiber. While it is understood that multiple higher levels of compaction (i.e., chromonema fiber ~100nm) exist, probably through histone mediated interactions, the precise size and structural characteristics of this organization remain elusive. Many models for interphase – as well as mitotic – chromatin organization describe chromatin fiber loops that are attached to a peripheral lamina or internal structural element (i.e., nuclear matrix). These loop attachment points called Matrix Attachment Regions or Scaffold Attachment Regions (MARs or SARs), are thought to have specific nucleotide sequences with a propensity for unwinding and forming single-stranded DNA and often found near the boundaries of genes (reviewed in (Kohwi and Kohwi-Shigematsu, 1995)).

Within the interphase nucleus compacted chromosomes occupy distinct regions, so-called 'territories', arranged radially in a non-random fashion that correlates with chromosome size and gene content (Cremer and Cremer, 2001; Tanabe et al., 2002). Chromatin within territories in organized as 'euchromatin' (open chromatin – active genes) or 'heterochromatin' (closed chromatin – inactive genes). Thus, within chromosomes there is a unique positioning of some genes that relates to active versus inactive expression states; some active genes will loop out from chromosome territories.

Furthermore, as cells differentiate there are changes in the positioning of genes into euchromatin versus heterchromatin (Arney and Fisher, 2004; Kosak and Groudine, 2004). Both long-range intrachromosomal and interchromosomal interactions between distinct genes and regulatory regions contribute to the control of gene expression (Spilianakis et al., 2005; Spilianakis and Flavell, 2004). Additionally these interactions appear to be linked with the frequency of chromosomal translocations associated with cancer (Roix et al., 2003).

The compartmentalization of chromosomes and positioning of genes is achieved in a manner that facilitates – or is facilitated by – the selective accessibility of regulatory proteins that control gene expression, replication, and repair (Verschure et al., 2003). There is a continuum of higher-order chromatin organization that appears to be dependent upon post-translational histone modifications, gene content, replication status and transcriptional activity. These points contribute to an emerging concept that a functional interplay exists between regulatory proteins and DNA to govern higher-order chromatin folding and organization. A compelling question that relates to cell fate determining regulatory proteins is how this functional interplay contributes to the regulation of gene expression for lineage commitment and progression.

Nuclear Compartmentalization of Regulatory Proteins: Nuclei contain many distinct compartments (referred to often as domains, foci, speckles, microenvironments, and bodies) that are comprised of localized concentrations of proteins. Perhaps the best known nuclear compartment is the nucleolus, where ribosomal genes reside and ribosomal biogenesis occurs (Dimario, 2004; Dundr and Misteli, 2001; Pombo et al.,

2000). Nucleoli are readily evident using light microscopy and have served as a paradigm for understanding the structure and function of nuclear domains. Nucleoli assemble following cell division from the congregation of multiple nucleolar organizing regions. Nucleolar formation is blocked in the presence of a RNA polymerase I inhibitor and is temperature sensitive, which indicates an energy dependent process that depends on ribosomal RNA transcription. The organization of regulatory factors and nucleic acids is heterogeneous throughout the nucleolar interior with distinct sub-compartments that reflect sites of rRNA synthesis, rRNA processing, and ribosome biogenesis. Furthermore, regulatory proteins rapidly exchange in and out of nucleoli, as revealed by photobleaching studies (Louvet et al., 2005). This result indicates that nucleolar localization of proteins observed by fluorescence microscopy is the manifestation of a steady-state local protein accumulation. Nucleolar function is linked with cell growth, proliferation, and differentiation, and recent work indicates that the nucleolus also plays an important role in controlling cell-cycle, senescence and stress responses, such as DNA damage (Dimario, 2004).

Technological advances in epifluorescence and confocal microscopy have lead to the detailed description of many other nuclear domains with a repertoire of functions including DNA replication and repair, as well as RNA splicing, processing, and transcription (Stein et al., 2003; Spector, 2003)). DNA replication proteins are distributed in punctate domains within the nucleus, referred to as 'replication factories', and colocalize with nascent replicated DNA, as visualized by BrdU labeling (reviewed in ((Cook, 1999)). Several proteins, such as proliferating cell nuclear antigen (PCNA), DNA

ligase I, and DNA polymerase are localized in these foci, which undergo cyclical assembly and disassembly and exhibit a diffuse distribution in all but the S phase of the cell cycle. These punctate sites are thought to provide optimal localized concentrations of regulatory protein to support the process of DNA replication.

Cellular mechanisms are in place to sense DNA damage and respond through an array of repair pathways that depend on the nature of the damage. These processes are linked with the formation of nuclear foci (Lisby and Rothstein, 2004). As an example, during late S, G2 and M phases of the cell cycle, repair of double-stranded DNA breaks is mediated by a homologous recombination mechanism downstream of ATM/ATR signaling. BRCA/Rad51 and Mre11/Rad50/Nbs DNA repair complexes rapidly form foci at sites of damage (Petrini and Stracker, 2003). These events involve interactions with the phosphorylated H2AX core histone variant that integrates into nucleosomes adjacent to sites of DSBs before the formation of repair foci. Similar to nucleolar formation, these events are activity driven and reflect the steady state accumulation of proteins engaged in the DNA repair process.

Speckles – also called SC35 domains – are compartments enriched in pre-messenger RNA splicing factors, exhibiting variability in size and shape, and localized to interchromatin regions of the nucleus (Pombo and Cook, 1996; Lamond and Spector, 2003). While often these splicing speckles are in juxtaposition with sites of active transcription (Shopland et al., 2003), their specific function remains in debate. Some evidence suggests that speckles function as storage sites of latent regulatory proteins that can supply splicing factors to active transcription sites (Spector, 2003). This concept

arises in part from studies that show inhibition of transcription or splicing results in the formation of enlarged speckles. Other evidence indicates that speckles have multi-functional roles that include active RNA processing (Shopland and Lawrence, 2000).

RNA polymerase II transcription domains are distributed in punctate sites throughout the nucleus. At both the fluorescence and electron microscopy levels these domains coincide with the labeling of nascent RNA transcription by Br-UTP, leading to the term transcription 'factories' (Cook, 1999; Pombo et al., 2000). Similar to RNA polymerase II, the basal transcriptional machinery, tissue-specific transcription factors, and chromatin remodeling factors also exhibit punctate distributions throughout the nucleus (Figure 1.3) (Young et al., 2005; Pombo et al., 1998; Dundr and Misteli, 2001; Stein et al., 2003; Zink et al., 2004).

While the domains containing, or comprised of, these proteins are principally thought to reflect sites of transcriptional activity – a concept supported by a preponderance of data – it remains formally possible that a subset of these nuclear compartments may reflect latent protein storage sites.

The organization of the proteins domains that are observed throughout the nucleus is often described qualitatively as punctate, with reference to the appearance by fluorescence microscopy of many distinct nuclear foci. Recent work, which is developed in chapter 3 of this thesis, describes and defines nuclear organization in quantitative terms that are utilized for comparative analyses. Such work has revealed that a quantitative 'signature' of nuclear organization can be uniquely defined for regulatory proteins and,

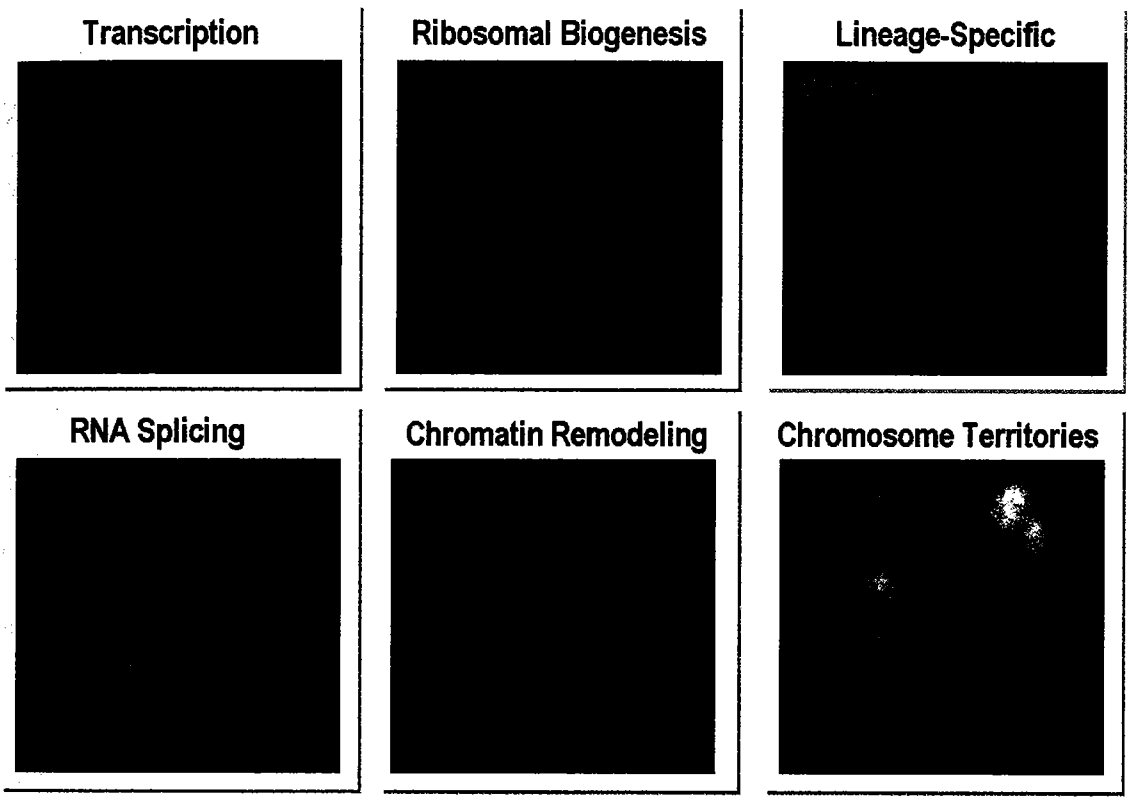

Figure 1.3 Nuclear Organizations of Proteins and Chromosomes
Nuclear proteins exhibit distinct punctate subnuclear distributions that appear to be coupled with unique regulatory roles. Several *in situ* immunofluorescence micrographs – captured by the author in the course of this thesis work – are shown as examples: RNA Polymerase II, Runx2, SC35, and Brg1 (primary calvarial cells) and UBF1 (Saos-2 cells). The organization of chromosomal territories (human Chromosomes 1 and Chromosomes 9) is shown as revealed by in situ hybridization (Ma et al., 1999).

as an example, can serve as a basis for statistical classification of biological function (Figure 1.4). Defining the molecular determinants that bring about these nuclear organizational signatures remains a fundamental biological problem.

Gene Expression in the Context of Nuclear Architecture:

Promoter Regulatory Elements: The primary level of organization in the control of gene expression is the arrangement of regulatory motifs encoded in the genome that delineate the promoters, enhancers, and silencers of genes (van et al., 2003; Stein et al., 2003). Promoter sequences define the RNA polymerase machinery that will drive transcription and possibly nuclear positioning of genes (e.g., RNA Pol I genes at the Nucleolus). The profile and relative proximity of binding sites within gene regulatory elements influence the expression of a given gene in both a temporal sense – with respect to cell cycle and developmental stage – and spatial sense – with respect to nuclear organization and developmental tissue patterns. The repertoire of gene regulatory motifs is a primary determinant for responsiveness to the range of biochemical signals that are received and processed by a cell.

Promoter Architecture and Chromatin Structure: A secondary level of gene expression control involves chromatin structure (Workman and Kingston, 1998; van et al., 2003). Chromatin organization and nucleosome positioning at gene regulatory regions can alter accessibility of transcription factors to binding elements as well as alter proximity between elements. Sequence-specific DNA binding proteins can interact with gene regulatory regions and recruit chromatin modifying factors to

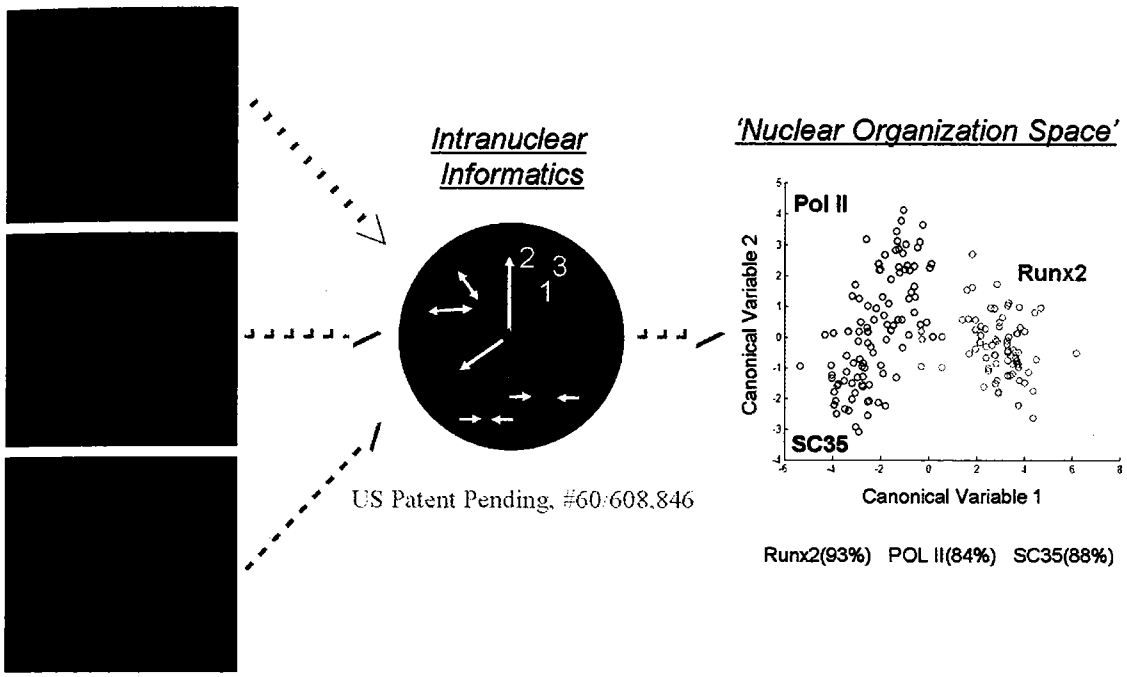

Figure 1.4 Discrimination of Regulatory Proteins based upon Quantitative Parameters of Nuclear Organization

Intranuclear informatics, described in depth in Chapter 3, was used to analyze the nuclear organization of Runx2, SC35, and RNA Polymerase II. Briefly, immunofluorescence image z-planes were obtained from deconvoluted z-series images stacks for each protein: Runx2 (75 images), RNA polymerase II and SC35 (50 images each). An automated image processing algorithm was applied to measure and compute from each image 25 parameters that collectively describe and define nuclear organization in quantitative terms. This multivariate data set was analyzed by canonical discriminate analysis to determine two variables ('canonical variables 1 and 2') that are linear combinations of the 25 parameters and that exhibit the greatest differences in nuclear organization between the three proteins. These two canonical variables are illustrated in a scatter-plot that can be abstractly defined as 'nuclear organization space'. Each data point reflects the nuclear organization determined on each of the two canonical variables from a single image of a protein (green = Runx2, blue = RNA Polymerase II, and red=SC35). By plotting the data in this way the distinct differences in nuclear organization between the proteins emerges as clusters of data points of the same color (i.e., protein). A linear discriminate function was also generated from the total 25 parameters. Using a cross-validation scheme the frequency with which the function can correctly classify an unknown image as being one of the three proteins was established (Runx2 = 93%, RNA Polymerase II = 84%, and SC35 = 88%). This analysis reveals that a quantitative 'signature' of nuclear organization can be uniquely defined for regulatory proteins, and that this signature can serve as a basis for statistical classification of biological function

alter gene expression in response to extracellular cues (Peterson and Logie, 2000; Peterson and Workman, 2000; Hassan et al., 2001). Post-translational modification of nucleosomes has emerged as an important regulatory component in this process (Schubeler et al., 2004; Berger, 2001; Jenuwein and Allis, 2001). Specific modifications, such as methylation of Histone H3 on Lysine 9, have been linked with initiating the ordered recruitment of factors which methylate DNA at CpG sites and ultimately lead to gene silencing (Schotta et al., 2004; Lachner et al., 2003). In contrast, methylation of Histone H3 on Lysine 4 facilitates the subsequent acetylation of nucleosomal histones and the activation of gene expression and may modulate the recruitment of bromodomain containing chromatin remodeling factors (Marmorstein and Berger, 2001). There is a growing list of histone modifications that lead to alterations in chromatin organization and regulate gene expression. Recent work indicates that histone modifications may provide epigenetic marks for active genes within the condensed chromosomes during the mitotic silencing of gene expression (Kruhlak et al., 2001; Kouskouti and Talianidis, 2005a). Gene regulation through histone modifications is linked with a functional interplay between sequence-specific transcription factors and DNA-dependent ATPase chromatin remodeling enzymes, such as the SWI/SNF complex. These chromatin remodeling factors alter nucleosomal histone-DNA interactions and nucleosome positioning to facilitate the recruitment of co-regulatory proteins and the formation of a pre-initiation complex for gene transcription (Imbalzano and Xiao, 2004; Peterson and Tamkun, 1995). Understanding how these chromatin remodeling events contribute to the control of cell growth and differentiation is an area of active scientific investigation.

Higher-Order Nuclear Architecture and Gene Expression: Recent work has revealed that the spatial positioning of genes in the nucleus, local chromatin structure at gene regulatory regions, and the organization of proteins that regulate gene expression are all functionally coupled (Moen, Jr. et al., 2004). Studies using artificially generated MMTV gene constructs and live cell imaging have revealed that alterations in gene localization and chromatin structure are rapidly generated within the nuclear milieu upon gene induction (Muller et al., 2001). Furthermore, work examining the organization of the endogenous Beta-Globin gene locus control regions reveals that upon transcriptional induction and cell differentiation the loci are selectively decondensed and relocalized within the nucleus (Tolhuis et al., 2002; Drissen et al., 2004). Thus there is precedence for developmental induction of gene expression that is accompanied by alterations in nuclear organization of chromosomes and associated regulatory proteins within the interphase nucleus. A compelling question is how the interactions between chromosomes and associated regulatory proteins are controlled during the nuclear reorganization that occurs during mitotic cell division.

Cell Cycle Dependent Aspects of Nuclear Organization:

Proliferation of cells is regulated by a complex network of growth factors, signaling pathways, transcription factors, metabolic regulators and structural proteins. These biochemical processes that support faithful DNA replication, mitotic spindle assembly, and partitioning of chromosomes to progeny cells delineate the 'cell cycle'. During the first divisions in the early embryo, cell cycle proceeds in a synchronous fashion with an invariable rate (Masui and Wang, 1998). When cell fate is specified, the

cycle becomes asynchronous and lengthens with the manifestation of so-called gap-phases (i.e., G1 and G2) between DNA synthesis and division (Gerhart et al., 1984; Masui and Wang, 1998; Masui and Wang, 1998; Masui, 1992). During G1 cells receive and integrate extracellular cues that signal cell growth and determine cell cycle exit or progression to support the tissue-level developmental program (Pardee, 1989; Galindo et al., 2005). In G2, cells acquire sufficient mass to support progeny cells (O'Farrell, 2001; Cooper, 2004). Furthermore, G1 and G2 provide checkpoints for repair of DNA damage and replication errors as well as options for aborting the cell cycle for the apoptotic program of cell death (Blagosklonny and Pardee, 2002; Kastan and Bartek, 2004; Lisby and Rothstein, 2004). The process of replication is coupled with a highly order, yet dynamic, re-localization of newly replicated DNA as well as a reorganization of nuclear domains comprised of replication regulatory factors (Ma et al., 1998).

Mitosis and cytokinesis require the concerted actions of multiple kinases, phosphatases, ubitquitin-mediated proteases and motor proteins, and are coupled with dramatic cell morphological changes that include nuclear envelope breakdown, cytoskeletal reorganization, spindle assembly and global condensation of chromosomes. As cells progress through mitotic division, there is a complete silencing of gene expression, nuclear reorganization, and global chromosome condensation to facilitate the segregation of the genetic material, associated regulatory factors, and cellular components into progeny cells (Burke and Ellenberg, 2002; Mitchison and Salmon, 2001). The organization of chromosomes and associated regulatory factors is sequentially restored following mitosis together with the resumption of gene expression

(Prasanth et al., 2003; Zaidi et al., 2003). Establishing determinants for this spatio-temporal nuclear organization is essential to understanding the cellular function in development and disease.

Contents of the Dissertation

Runx2 proteins are a paradigm for addressing the hypothesis that components of nuclear architecture support the program of gene expression for cell proliferation and differentiation. Using the Runx2 model system this thesis demonstrates the requirements for chromatin remodeling during the Runx2 dependent osteoblast differentiation. This works establishes molecular determinants for nuclear organization of Runx2 transcription factor domains that are coupled with competency for osteoblast differentiation. In a series of the three final chapters this thesis reveals that the partitioning and domain organization of Runx2 transcription factors during mitotic division is coupled with the maintenance of lineage-specific gene regulation in progeny cells following mitotic cell division; and that control of ribosomal gene expression and cell growth through mitosis and in progeny cells are fundamental components of establishing and maintaining cell identity.

Chapter 2: A model has emerged for control of cellular differentiation that involves the combined contribution of tissue specific transcription factors and chromatin remodeling complexes. Several lines of evidence suggest that the recruitment of chromatin remodeling factors may be coupled to BMP2 signaling and Runx2 mediated

gene expression for the commitment of progenitor cells into the osteogenic lineage. Conserved from yeast to humans, SWI/SNF complexes alter chromatin structure in an ATP-dependent manner and provide a critical function for the regulation of gene expression (Workman and Kingston, 1998; Sif, 2004). Chapter 2 addresses the requirement of SWI/SNF activity for induction of the osteoblast phenotype. The expression of Brg1, an essential component of the SWI/SNF complex, was identified in developing skeletal structures of the mouse embryo and in *ex vivo* osteoblast cultures. Functional studies were then carried out to that establish the requirement of SWI/SNF for the initiation of Runx2-dependent BMP-2 induction of osteoblast differentiation. This chapter demonstrates that SWI/SNF activity is required for initiating the program of gene expression obligatory for development of the osteoblast phenotype.

Chapter 3: This section describes a novel approach, intranuclear informatics, to examine the nuclear organization of protein domains from digital microscopic images. An image-processing algorithm is developed to measure and compute quantitative parameters that describe and define nuclear organization. The result is a multivariable data-set that can be used for exploratory analysis techniques and for quantitatively testing specific biological hypotheses. By the application of intranuclear informatics this section elucidates that Runx2 nuclear organization has an interphase 'signature' that is restored following mitosis. Furthermore, our analysis of C-terminal mutant proteins provides evidence that nuclear organization of Runx2 foci is functionally linked with tissue specific gene regulatory functions.

Chapter 4: Concomitant with transcriptional silencing, gross alterations of nuclear organization and re-localization of regulatory complexes happen during mitosis. A fundamental question is how cells restore nuclear distribution of tissue specific transcription factors in progeny cells to regulate post-mitotic phenotypic gene transcription. This concept is addressed using the Runx family of lineage-specific transcription factors as a model system. By the combined use of *in situ* immunofluorescence microscopy and image quantitation, Chapter 4 documents progressive mitotic changes in the distribution of Runx foci and sequential re-organization of nuclear proteins involved in gene expression. The interphase subnuclear organization of Runx foci is selectively restored in telophase with equal partitioning of the protein into progeny nuclei. Thus a dynamic spatial distribution of Runx transcription factors in parallel with chromosomal partitioning to sustain balanced expression of phenotypic genes post-mitotically.

Chapter 5: Osteogenic cell fate decisions and subsequent proliferation of osteoprogenitor cells is controlled by Runx2 (Galindo et al., 2005; Lian et al., 2004; Pratap et al., 2002; Westendorf and Hiebert, 1999; Thomas et al., 2004). A mechanism must be operative that ensures Runx2 dependent regulation of this osteogenic identity through multiple mitotic cell divisions. Chapter 5 combines mitotic cell synchronization, expression profiling, chromatin immunoprecipitation, and RNA interference to investigate this mechanism. During mitosis Runx2 directly interacts with a novel set of cell fate and cell cycle related target genes that exhibit distinct modifications in histone acetylation and methylation. This works indicates that Runx transcription factors

reinforce cell fate through an epigenetic mechanism that retains phenotypic gene expression patterns following cell division

Chapter 6: This chapter describes that Runx2 is retained in large discrete foci that are symmetrically positioned on sister chromatids within the condensed mitotic chromosomes. These chromosomal foci are associated with open chromatin at nucleolar organizing regions; co-localize with the RNA polymerase I transcription factor, UBF1, and transition into nucleoli during interphase. Specific spatial and temporal changes in the binding of Runx2 throughout rDNA repeats during cell cycle progression are revealed by chromatin immunoprecipitation analysis. Reduction of Runx2 levels by siRNA activates rRNA transcription, while induction of Runx2 directly represses ribosomal biogenesis. Furthermore, Runx2 repression of ribosomal gene expression is associated with growth inhibition and expression of lineage-specific genes. This work establishes that Runx2 not only controls lineage commitment and cell proliferation by regulating RNA polymerase II transcription, but also acts as a cell cycle dependent suppressor of RNA Polymerase I mediated rRNA synthesis.

CHAPTER II:

The SWI/SNF Chromatin Remodeling Complex is Obligatory for BMP2 Induced, Runx2-Dependent Skeletal Gene Expression that Controls Osteoblast Differentiation

ABSTRACT

Development of bone tissue requires maturation of osteoblasts from mesenchymal precursors. BMP2, a member of the TGFβ superfamily, and the Runx2 (AML3/Cbfa1) transcription factor, a downstream BMP2 effector, are regulatory signals required for osteoblast differentiation. While Runx2 responsive osteogenic gene expression has been functionally linked to alterations in chromatin structure, the factors that govern this chromatin remodeling remain to be identified. Here we address the role of the SWI/SNF chromatin remodeling enzymes in BMP2-induced, Runx2-dependent development of the osteoblast phenotype. For these studies we have examined, calvarial cells from wild-type mice and mice that are homozygous for the Runx2 null allele, as well as the C2C12 model of BMP2 induced osteogenesis. By the analysis of microarray data we find that several components of the SWI/SNF complex are regulated during BMP2-mediated osteoblast differentiation. Brg1 is an essential DNA dependent ATPase subunit of the SWI/SNF complex. Thus, functional studies were carried out using a fibroblast cell line that conditionally expresses a mutant Brg1 protein, which exerts a dominant negative effect on SWI/SNF function. Our findings demonstrate that SWI/SNF is required for BMP2- induced expression of alkaline phosphatase, an early marker reflecting Runx2 control of osteoblast differentiation. In addition, Brg1 is expressed in cells within the developing skeleton of the mouse embryo as well as in osteoblasts ex vivo. Taken together these results support the concept: that BMP2 mediated osteogenesis requires Runx2 and demonstrate that initiation of BMP2-induced, Runx2 dependent skeletal gene expression requires SWI/SNF chromatin remodeling complexes.

INTRODUCTION

Bone Morphogenetic Proteins (BMP) are key regulators of bone formation. BMP2 induction of the osteogenic phenotype is observed in several non-osseous mesenchymal cells that include pluripotent C3H10T1/2 cells as well as NIH3T3 fibroblasts, and pre-myogenic C2C12 cells (Si et al., 1999; Katagiri et al., 1994; Wang et al., 1993; Ahrens et al., 1993). BMP2 signals are directed to the nucleus through Smad heterodimers that converge with Runx2, a transcription factor required for osteoblast differentiation, to regulate the expression of osteogenic genes (Lee et al., 2000; Zaidi et al., 2002b; Kobayashi et al., 2000; Selvamurugan et al., 2004a; Franceschi and Xiao, 2003; Ito and Miyazono, 2003). The mechanisms by which BMP2 signaling and Runx2 are integrated at gene promoters for development of the osteoblast phenotype are minimally understood. Runx2 activation of the bone related osteocalcin gene has been functionally linked to alterations in chromatin structure (Javed et al., 1999). Although Runx proteins alone lack the ability to remodel chromatin, these transcriptional regulators interact with several factors that have chromatin remodeling activity (Javed et al., 2000; Paredes et al., 2002; Lian and Stein, 2003; Gutierrez et al., 2000). Together these results suggest that the recruitment of chromatin remodeling factors may be coupled to BMP2 signaling and Runx2 mediated gene expression for the commitment of progenitor cells into the osteogenic lineage.

Chromatin remodeling has emerged as a fundamental parameter for control of various physiological events, including steroid hormone and stress response, as well as cellular differentiation (de la Serna et al., 2000; de la Serna et al., 2001; Pedersen et al.,

2001; Kowenz-Leutz and Leutz, 1999; Muchardt and Yaniv, 1993; Chiba et al., 1994). Several factors alter chromatin structure by perturbing nucleosome stability or position in an ATP-dependent manner (e.g., SWI/SNF complexes) or by covalently modifying histones (e.g., histone acetyltransferase) (Workman and Kingston, 1998). A key step in chromatin-regulated control of transcription is the ordered recruitment of chromatin remodeling factors to gene promoters via interactions with sequence-specific transcription factors (Hassan et al., 2001; Agalioti et al., 2000; Soutoglou and Talianidis, 2002). Thus, a model has emerged for the combined contribution of tissue specific transcription factors and chromatin remodeling complexes to control cellular differentiation.

Conserved from yeast to humans, SWI/SNF complexes alter chromatin structure in an ATP-dependent manner and provide a critical function for the regulation of gene expression (Workman and Kingston, 1998; Sif, 2004). These multisubunit complexes are distinguished by their essential DNA dependent ATPase subunit, which in higher eukaryotes is either the Brg or Brm protein (Sif et al., 2001; Wang et al., 1996b). Recent studies using *in vitro* cell differentiation models have shown that SWI/SNF complexes support transcriptional control of myogenic, adipocytic, and myeloid differentiation (de la Serna et al., 2001; Pederson, 2001; Kowenz-Leutz and Leutz, 1999).

Here we have addressed the requirement of SWI/SNF activity for induction of the osteoblast phenotype. We first demonstrate that alkaline phosphatase (APase) is a marker for BMP2-induced Runx2-dependent osteoblast differentiation. By analysis of microarray profiles of BMP2-induced osteoblast differentiation, we find that expression

of several SWI/SNF subunits is altered. The expression of Brg1, an essential component of the SWI/SNF complex, was identified in developing skeletal structures of the mouse embryo and in *ex vivo* osteoblast cultures. Functional studies were then carried out to establish the requirement of SWI/SNF for initiation of osteoblast differentiation. Our findings demonstrate that SWI/SNF activity is required for initiating the program of gene expression obligatory for development of the osteoblast phenotype.

MATERIALS AND METHODS

Cell Isolation and Culture Conditions

Primary mouse calvarial cells (17.5 dpc) were isolated from wild-type and Runx2 null mice, as described in (Pratap et al., 2003), and maintained in α-MEM with 10% FBS and 2 mM L-Glutamine. B22 cells were previously generated which have an inducible Flag-tagged BRG1 transgene containing a mutation in the ATP binding site (Figure 2.5b, (de la Serna et al., 2001; Khavari et al., 1993)). Tet-VP16 cells were generated from NIH-3T3 cells and contain a stably integrated tet-tA transgene that encodes the Tet-VP16 regulator. B22 cells were generated from Tet-VP16 cells and contain both the Tet-tA transgene (Tet-off) and the Flag-tagged BRG1 mutant transgene (Figure 2.5a). Mutant Brg1 has been previously shown in this cell line to associate with endogenous components of the SWI/SNF complex, but is non-functional (Figure 2.5d), (de la Serna et al., 2000). Expression of the mutant transgene is repressed in cells grown in the presence of 2 μg/ml tetracycline; whereas growth in the absence of tetracycline induces expression of the mutant protein as shown by western blot (Figure 2.5c). Both B22 and the Tet-VP16 cells were maintained in DMEM + 10% CS + 4 mM L-Glutamine.

Primary rat osteoblasts isolated from fetal calvarial tissue (20 dpc) were cultured under osteogenic culture conditions essentially as described (Owen et al., 1990). ROS 17/2.8 cells were maintained in F12 medium with 5% FBS and 2mM L-Glutamine.

Assessment of Alkaline Phosphatase Activity

For phenotypic rescue experiments Runx2 deficient calvarial cells (Komori et al., 1997) were transduced with an adenovirus vector encoding human Runx2 protein under the control of a CMV promoter or the corresponding empty vector (a kind gift from John Robinson, Wyeth Research, Collegeville, PA). Briefly, viral particles were administered at 50 MOI in α-MEM with 1% FBS, incubated for 1 h at 37°C. After infection, free virus was aspirated, and cells were washed twice in serum-free MEM. Cells were then fed with fresh medium containing 10% FBS and, where indicated, 100 ng/ml BMP2 (a kind gift from Dr. John Wozney, Wyeth Research, Cambridge, MA). Media was changed every second day, with fresh BMP2 where indicated and cultured for one week. Cells were then fixed in 2% paraformaldehyde and stained for alkaline phosphatase activity, detected by colorimetric reaction using a 0.1M Tris maleate buffer (pH8.4) containing 0.05% Naphthol AS-MX Phosphate disodium salt, 2.8% NN'-dimethyl formamide, and 0.1% Fast Red salt (Sigma Chemical Co.; St. Louis, MO). Staining was carried out at 37°C for 10 minutes (Burstone, 1962). In control experiments cells were transduced with adenoviral particles with empty vector (data not shown).

B22 and Tet-VP16 cells were grown on collagen type I coated plates (14 ng/mm^2) with media changes every second day. Where indicated 2 μg/ml of Tetracycline was added to suppress transgene expression. After four days in culture, cells reached confluence and, where indicated, cells were grown in media containing 200 ng/ml rh-BMP2. After 7 and 14 days in culture, cells were fixed in 2% paraformaldehyde and stained for alkaline phosphatase activity as described above.

Real-Time PCR Analysis

B22 and Tet-VP16 control cells were grown to confluence as described above and transduced with 200 ng/ml rh-BMP2. Total RNA was isolated from cells at the indicated time points using Trizol reagent (Invitrogen, Carlsbad, CA). Total RNA was purified using the DNA-Free RNA kit (Zymo Research Corporation, Orange CA). cDNA was generated from purified RNA using a reverse transcription reaction with Oligo-dT primers (Invitrogen Corporation, Carlsbad, CA). cDNA was then subjected to Real-Time PCR reaction using TaqMan chemistry (Applied Biosystems, Inc., Foster City, CA). Primers and probes for rodent GAPDH were purchase from Applied Biosystems, Inc. and mouse alkaline phosphatase (APase) primers and probes were as follows:

(Forward 5'-CTGCAGGATCGGAACGTCAA-3')

(Reverse 3'-CTCTTCCCACCATCTGGGC-5')

FAM-MGB probe (5'-CAATTAACATCGACGCTGC-3')

Amplicon quantities were determined relative to a standard curve generated from a serial dilution of pooled cDNA from all samples. APase quantities were normalized to GAPDH.

Western Blot Analysis

Total protein was isolated from primary rat calvarial osteoblasts at the indicated time in culture. Briefly, cells were lysed on the plate by adding SDS lysis buffer (2% SDS, 10 mM dithiothreitol, 10% glycerol, 2 M urea, 1.0 mM phenylmethylsulfonyl fluoride, 10 mM Tris-HCl, pH 6.8, 0.002% bromphenol blue, complete 1× complete protease

inhibitor mixture, Roche Molecular Biochemicals, Indianapolis, IN). Proteins were resolved by SDS-PAGE, transferred to a Immobilon-P PVDF transfer membrane (Millipore Corporation, Bedford MA). Blots were probed with either rabbit polyclonal antibodies to Brg1 (1:2000; [H-70] Santa Cruz Biotechnology) or mouse monoclonal antibody to INI1 (BAF47) (1:100; B33720 Transduction Laboratories, Lexington, KY). Appropriate HRP conjugated secondary antibodies were purchased from Santa Cruz Biotechnology, Santa Cruz, CA. ECL western immunoblot detection reagent was used to visualize proteins (Amersham Biosciences, Piscataway, NJ).

In Situ Immunofluorescence Microscopy

Mouse embryos at 18.5 dpc were fixed in paraformaldehyde, embedded in paraffin, and heads were serial sectioned at 8 μm for immunolabeling using standard procedures. Slides of serial sections were stained by H&E and by indirect immunofluorescence. Antibodies for indirect immunofluorescence included rabbit anti-Brg1 (1:200; [H-70]), rabbit anti-Runx2 (1:200; [M-70], Santa Cruz Biotechnology, Santa Cruz, CA), and donkey anti-rabbit Alexa 488 (1:800, Molecular Probes, Eugene, OR). DNA was visualized by DAPI (4', 6-diamidino-2-phenylindole) staining.

Primary osteoblasts isolated from mouse calvaria (18.5dpc) were grown on gelatin-coated coverslips and processed for *in situ* immunofluorescence. In brief, cells were rinsed twice with PBS and fixed in 3.7% formaldehyde in PBS for 10 minutes on ice. After rinsing once with PBS, the cells were permeabilized in 0.1% Triton X-100 in PBS, and

rinsed twice with PBSA (0.5% bovine serum albumin in PBS) followed by antibody staining. Cells were double-labeled for Runx2 (green) and Brg1 (red). Affinity purified Brg1 rabbit polyclonal antibodies (1:200; (de la Serna et al., 2000)), Runx2 monoclonal antibody (a generous gift from Ito Y., Institute of Molecular Cell Biology, Singapore) (Zhang et al., 2000a) and anti-rabbit Alexa 568 and anti-mouse Alexa 488 (1:800, Molecular Probes, Eugene, OR) were used. To determine the degree of Runx2 and Brg1 colocalization image cross-correlation was performed essentially as described in (Gupta et al., 2003). Immunostaining of both cells and tissue sections was recorded using an epifluorescence Zeiss Axioplan 2 (Zeiss Inc., Thorwood, NY) microscope attached to a CCD camera. Cell images were deconvoluted using Metamorph Imaging Software (Universal Imaging Corp., Downingtown, PA).

RESULTS

Alkaline phosphatase expression reflects BMP2 induced and Runx2 dependent initiation of osteoblast differentiation

Runx2 null mice are characterized by a complete absence of bone formation due to a defect in osteoblast differentiation (Komori et al., 1997). Previous studies have shown that Runx2 cooperates with BMP activated receptor Smads to induce osteoblast differentiation (Kobayashi et al., 2000; Lee et al., 2000; Zaidi et al., 2002b; Ito and Miyazono, 2003; Franceschi and Xiao, 2003; Selvamurugan et al., 2004b). We used Runx2 null cells to determine the extent to which BMP2 signaling promotes osteoblast differentiation in the presence or absence of Runx2, as reflected by alkaline phosphatase (APase) activity. Primary cultures of cells isolated from the calvaria of Runx2 null and wild-type mouse embryos were treated with BMP2 and/or exogenously expressed Runx2 for seven days and monitored daily for APase activity. APase activity was detected in untreated wild-type calvarial cultures when cells reached confluence (Figure 2.1) and was stimulated in cells grown in the presence of BMP2 alone. While exogenous Runx2 expression (by adenovirus infection) alone had a minimal effect on APase activity in wild-type culture, the presence of both BMP2 and exogenous Runx2 resulted in a synergistic induction of APase activity. In contrast, APase activity remained nearly undetectable in Runx2 null cells, as well as in null cells grown in the presence of either BMP2 or exogenously expressed Runx2. Notably, BMP2 treatment in combination with exogenous Runx2 expression in Runx2 null cells resulted in a synergistic induction of

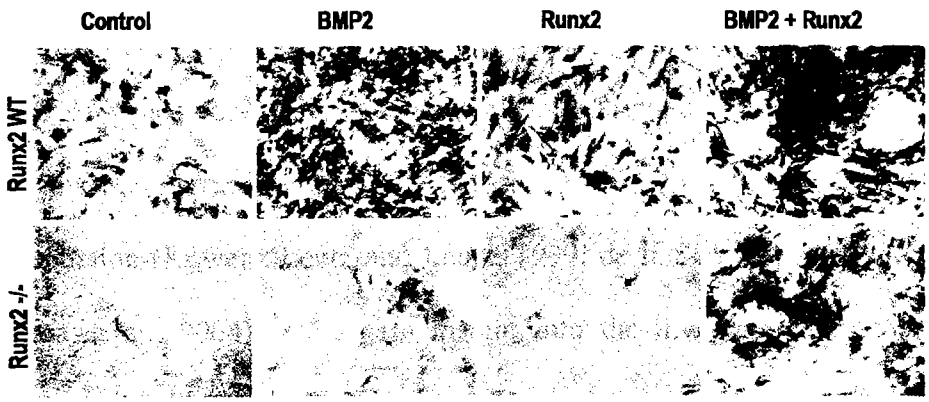

Figure 2.1 BMP2 Signaling and Runx2 Synergistically Promote Osteoblast Differentiation
The dependence of Runx2 expression for BMP2 induced alkaline phosphatase (APase) activity was assessed using mouse calvarial cells (17.5 dpc) from wild type (WT) or Runx2 null mice. Minimal APase activity was detected in WT cells grown for seven days in the absence of BMP2 and no expression was observed in Runx2 null cells grown under the same conditions. Induction of APase activity is observed in WT cells treated with BMP2 (100 ng/ml) or exogenous Runx2 delivered by adenoviral vector. In contrast no induction was observed in Runx2 null cells for either treatment alone. Notably, the combination of BMP2 (100 ng/ml) with exogenous Runx2 expression induced APase activity in both WT and Runx2 null cells.

APase activity (Figure 2.1). This finding directly demonstrates that BMP2 induction of the osteoblast phenotype requires Runx2.

BMP2 induced osteoblast differentiation is associated with the temporal expression of SWI/SNF chromatin remodeling subunits

Chromatin remodeling is required to support developmental activation and suppression of genes for phenotype development. Previous studies have shown that SWI/SNF chromatin remodeling activity is essential for myeloid, adipocyte, and muscle cell differentiation (Kowenz-Leutz and Leutz, 1999; de la Serna et al., 2001; Pederson, 2001; Salma et al., 2004). To gain insight into the involvement of the SWI/SNF complex in osteogenic differentiation, we analyzed microarray gene expression data from BMP2-induced osteoblast differentiation of premyogenic C2C12 cells. Induction of the osteoblast phenotype in this system is reflected by the upregulation of both Runx2, within 2 hours, and APase expression, by 16 hours(Balint et al., 2003). We find that in response to BMP2 treatment (300 ng/ml) there are temporal alterations in expression of Brg1, BAF53a, BAF57, BAF60a, BAF155, and BAF250 at 12 and 24 hours after BMP2 treatment (Figure 2.2). These observations provided a basis for exploration of the hypothesis that the chromatin remodeling activity of SWI/SNF is functionally linked to BMP2-induced osteoblast differentiation.

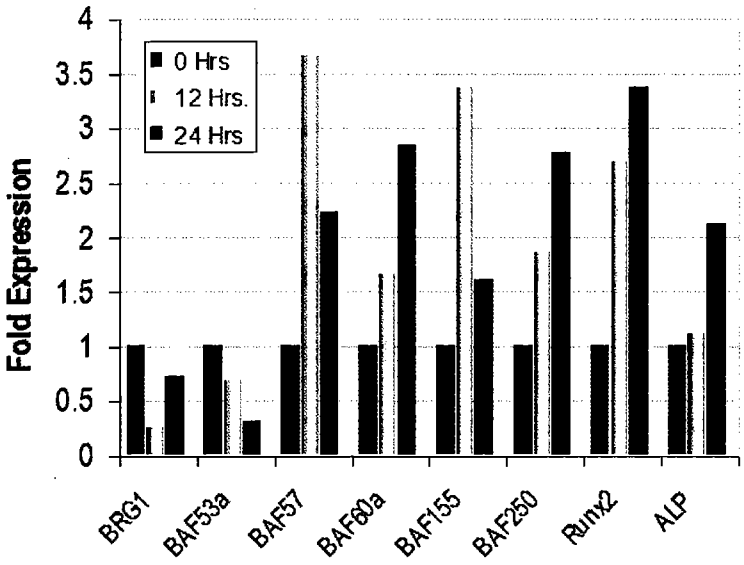

Gene	GenBank Accession Number
BRG1	U29175
BAF53a	AF041474
BAF57	AF036262
BAF60a	U66617
BAF155	U66615
BAF250	AB001895
RUNX2	L40992
ALP	AB011405

Figure 2.2. Gene Microarray Analysis of BMP2 Induced Osteoblast Differentiation Reveals Temporal Alterations in the Expression of Components of the SWI/SNF Complex
Gene microarray expression data from a timecourse in which premyogenic C2C12 cells were induced to differentiation toward the osteogenic lineage by BMP2 treatment (Balint et al., 2003) were analyzed to assess changes in mRNA accumulation for subunits of the SWI/SNF chromatin remodeling complex. Temporal alterations were observed in the expression of each of the SWI/SNF genes that is represented in the microarray data set. For comparison the osteogenic induction of Runx2 as well as APase gene expression is shown. Data were normalized to the initial time point.

SWI/SNF components are expressed in the developing skeleton in vivo and in osteoblasts ex vivo

We examined the involvement of SWI/SNF complexes during osteogenic differentiation initially by assessing Brg1 expression in developing skeletal structures *in vivo*. Mouse embryos isolated at 18.5 days post coitum (dpc) were examined by immunofluorescence histochemistry for the expression of Brg1 and Runx2 proteins. As shown in figure 2.3, both Brg1 and Runx2 proteins are detectable in the nuclei of cells in the developing exoccipital bone. This pattern of Brg1 expression is consistent throughout skeletal components, all of which were also positive for the key osteogenic regulatory protein, Runx2. These observations are consistent with a requirement for SWI/SNF chromatin remodeling activity to supported Runx dependent skeletal gene expression. We further find by western blot and *in situ* immunofluorescence analyses that Brg1 and Ini1, essential components of the SWI/SNF complex, are expressed in osteoblasts *ex vivo* (Figure 2.4). While the level of Ini1 protein remains constitutive, Brg1 reproducibly exhibits two forms with differing electrophoretic migration at the onset of cellular multilayering and maturation, but, one form at early and late stages of differentiation. Taken together our results suggest a functional relationship between the expression of components of the SWI/SNF chromatin remodeling complex and osteoblast differentiation.

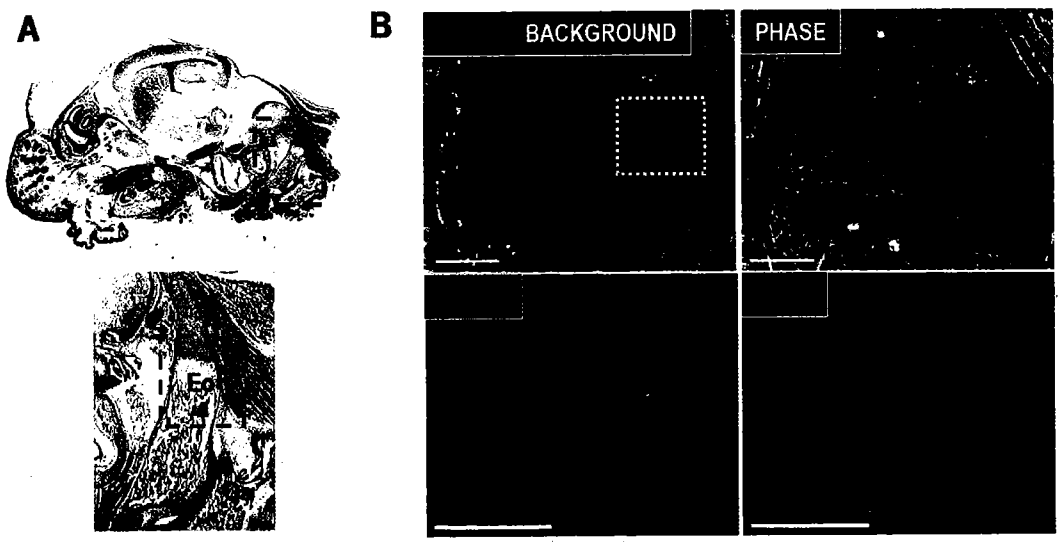

Figure 2.3. SWI/SNF Factors Are Expressed In Developing Skeletal Structures
Mouse embryos at 18.5dpc were fixed in paraformaldehyde, embedded in paraffin, and heads were serial sectioned at 8μm. Slides of serial sections were stained by H&E dye (A) and by indirect immunofluorescence (B). Labeled skeletal structures are as follows: Exoccipital (Eo) and Occipital Arch (Oa). Indirect immunofluorescence was performed on adjacent serial sections for Runx2 and Brg1. The Runx2-background image shows the growth plate region of the exoccipital bone. This image was generated by overlaying the Runx2 image with an image that reflects sample auto-fluorescence; in this image background signal is red, autofluorescence signal is yellow, and specific Runx2 signal is green. Staining for Runx2 (green, lower left panel) is from the white inset in the Runx2-background image; and staining for Brg1 (red, lower right panel) is from an adjacent serial section. (White bars: upper panel, 100 μm; lower panel, 50 μm).

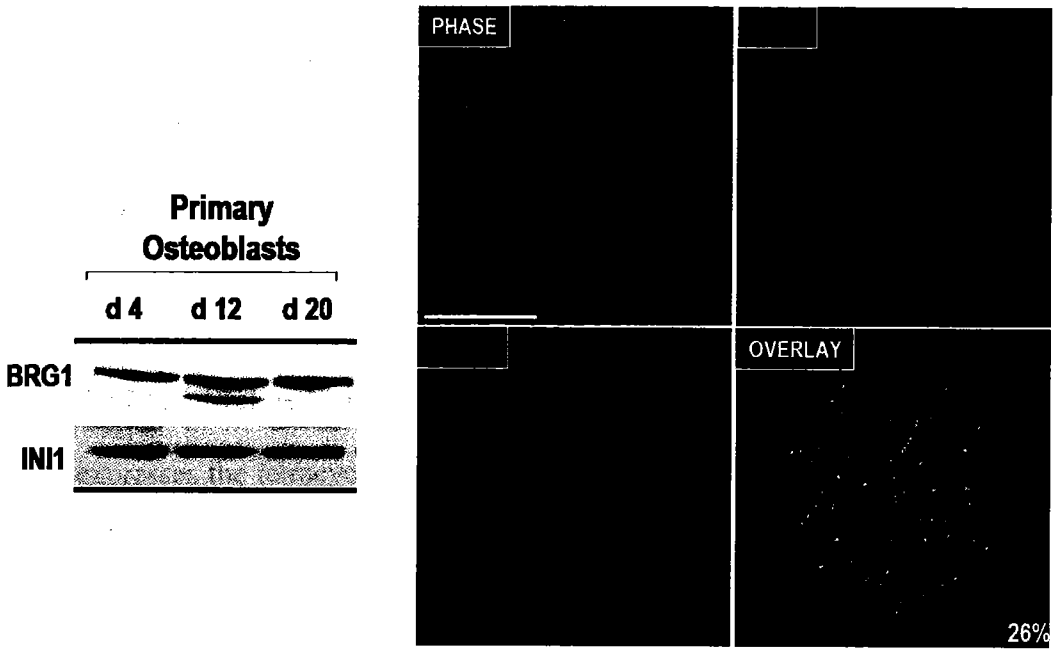

Figure 2.4. SWI/SNF Factors Are Expressed in Primary Osteoblasts
Normal rat diploid osteoblasts were cultured for the indicated time (days). Total protein was isolated and western blot analysis was performed using antibodies to Brg1 and INI1 (left panel). Primary osteoblasts isolated from mouse calvaria (17.5 dpc) were grown on gelatin-coated coverslips and processed for *in situ* immunofluorescence. Cells were double-labeled for Runx2 (green) and Brg1 (red). As shown both Runx2 and Brg1 are organized in punctate subnuclear foci, and subset of which colocalize (26%), as determined by image cross-correlation analysis. White bar is 10 μm.

SWI/SNF Complex is required for BMP2-Induced Alkaline Phosphatase gene expression

To determine directly whether there is a role for SWI/SNF-mediated chromatin remodeling in BMP2 induced osteoblast differentiation, we utilized the B22 cell line that contains a stably integrated tetracycline inducible transgene encoding a flag-tagged Brg1 protein with a point-mutation in the ATP binding domain (Figure 2.5A,B). This mutant Brg1 associates with components of the SWI/SNF complex, forming catalytically non-functional complexes (de la Serna et al., 2000; de la Serna et al., 2001) (Figure 2.5C). Mutant Brg1 protein expression reaches maximal levels within 3 days (Figure 2.5D) after removal of tetracycline. As a control we used the B22 parental cell line, Tet-VP16, which expresses the tetracycline responsive repressor protein. B22 cells and the parental Tet-VP16 cell lines express equivalent levels of endogenous Runx2 protein (data not shown).

We examined BMP2-induced osteoblast differentiation in the B22 cells in the absence or presence of the mutant Brg1 protein, +/- tetracycline respectively. We find that BMP2 treatment results in an induction of APase activity in cells expressing endogenous wild-type Brg1 protein (Figure 2.6A). APase expression was detectable as early as four days following BMP2 treatment (data not shown) and increased progressively over time in culture. By day 14 robust expression of APase was evident in multilayered tissue-like nodules. Strikingly, the presence of the dominant negative Brg completely blocked the induction of APase by BMP2. APase remained undetectable

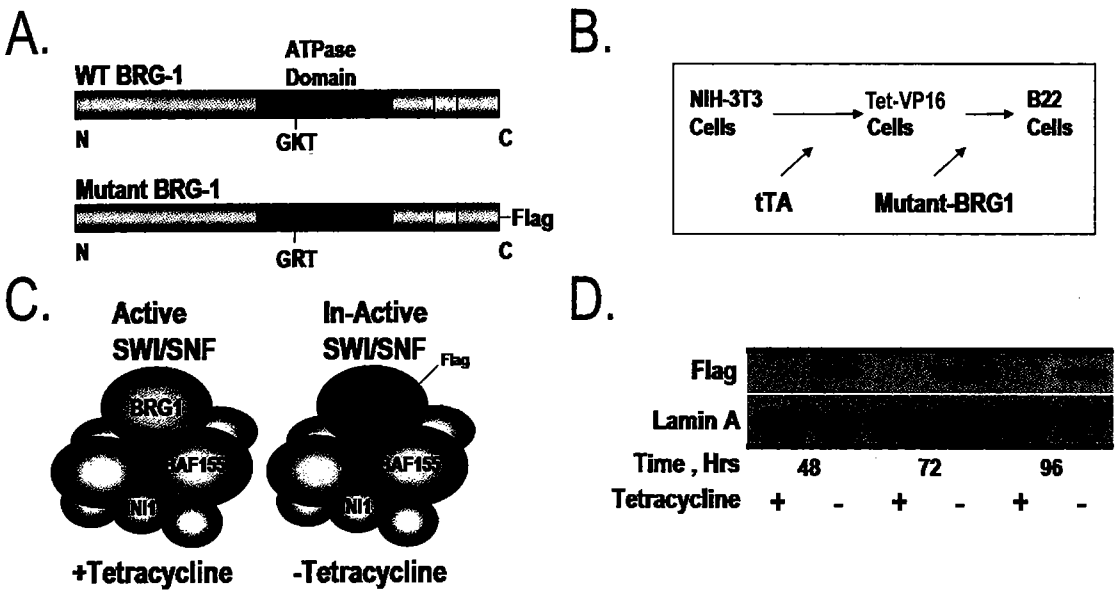

Figure 2.5. Tetracycline Inducible (Tet-Off) Dominant Negative SWI/SNF Stable Cell Line **A.** B22 cells have an inducible flag-tagged BRG1 transgene containing a mutation in the ATP binding site (K to R). **B.** Tet-VP16 cells were generated from NIH-3T3 cells and contain a stably integrated Tet-tA transgene, which encodes the Tet-VP16 regulator. B22 cells were generated from Tet-VP16 cells and contain both the Tet-tA transgene and the flag-tagged BRG1 mutant transgene. **C.** Mutant Brg1 has been previously shown in this cell line to associate with components of the SWI/SNF complex, but is non-functional. **D.** Cells grown in the presence of 2 ug/ml Tetracycline repress the mutant transgene; whereas removal of Tetracycline induces expression of the mutant protein as shown by western blot. Maximum levels of the mutant Brg1 protein are observed within three days.

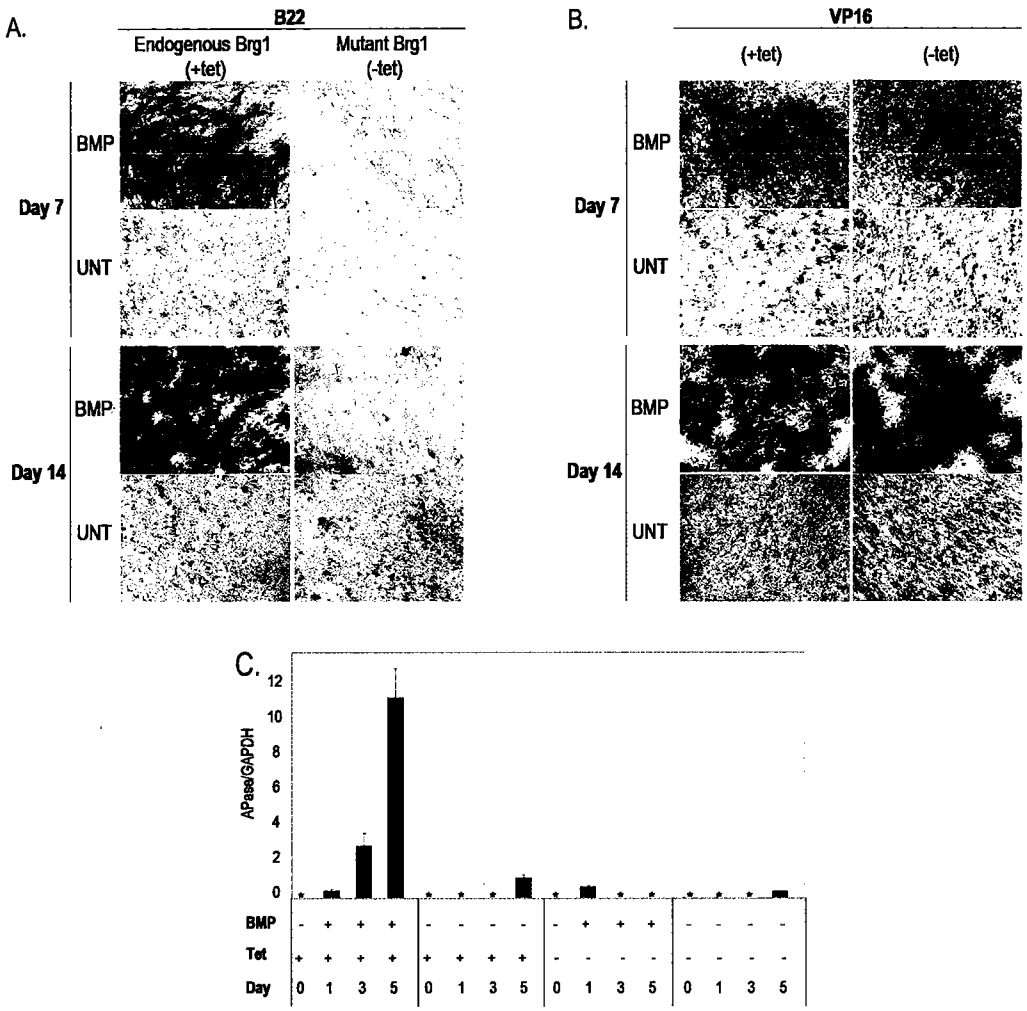

Figure 2.6. SWI/SNF Complex is Required for BMP2 Induced Alkaline Phosphatase Gene Expression

A. and **B.** B22 and tet-VP16 cells were growth on collagen type I coated plates with media changes every second day. Where indicated 2 ug/ml of Tetracycline was added to suppress transgene expression. After four days in culture, cells reached confluence and, where indicated, were grown in media containing 200 ng/ml rh-BMP2. After 7 and 14 days in culture, cells were fixed in paraformaldehyde and stained for alkaline phosphatase activity. B22 cells were isolated from each treatment on days 0, 7, and 14 to confirm by western blot the expression of the mutant-Brg1 protein (data not shown). **C.** B22 cells were grown and treated as described above. RNA was extracted at the indicated time points and processed for real-time PCR analysis using primers and probes for mouse APase and GAPDH. Amplicon quantities were determined relative to a standard curve generated from a serial dilution of pooled cDNA from all samples (n=2). APase quantities were normalized to GAPDH and (*) indicates undetectable APase mRNA.

even after 14 days of chronic BMP2 treatment in the presence of the mutant Brg1 protein. By using Tet-VP16 cells, we confirmed that induction of the tetracycline responsive transactivator alone did not inhibit APase activity (Figure 2.6B). We further confirmed by quantitative RT-PCR that the inhibitory effects of the mutant Brg1 protein on APase activity occurred at the level of gene expression (mRNA) (Figure 2.6C). These findings indicate that inhibition of SWI/SNF function does not simply delay induction of the osteoblast phenotype but abrogates completion of the BMP2 signaling pathway. Thus SWI/SNF chromatin remodeling activity is essential for induction of the osteogenic lineage.

DISCUSSION

We have combined molecular, biochemical, cellular, and *in vivo* approaches to demonstrate that SWI/SNF chromatin remodeling activity is obligatory for skeletal gene expression that supports osteoblast differentiation. Our findings in Runx2 null cells show that BMP2 mediated induction of the osteoblast phenotype requires Runx2. However, BMP2 and Runx2 protein are not sufficient to promote osteoblast differentiation in the presence of a dominant negative SWI/SNF chromatin remodeling complex.

The concept that chromatin remodeling factors, including SWI/SNF, mediate induction of the osteoblast phenotype is supported by specific modifications in chromatin structure that correlate with basal and vitamin D enhanced gene expression of the bone-specific osteocalcin (OC) promoter and that require promoter binding of Runx proteins (Javed et al., 1999; Montecino et al., 1996). These chromatin alterations include nucleosome displacement and covalent histone modifications (Montecino et al., 1996; Shen et al., 2002; Sierra et al., 2003a), and are consistent with the involvement of ATP-dependent chromatin remodeling as well as histone acetyltransferase activity. Runx proteins are not competent to remodel chromatin (Gutierrez et al., 2002), but interact with coregulatory proteins and chromatin remodeling factors (Gutierrez et al., 2002; Javed et al., 1999). Thus Runx2 may have a functional role in directing structural alterations in the chromatin organization of skeletal gene promoters to support osteoblast differentiation. Runx2 null mice do not develop a mineralized skeleton and osteoblast differentiation is compromised (Komori et al., 1997). Together these results predict that the coordination of chromatin alterations is a requirement for the onset of bone formation.

Our findings that both Runx2 and SWI/SNF are required for BMP2 mediated induction of osteogenic differentiation strongly support this concept.

The consequences of null mutations in different subunits of the SWI/SNF complex have been examined *in vivo*. From these studies it is evident that SWI/SNF function is required for embryonic development (Guidi et al., 2001; Klochendler-Yeivin et al., 2000; Roberts et al., 2000; Bultman et al., 2000). With regard to skeletal development, it is known that fourteen percent of Brg1 null heterozygous mice exhibit exencephaly at embryonic day 16.5-18.5 (Bultman et al., 2000). This craniofacial defect that is characterized in part by the absence of a calvarium (Ohyama et al., 1997; Bultman et al., 2000), supports a role for Brg1 in skeletal formation. Also, mice that are heterozygous for a BAF155 null allele, a subunit of the SWI/SNF complex, exhibit exencephaly with a similar penetrance as observed for the Brg1 heterozygote mice (Kim et al., 2001). These genetic observations further indicate a role for the SWI/SNF chromatin remodeling complex in skeletal development. Our demonstration that essential components of the SWI/SNF complex are expressed in developing skeletal structures, as well as throughout osteogenic differentiation of cells isolated from the calvarium, is consistent with such a role.

The rules that govern functional interrelationships between chromatin remodeling and transcriptional control of skeletogenesis remain to be comprehensively established. However, our studies suggest that the SWI/SNF chromatin remodeling enzymes are essential for the initiation of BMP2-induced Runx2-dependent skeletal gene expression that is required for osteoblast differentiation.

CHAPTER III:

Quantitative Signature for Architectural Organization of Regulatory Factors Using Intranuclear Informatics

ABSTRACT

Regulatory machinery for replication and gene expression is punctately organized in supramolecular complexes that are compartmentalized in nuclear microenvironments. Quantitative approaches are required to understand the assembly of regulatory machinery within the context of nuclear architecture and to provide a mechanistic link with biological control. We have developed "intranuclear informatics" to quantify functionally relevant parameters of spatially organized nuclear domains. Using this informatics strategy we have characterized post-mitotic reestablishment of focal subnuclear organization of Runx (AML/Cbfa) transcription factors in progeny cells. By analyzing point mutations that abrogate fidelity of Runx intranuclear targeting, we establish molecular determinants for the spatial order of Runx domains. Our novel approach provides evidence that architectural organization of Runx factors may be fundamental to their tissue specific regulatory function.

INTRODUCTION

The architectural organization of nucleic acids and cognate factors in subnuclear microenvironments is linked with gene regulation, replication and repair (Stein et al., 2000a; Stein et al., 2000b; Lemon and Tjian, 2000; Dundr and Misteli, 2001; Iborra and Cook, 2002; Spector, 2003; Stein et al., 2003). Spatio-temporal changes in this subnuclear organization accompany cell cycle progression and cell differentiation (Ma et al., 1998; Francastel et al., 2000). Perturbations in subnuclear organization have been functionally related with compromised gene expression that accompanies the onset and progression of disease (Dyck et al., 1994; Karpuj et al., 1999; McNeil et al., 1999). Traditionally, biological control of gene expression has been experimentally addressed by the identification and characterization of promoter elements and cognate regulatory and co-regulatory proteins, as well as by mechanistically defining the dynamics of chromatin structure and nucleosome organization. It is becoming increasingly evident that regulatory parameters of gene expression are operative within a higher-order subnuclear organization of nucleic acids and regulatory proteins. Observations made by epifluorescence and confocal microscopy have provided the initial insight into assembly of nuclear microenvironments that support the combinatorial compartmentalization of regulatory factors and chromosomal domains (Cook, 1999; Stein et al., 2000a; Stein et al., 2000b; Stein et al., 2003; Spector, 2003). Quantitative strategies are necessary to mechanistically associate the subnuclear organization of regulatory factors with biological control.

Here we describe a novel approach, intranuclear informatics, to examine the subnuclear organization of regulatory factor domains from digital microscopic images. Intranuclear informatics utilizes parameters with biologically relevant variability to characterize subnuclear organization. We have developed an image-processing algorithm to acquire and evaluate these parameters of subnuclear organization. The result is a multivariable data-set that can be used for exploratory analysis techniques and for quantitatively testing specific biological hypotheses.

Runx transcription factors provide a paradigm for compartmentalization of gene expression and nuclear matrix association of regulatory proteins (Lian and Stein, 2003). A conserved intranuclear targeting signal (NMTS) within the C-terminus directs Runx factors to matrix associated subnuclear sites that support transcriptional control in the interphase nucleus (Choi et al., 2001; Zaidi et al., 2001a; Zeng et al., 1997). By the application of intranuclear informatics we elucidate that Runx regulatory proteins exhibit an interphase architectural signature that is restored following mitosis. Furthermore, our analysis of NMTS mutant proteins provides evidence that architectural association of Runx factors may be fundamental to their tissue specific gene regulatory functions. Thus, intranuclear informatics quantitatively bridges the spatial organization of protein domains with regulatory determinants of biological control.

MATERIALS AND METHODS

Cell Culture and Transfections

ROS 17/2.8 osteosarcoma cells were maintained in F12 with PS, 2mM L-glutamine, and 5% FBS. Hela cells were maintained in DMEM with PS, 2mM L-glutamine, and 10% FBS. Exponentially growing HeLa cells were transfected using with 500ng of either HA-tagged wild-type Runx2, an HA-tagged C-terminal deletion, or one of the five HA tagged NMTS point mutants for 24hrs with Superfectamine (Invitrogen, San Diego, CA).

Immunofluorescence

Hela and Ros cells were grown on gelatin-coated coverslips (BD Biosciences, Lexington, KY). Cells were processed for *in situ* immunofluorescence as described (Javed et al., 2000). In brief, cells were rinsed twice with ice-cold PBS and fixed in 3.7% formaldehyde in PBS for 10 minutes on ice. After rinsing once with PBS, the cells were permeabilized in 0.1% Triton X-100 in PBS, and rinsed twice with PBSA (0.5% bovine serum albumin [BSA] in PBS) followed by antibody staining. Antibodies and their dilutions used are as follows: rabbit polyclonal antibodies against Runx2 (1:200; Oncogene, Carlsbad, CA) and rabbit polyclonal antibodies against HA-epitope (1:500, Santa Cruz Biotechnology, Santa Cruz,CA). The secondary antibodies used were either anti rabbit or mouse Alexa 568 or Alexa 488 (1:800, Molecular Probes, Eugene, OR).

Image acquisition and restoration

Immunostaining of cell preparations was recorded using a CCD camera attached to an epifluorescence Zeiss Axioplan 2 microscope (Zeiss Inc., Thorwood, NY). For Runx2 interphase/telophase studies single image planes were acquired and deconvoluted using the Metamorph Imaging Software (Universal Imaging Corp., Dowingtown, PA). For NMTS mutation experiments Z-series image stacks were acquired at 0.25 micron intervals with 67 nm/pixel (xy). Restoration of images was carried out by 3-D deconvolution using a measured point-spread function as described in (Carrington et al., 1995).

Image processing

We have developed an image processing algorithm which automatically performs image segmentation, feature extraction, and parameter computation. Our algorithm requires the input of any number of image pairs and a text-file, which lists the name of the images to be analyzed. For each pair of images, one is the digital micrograph and a second is the nuclear mask image. The nuclear mask, which is generated using Metamorph imaging software or Adobe Photoshop (Adobe Systems Inc., San Jose, CA), is utilized to eliminate intensity data that is located outside the nucleus and restrict analysis to intensity data within the nucleus. For mitosis studies we analyzed a single image plane per cell. For NMTS mutation studies we analyzed z-section images from deconvoluted Z-series stacks. Image segmentation is carried out using a threshold technique, where the selected threshold is the intensity value that maximizes the number of detectable nuclear domains. The image analysis is implemented using the MATLAB®

image processing and statistics toolboxes (The Mathworks Inc., Natick, MA) and Metamorph Imaging Software (Universal Imaging Corp., Downingtown, PA).

Image Feature Extraction

Our algorithm extracts the total number of domains within the nucleus, the size of each domain, the location of each domain-centroid in image pixel coordinates, the nuclear cross-sectional area and the nuclear cross-sectional perimeter from the segmented and mask images. From these measurements we determine the following statistics for both domain size and nearest neighbor distances: mean, median, variance, standard deviation, index of dispersion, coefficient of variation, skewness, and kurtosis. The index of dispersion and coefficient of variation are mean normalization measures of variation and standard deviation, respectively. Skewness reflects of the degree of asymmetry in the distribution with positive values indicating right skewness and negative values indicating left skewness. Kurtosis is a measure of the peakedness of the distribution: positive values indicate a tall peak and negative values indicate a flat peak (or plateau) (Norman, 2000). To assess the spatial domain randomness we measured Euclidean nearest neighbor distances (NN distance) between domain centroids. The mean and variance of the Euclidean nearest neighbor distances between domains is compared to a Poisson point-process of an equivalent density (i.e., domains per unit nuclear area); standard error is also measured (Clark and Evans, 1954). Expected nearest neighbor distance parameters are corrected for edge effects (Donnelly, 1978; Sinclair, 1985). The ratio of observed (Ro) to expected (Re) mean nearest neighbor distances is

referred to as the Clark and Evans statistic (Ro/Re<1, clustered; Ro/Re=1, random; Ro/Re>1, ordered) (Clark and Evans, 1954). We also examined the radial position of domains within the nucleus. This statistic is determined by measuring the mean distance from each domain centroid to the nuclear centroid (mean domain radius) and the mean distance from the nuclear centroid position to the each perimeter pixel (mean perimeter radius); for a circle this would be the radius. The ratio of the two values is the mean relative domain radius. Value between 0 and 0.5 reflect a tendency for domains to be positioned in the nuclear interior and values between 0.5 and 1 reflect a tendency for domains to be positioned toward the nuclear periphery.

Statistical Analyses

For mitosis studies ANOVA tests were conducted on subnuclear organization data to determine the significance of observed differences in each parameter. Asterisks indicate parameters with differences that are considered to be statistically significant on a 0.05 level. P-values were adjusted to account for the false-discovery rate; asterisks are indicative of this adjustment. Analysis was performed using the general linear model (GLM) procedures in SAS/STAT (Sas Institute Inc., Cary, NC). These statistical tests were conducted to compare among telophase nuclei (T_1 and T_2) and interphase (I). We analyzed 60 nuclei for Runx2; twenty for each nucleus (see supplemental information for the complete dataset). For NMTS studies, statistical tests were conducted to compare among wild-type Runx2 and each of the five mutants. In total, 330 Z-sections were analyzed, 55 for each protein from two independent experiments (see supplemental

information for the complete dataset). Five Z-sections were analyzed per cell to account for within cell variability. Thus, the effect of NMTS mutation was assessed using a repeated measure ANOVA at a 0.05 level.

Factor Analysis was performed on parameters of subnuclear organization for each of the wild-type Runx and the five mutant proteins using the data obtained from 330 nuclear images. This analysis represents the observed subnuclear organization parameters in terms of a smaller number of uncorrelated "Factors" (or groups of parameters) that account for most of the information contained in the complete data set (Norman, 2000). Factors are extracted using principal component analysis and rotated using the varimax method. Factors scores were computed for each image and represent the sum of the standardized subnuclear organization parameters multiplied by their respective Factor loadings. Factor loading refers to the correlation of each subnuclear organization parameter with a particular Factor. Factor loadings greater than 0.65 were considered to be significant. This analysis was carried out using the Factor procedure in SAS/STAT.

Hierarchical cluster analysis was performed on mean subnuclear organization parameters from wild-type Runx and the five mutant proteins using the data from 330 nuclear images. Cluster analysis was performed using the Euclidean distance metric with complete linkage. Clusters were displayed using a dendrogram. Cluster analysis was carried out using the cluster procedure in SAS/STAT.

RESULTS

Intranuclear Informatics: A signature of nuclear architecture for regulatory proteins

We have developed intranuclear informatics to characterize spatially organized protein domains within the nucleus in terms of parameters with inherent biological variability. The conceptual framework for quantifying nuclear organization is outlined in Figure 3.1 and briefly described here. Alterations in size and number of protein domains with respect to physiological conditions, cell cycle stage, and/or cellular differentiation have been observed (Ma et al., 1998; Stenoien et al., 2001; Nielsen et al., 2002; Zaidi et al., 2003). Intranuclear informatics exploits this variability in domain size and number, to elucidate changes between different biological conditions (Figure 3.1). Another prominent feature of nuclear organization is the non-random localization of chromosome territories and protein domains (Noordmans et al., 1998; Cremer and Cremer, 2001; Shiels et al., 2001; Kozubek et al., 2002; Tanabe et al., 2002). Our approach employs first-order nearest neighbor statistics, commonly used in ecological studies (Clark and Evans, 1954; Sinclair, 1985), to characterize the spatial randomness of nuclear microenvironments (Figure 3.1). Finally, the radial position of regulatory machinery for replication and transcription is functionally interrelated with the location of chromosomal territories as well as chromatin structure (Ma et al., 1998; Cook, 1999; Cremer and Cremer, 2001; Tumbar and Belmont, 2001; Kozubek et al., 2002). Intranuclear informatics establishes the placement of regulatory foci within the context of nuclear morphology (Figure 3.1). Based on these biological observations, our approach

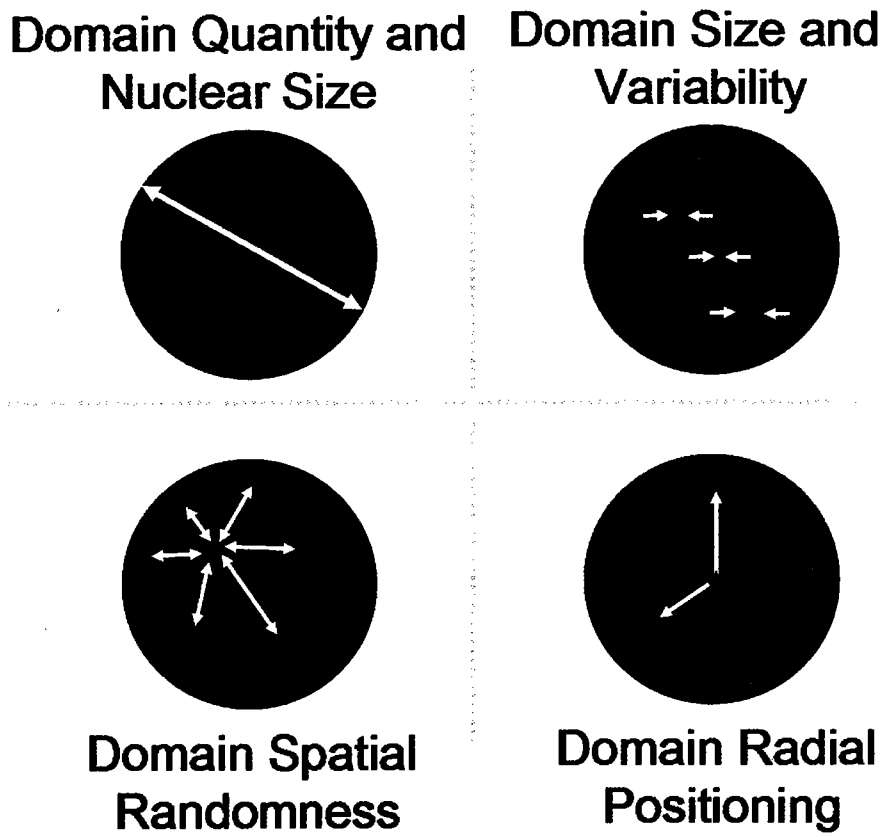

Figure 3.1: Conceptual framework for the quantitation of subnuclear organization by Intranuclear Informatics.
Four main groups of parameters, selected on the basis of inherent biological variability, are examined. Parameters that describe domain quantity and nuclear size comprise group 1 (upper left panel). Group 1 includes: number of domains and domain density. Parameters that describe domain size and variability comprise group 2 (upper right panel). Group 2 includes: domain size mean, median, standard deviation, variance, skewness, kurtosis, coefficient of variation, and index of dispersion. Parameters that describe the domain spatial randomness, which is based on domain nearest neighbor distances, comprise group 3 (lower left panel). Group 3 includes: domain nearest neighbor mean, median, standard deviation, variance, skewness, kurtosis, coefficient of variation, index of dispersion, domain density, nearest neighbor distance mean and variance expected for a random distribution, ratios between actual and expected mean and variance, and the standard error in the nearest neighbor distances. Parameters that characterize the radial position of domains comprise group 4 (lower right panel). Group 4 includes: mean perimeter radius, mean domain radius, mean relative domain radius.

describes and defines intranuclear organization utilizing twenty-five parameters, evaluated from digital fluorescence microscopic images. We have developed an image-processing and statistical algorithm to acquire measurements and compute the parameters from any number of images. The resulting data are then analyzed to quantitatively address specific biological questions using statistical approaches such as Factor analysis and multivariate clustering techniques. In summary, intranuclear informatics incorporates the principal features of intranuclear organization to provide a vehicle for quantitatively defining nuclear structure-function interrelationships.

Intranuclear informatics reveals that the post-mitotic restoration of Runx subnuclear domain organization is functionally conserved

The hematopoietic and osteogenic Runx transcription factors are involved in tissue-specific gene expression and support cell differentiation (Tracey and Speck, 2000; Komori, 2002; Lutterbach and Hiebert, 2000; Lian and Stein, 2003). In the interphase nucleus Runx proteins are associated with the nuclear matrix and are organized into punctate domains (Zaidi et al., 2001a; Zeng et al., 1997). These nuclear microenvironments spatially coincide with sites of active transcription and colocalize with several coregulatory proteins (Thomas et al., 2001; Javed et al., 2000; Lian and Stein, 2003; Harrington et al., 2002; Zaidi et al., 2002b; Westendorf et al., 2002; Kundu et al., 2002; Zaidi et al., 2004). These observations suggest a direct link between the activity of Runx proteins and their spatiotemporal organization within the nucleus. We have recently demonstrated that Runx1 and Runx2 protein domains persist during

mitosis, and undergo spatial and temporal reorganization resulting in equal partitioning into progeny nuclei (Zaidi et al., 2003). These mitotic alterations reflect natural perturbations in both nuclear structure and function and serve as a biological template for understanding Runx domain organization. Together, the dynamic distribution of Runx proteins provides a model for quantitative and comparative analysis of the subnuclear organization of regulatory proteins.

Here we have applied intranuclear informatics to understand the spatial organization of endogenous Runx2 domains in the interphase nucleus as well as following mitosis. Immunofluorescence microscopy confirms that the protein is distributed in punctate subnuclear domains (Figure 3.2). We analyzed and compared twenty-five parameters of subnuclear organization among interphase and in both telophase nuclei. Our quantitative results show that most parameters are comparable between interphase and telophase for Runx2. As expected telophase nuclei are significantly smaller than interphase. The number of domains is equivalent between progeny telophase nuclei and higher in the interphase. This observation is consistent with the mitotic partitioning of Runx proteins (Zaidi et al., 2003) (Figure 3.2). We further find that Runx2 domains exhibit a non-random organization with spatial order. We conclude that the post-mitotic restoration of Runx subnuclear organization is functionally conserved in progeny cells.

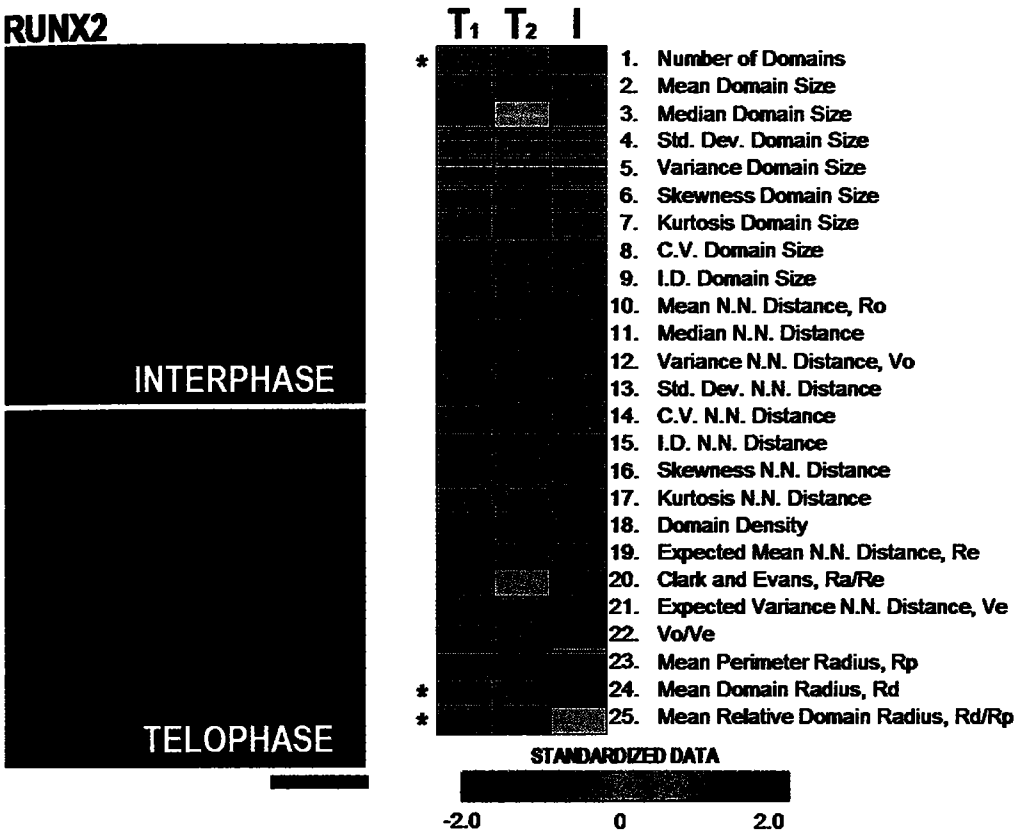

Figure 3.2: Post-mitotic restoration of the spatially ordered Runx subnuclear organization is functionally conserved.

ROS 17/2.8 osteosarcoma cells (right panel) were subjected to *in situ* immunofluorescence microscopy for endogenous Runx2. Runx2 is distributed at punctate subnuclear domains throughout the interphase and telophase nucleus (left panels). Subnuclear organization parameters were computed from deconvoluted images for Runx2 for interphase nuclei, (I) and both progeny telophase nuclei, denoted at random as telophase nucleus 1, (T_1) or telophase nucleus 2, (T_2). A color map has been applied to the standardized data assigning red to higher values and green to lower values (see supplemental information at http://jcs.biologists.org/cgi/content/full/117/21/4889/DC1). Each increment of one reflects one (row) standard deviation (inner left and right panels). ANOVA was performed to assess the significance of observed differences between T_1, T_2, and I. Asterisks indicate statistically significant differences based on a 0.05 level with correction for false discovery rate. Bonferroni's multiple comparison tests were use to determine which nuclei differed significantly at a 0.05 level. In each case significant differences were observed between each telophase (T_1,T_2) and interphase nuclei (I), but difference were not observed between telophase nuclei. Overall mean Clark and Evans statistics (Ro/Re) were 1.4 for Runx2, indicating a non-random organization with spatial order. Black bar indicates 10μm.

Intranuclear informatics establishes molecular determinants for the spatial domain organization of Runx transcription factors

A viable candidate for elucidating the underlying requirements for Runx domain organization is the nuclear matrix targeting signal (NMTS). The NMTS is a conserved and unique Runx protein motif that is necessary and sufficient for directing the protein to matrix associated intranuclear sites (Zaidi et al., 2001a; Zeng et al., 1997). Biochemical, cellular, and in vivo genetic approaches have established the requirement of the NMTS and associated functions in Runx control of cell differentiation and tissue-specific development (Choi et al., 2001; Yergeau et al., 1997). Importantly, mutations in Runx proteins that alter subnuclear targeting are associated with skeletal disease and leukemia (McNeil et al., 1999; Choi et al., 2001; Barseguian et al., 2002; Zhang et al., 2000b).

Our experimental strategy combines mutagenesis, microscopy, and intranuclear informatics to understand the contribution of the NMTS to Runx domain organization. We examined wild-type Runx2, a C-terminal deletion (Runx2-ΔC) that lacks the NMTS, as well as four NMTS point mutations, using immunofluorescence microscopy. These mutants exhibit varying degrees of compromised intranuclear targeting and selective alterations in physical and functional protein-protein interactions (Zaidi et al., 2002b; Zaidi et al., 2004), [our unpublished observations]. Our intranuclear informatics analysis was performed on deconvoluted images (n=330) from nuclei of cells expressing these proteins. All of the Runx proteins localize to punctate domains within the nucleus (Figure 3.3). Initial evaluation of subnuclear organization data reveals that there are significant differences in seventeen of twenty-five parameters, as identified by ANOVA.

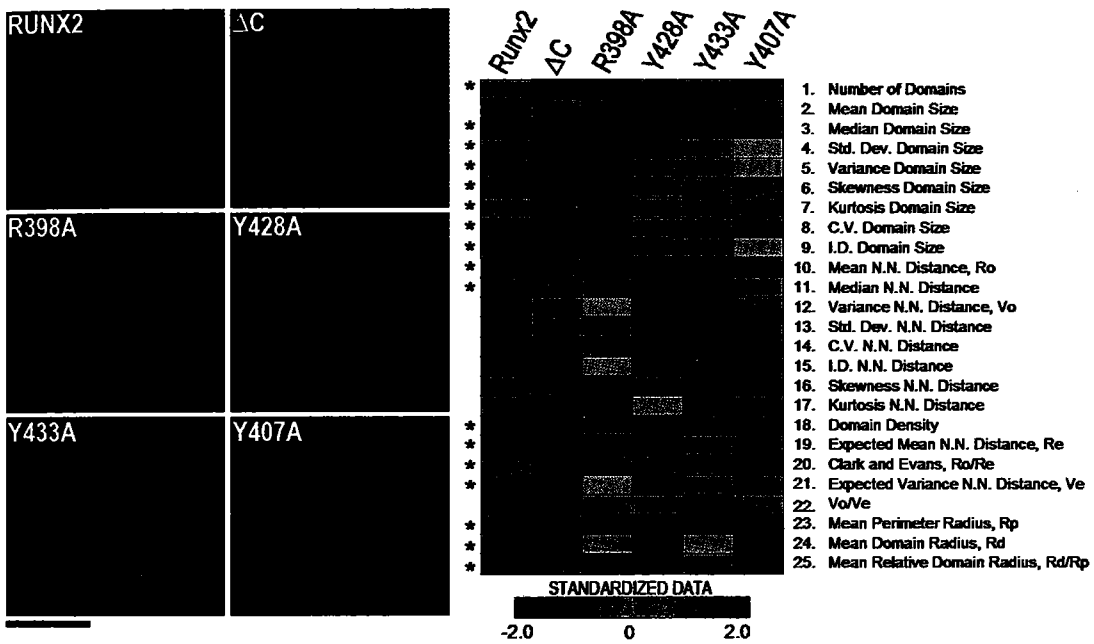

Figure 3.3: Mutation of NMTS alters the interphase Runx subnuclear organization. Point mutations within the Runx2 NMTS were generated using PCR-mediated mutagenesis. Deconvoluted images were analyzed of whole cells (HeLa) expressing either HA-tagged wild-type Runx2, an HA-tagged C-terminal deletion or one of the four HA-tagged NMTS point mutants. As shown, each of these mutants and wild-type Runx exhibits a punctate subnuclear distribution (left panel). Standardized mean subnuclear organization data for the indicated proteins are shown (right panel). A color map has been applied to the standardized values assigning red to higher values and green to lower values (see supplemental information at http://jcs.biologists.org/cgi/content/full/117/21/4889/DC1). Using a repeated-measure analysis of variance (ANOVA) we detect significant differences at a 0.05 level in 17 of 25 parameters measured, as indicated by asterisks. Black bar indicates 10μm.

In contrast, parameters that reflect variation in nearest neighbor distances are not significantly altered by the mutations. These results are schematically demonstrated by a color representation of standardized data (Figure 3.3). Collectively, our observations indicate that there are indeed alterations in the spatial domain organization of Runx proteins as a consequence of mutations in the NMTS.

Our analysis reveals that R398A and Y407A mutants share most of the properties with the wild-type protein; except for a reduction in the domain radial positioning for the Y407A mutant protein, and an increase in the domain size variability for the R398A mutant protein. Significant alterations in subnuclear organization were observed for the Y428A, Y433A, and ΔC mutations. It has been proposed that nuclear microenvironments represent the steady state local accumulation of proteins resulting from dynamic molecular interactions providing threshold concentrations of regulatory factors for combinatorial control (Stein et al., 2000a; Stein et al., 2000b; Misteli, 2001; Stein et al., 2003). Consistent with this concept, the Y428A mutant, which has a significant reduction in the mean and variability in domain size (Figure 3.3), functionally abrogates interactions between Smad and Runx, thereby blocking integration of TGFβ signals at matrix-associated subnuclear sites (Zaidi et al., 2002b). Furthermore, impairment of Src/YAP signaling by the Y433A mutation correlates with a decrease in average domain size (Figure 3.3). Similarly, deletion of the C-terminus of Runx2 abolishes interactions with several known co-regulators and results in reduced domain size and variability (Hanai et al., 1999; Javed et al., 2000; Westendorf et al., 2002; Thomas et al., 2001) (Figure 3.3). Hence, the reduction in Runx domain size is likely to

Factor	Common Domain Characteristic	Constituent Parameters	Loadings
A	Size Properties	Mean Domain Size	0.66
		Standard Deviation in Domain Size	0.94
		Variance in Domain Size	0.93
		Skewness in Domain Size	0.9
		Kurtosis in Domain Size	0.9
		Coefficient of Variation in Domain Size	0.95
		Index of Dispersion in Domain Size	0.97
B	Packing	Mean Domain Nearest Neighbor Distance (Observed), Ro	0.94
		Median Domain Nearest Neighbor Distance	0.91
		Domain Density	-0.91
		Mean Domain Nearest Neighbor Distance (Expected), Re	0.9
		Variance in Domain Nearest Neighbor Distance (Expected), Ve	0.88
C	Spatial Randomness	Variance in Domain Nearest Neighbor Distance (Observed), Vo	0.87
		Standard Deviation in Domain Nearest Neighbor Distance	0.85
		Coefficient of Variation in Domain Nearest Neighbor Distance	0.95
		Index of Dispersion in Domain Nearest Neighbor Distance	0.92
		Vo/Ve	0.96

TABLE 3.1: Factor analysis of subnuclear organization

The covariance structure between the twenty-five subnuclear organization parameters measured on wild-type and mutant images (n=330) indicates that there is a large degree of correlation between parameters (data not shown). Factor analysis was carried out to represent the observed subnuclear organization parameters in terms of a smaller number of uncorrelated variables. The strategy reduces the twenty-five parameters to a subset of three factors which retain the information (variability) contained within the entire data set. In multivariate analysis, "Factors" reflect groups of correlated parameters that are related to a common property of subnuclear organization. Each of the Factors has a biological interpretation based upon the grouped subnuclear organization parameters. We restricted our analysis to the first three Factors (referred to as A,B, and C), as they reflect meaningful aspects of the domain spatial. Factor A which represents, "domain size properties", accounts for approximately 30% of the information describing the subnuclear organization of the wild-type Runx and mutant images (i.e., 30% of the variation). The domain size properties are highly correlated with parameters that describe the variability in domain size and to a lesser degree the mean domain size. Factor B, which reflects "domain packing" describes 23% of the variation and is directly correlated with parameters that characterize the mean nearest neighbor distances and inversely related to domain density. "Packing" indicates that this factor relates the number of domains with the distances between domains. Factor C, which reflects "domain spatial randomness", describes 10% of the variation and is directly correlated with parameters that described the variability in domain nearest neighbor distance.

be a consequence of abrogated and/or altered protein-protein interactions. We further find that the NMTS may contribute to the spatial distribution of domains within the nucleus. This is evidenced by a reduced variability in domain nearest-neighbor distances for Y428A, Y433A, and the ΔC protein. In addition, the Runx2-ΔC protein which has abrogated subnuclear targeting, exhibits a significant increase in mean domain nearest neighbor distances as well as in domain density. We conclude that NMTS mediated intranuclear targeting is a functional determinant for the characteristic spatially ordered distribution of Runx domains.

Intranuclear informatics selectively discriminates between the subnuclear organization of wild type and mutant Runx protein domains

To identify on a broader level the biological features of subnuclear organization that are predominantly influenced by the NMTS mutations we used Factor analysis, a multivariate analytical tool for grouping related parameters ("Factors"). Three Factors that capture a large proportion of the biological variability and are readily interpretable describe the domain size (Factor A), the domain packing (Factor B) and the domain spatial randomness (Factor C) (Table 3.1). We evaluated the subnuclear distribution of each protein by calculating "Factor Scores" and generated star-plots to compare wild-type Runx2 with each of the NMTS mutants (see Figure 3.4 legend and Methods for details). Differences are evident in all three Factors. Our analysis of these changes reveals that NMTS mutations have selective effects on Runx subnuclear organization (Figure 3.4). Based upon the observed differences we can categorize the proteins into

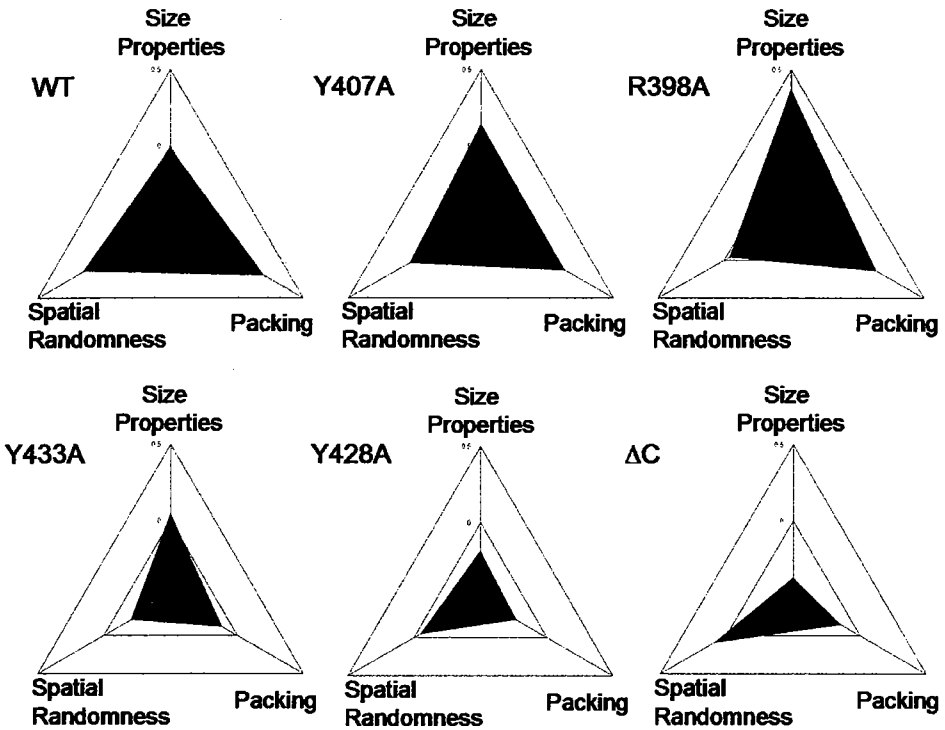

Figure 3.4: Discrimination between wild-type Runx2 and NMTS mutants on the basis of domain size, packing, and spatial randomness.
To understand the subnuclear organization of the wild-type Runx protein and the five mutants, we analyzed Factors scores, which reflect the sum of standardized subnuclear organization parameters multiplied by respective factor loadings. Factor scores assign a value to each of the unobservable Factors (Factor A: Domain Size Properties, Factor B: Domain Packing, and Factor C: Domain Spatial Randomness). Using the data acquired from the 330 nuclear image sections, we computed Factor scores for wild-type and each of the mutants and analyzed star-plots of these scores on three axes (see supplemental information at http://jcs.biologists.org/cgi/content/full/117/21/4889/DC1). The center of the star-plot has a value of -0.5, the end of each axis has a value of 0.5, and the mid-point on each axis is zero; these values are in standardized units. The three mean Factor scores for each protein define the points of a filled triangle that has been drawn to illustrate the similarities and differences among each of the proteins. Based upon the shape of each of the filled triangles, we can discriminate two groups of domain organizations: one comprised of the wild-type Runx2 protein along with the Y407A and R398A mutants and a second group containing Y433A, Y428A, and the functionally compromised Runx2-ΔC mutant. Differences in the shape of the triangles highlight the selective alterations in subnuclear organization as a consequence of NMTS mutations.

two groups. One group contains wild type Runx2, R398A and Y407A which exhibit similar spatial randomness and domain packing. The second group contains the remaining mutants with similar effects on domain packing, but selective effects on size and spatial randomness. While Y428A and Y433A mutants display similar changes in spatial randomness, domain size alterations are common between the Y428A mutant and the Runx2-ΔC protein. Of all the mutants, the Runx-ΔC protein has the most prominent effect on the three Factors collectively. Notably, this mutant protein exhibits compromised subnuclear targeting, fails to promote osteoblast differentiation, and has been linked to the human disease cleidocranial dysplasia (CCD) (Choi et al., 2001; Zhang et al., 2000b). Taken together, our analysis selectively distinguishes between wild-type Runx2 and NMTS mutant proteins based upon the three Factors of subnuclear organization.

Intranuclear informatics quantitatively bridges the spatial organization of protein domains with regulatory determinants of biological control

We have demonstrated that mutations in the NMTS have selective and specific effects on the architectural signature of Runx proteins (Figures 3.3 and 3.4). Consequently, it is important to comprehensively assimilate all the data to establish the overall degree of domain organizational similarity among wild-type and the mutants. Here we utilized hierarchical cluster analysis to group each protein on the basis of the twenty-five parameters that describe and define their subnuclear organization (Figure 3.5). The dissimilarity between the subnuclear organization of wild-type and the

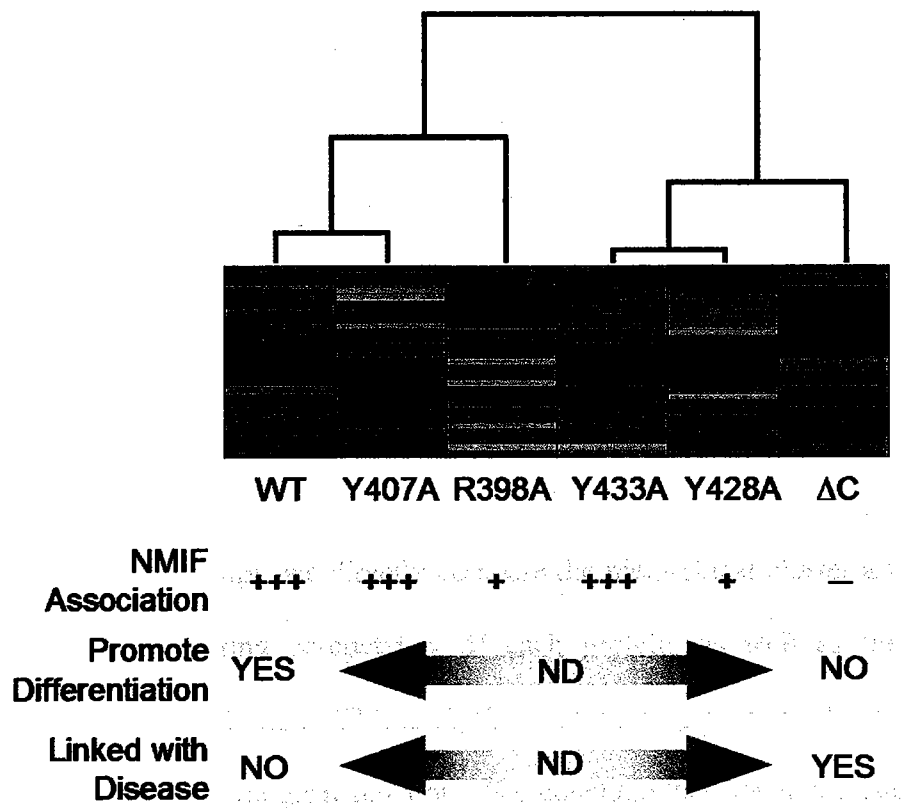

Figure 3.5: The subnuclear organization of Runx domains is linked with subnuclear targeting, biological function, and disease.
In order to determine the extent to which the subnuclear organization of each mutant differs from wild-type we performed hierarchical cluster analysis using the Euclidean distance matrix and complete linkage. Cluster organization is illustrated using a dendrogram. Subnuclear organization data is presented in a compressed form with a color map as described in figure 3.3. As shown there are two main clusters: one including wild-type and one including the Runx2-ΔC protein, which does not contain the NMTS. We find a clear parallel between this cluster analysis and our Factor analysis, particularly with respect to the clustering of Runx2-ΔC with Y433A and Y428A. This parallel lends strength to the observed clusters. Shown at the bottom is a symbolic representation of the extent to which each protein associates with the nuclear matrix as determined by biochemical fractionation and western blot analysis (i.e., ranging for "+++" (associated) for wild-type to "–" (no association for Runx2-ΔC) (Zaidi et al., 2001a; Choi et al., 2001) [and our unpublished observations]. We find a correlation between subnuclear organization and nuclear matrix association. The schematic below indicates whether a protein will promote differentiation or is involved in disease (i.e., cleidocranial dysplasia) [yes, no, or not determined (ND)].

functionally compromised Runx2-ΔC mutant is evident by the presence of two distinct clusters. This mutation removes the entire C-terminus including the subnuclear targeting signal and associated functions; homozygosity for the Runx2-ΔC allele results in embryonic lethality (Choi et al., 2001). We find that the subnuclear organization of Y433A and Y428A mutation is similar to that of the Runx2-ΔC mutant. This observation is in agreement with our Factor Analysis and is consistent with the evidence that these mutant proteins are functionally compromised and are incompetent for integrating physiological signals, which include BMP/TGFβ and Src/YAP signaling (Zaidi et al., 2001a; Zaidi et al., 2004). To provide further insight into the Runx nuclear structure-function relationships, we directly compare the hierarchical cluster arrangement with the intranuclear targeting competency of each protein, as well as their contribution to development and disease. This analysis reveals a link between Runx subnuclear domain organization and biological function. We conclude that the architectural organization of Runx transcription factors within the nucleus is fundamental to their tissue specific regulatory function.

CONCLUSION

Knowledge of the biochemical and genetic components of gene regulation, replication, and repair far exceeds our understanding of the integration of these processes within the context of nuclear architecture (Stein et al., 2000a; Stein et al., 2000b; Lemon and Tjian, 2000; Dundr and Misteli, 2001; Iborra and Cook, 2002; Spector, 2003; Stein et al., 2003). Here we have established a bioinformatics approach to describe and define organization of protein domains within the nucleus. Intranuclear informatics provides the quantitative platform to capture the relevant parameters of subnuclear organization and relate them to the fundamental requirements for biological control. Using this approach, we have demonstrated that the focal subnuclear organization of Runx proteins is conserved in progeny cells. Our strategy has enabled us to discriminate between functional and non-functional Runx proteins based, upon their domain organization within the nucleus. Furthermore, we have identified an architectural signature of Runx transcription factors that is coupled with fidelity of intranuclear targeting. In a broader context, intranuclear informatics can be applied to analyze subtle alterations in any spatially organized nuclear microenvironments under normal and pathological conditions.

CHAPTER IV:

Mitotic partitioning and selective reorganization of tissue specific transcription factors in progeny cells

ABSTRACT

Post-mitotic gene expression requires restoration of nuclear organization and assembly of regulatory complexes. The hematopoietic and osteogenic Runx (Cbfa/AML) transcription factors are punctately organized in the interphase nucleus and provide a model for understanding the subnuclear organization of tissue specific regulatory proteins following mitosis. Here we have used quantitative *in situ* immunofluorescence microscopy and quantitative image analysis to show that Runx factors undergo progressive changes in cellular localization during mitosis while retaining a punctate distribution. In comparison, the acetyl transferase p300 and acetylated histone H4 remain localized with DNA throughout mitosis while the RNA processing factor SC35 is excluded from mitotic chromatin. Subnuclear organization of Runx foci is completely restored in telophase and Runx proteins are equally partitioned into progeny nuclei. In contrast, subnuclear organization of SC35 is restored subsequent to telophase. Our results show a sequential reorganization of Runx and its co-regulatory proteins that precedes restoration of RNA processing speckles. Thus, mitotic partitioning and spatio-temporal re-organization of regulatory proteins together render progeny cells equivalently competent to support phenotypic gene expression.

INTRODUCTION

In the interphase nucleus, many tissue-restricted transcription factors are architecturally organized at punctate subnuclear sites that are associated with the nuclear matrix scaffold (Guo et al., 1995; Merriman et al., 1995; van Steensel et al., 1995; Htun et al., 1996; McNeil et al., 1998; Stenoien et al., 1998; Tang et al., 1998; Cook, 1999; Verschure et al., 1999; Bangs et al., 1998; Zeng et al., 1997; Zeng et al., 1998; Zaidi et al., 2001a; DeFranco, 2002; Stein et al., 2000b; Stenoien et al., 2000; Berezney, 2002; Berezney and Jeon, 1995). These nuclear matrix associated intranuclear foci are linked to transcriptional activation and suppression as well as contain co-regulatory proteins and signaling molecules (Zaidi et al., 2002a; Zaidi et al., 2001b; Stein et al., 2000c; Wei et al., 1998; Stein et al., 2002). Compromised nuclear matrix targeting and/or altered gene dosage of regulatory proteins is associated with pathological conditions (Zhang et al., 2000a; Choi et al., 2001; McNeil et al., 1999). Gross alteration of subnuclear organization (Nickerson and Penman, 1992b; Hendzel et al., 1997; Wagner et al., 1986; Capco and Penman, 1983; Fan and Penman, 1971) and re-localization of regulatory complexes occur concomitant with transcriptional silencing during mitosis (Buendia et al., 2001; Johansen, 1996; Gottesfeld and Forbes, 1997). A fundamental question therefore is how cells restore subnuclear distribution of tissue specific transcription factors in progeny cells to regulate post-mitotic phenotypic gene transcription.

Runx (Cbfa/AML) proteins are tissue-specific transcription factors that control hematopoietic and osteogenic lineage commitment [reviewed in (Lund and van Lohuizen, 2002)]. Runx factors bind to DNA in a sequence specific manner, are targeted to

transcriptionally active subnuclear foci, and are required for maintenance of chromatin architecture of target genes in the interphase nucleus (Ogawa et al., 1993; Zeng et al., 1997; Zeng et al., 1998; Javed et al., 1999; Zaidi et al., 2001a; Harrington et al., 2002). Perturbed subnuclear organization and/or altered physiological levels of Runx proteins are associated with genetic disorders and tumorigenesis (Otto et al., 1997; Zhang et al., 2000a; McNeil et al., 1999; Choi et al., 2001; Telfer and Rothenberg, 2001). Runx protein levels persist through the proliferation of lineage-committed cells (Pratap et al., 2003).

While the rules that govern mitotic chromosome segregation are longstanding (Nasmyth, 2002), only a limited number of studies have addressed redistribution of regulatory proteins during mitosis (Mancini et al., 1994; Nickerson and Penman, 1992a; Reyes et al., 1997; Berube et al., 2000; Tang and Lane, 1999). By the combined use of *in situ* immunofluorescence microscopy and image quantitation, here we have documented progressive mitotic changes in the distribution of Runx foci and sequential re-organization of nuclear proteins involved in gene expression. The interphase subnuclear organization of Runx foci is selectively restored in telophase with equal partitioning of the protein into progeny nuclei. Thus we have shown a dynamic spatial distribution of Runx transcription factors in parallel with chromosomal partitioning to sustain balanced expression of phenotypic genes post-mitotically.

MATERIALS AND METHODS

Cell Culture and Cell Synchronization.

Hematopoietic (Jurkat lymphoma) and osteogenic (Rat osteosarcoma ROS 17/2.8) cells were maintained in F12 medium containing 5% fetal bovine serum (Gibco Life Technology, Grand Island, NY) and RPMI medium supplemented with 10% fetal bovine serum, respectively. ROS 17/2.8 cells were synchronized in early S phase by double thymidine block as described elsewhere (Stein et al., 1998) and subjected to *in situ* immunofluorescence analyses.

In Situ Immunofluorescence Microscopy.

Synchronized cells, grown on gelatin-coated coverslips, were processed for *in situ* immunofluorescence as described (Javed et al., 2000). In brief, cells were rinsed twice with ice-cold PBS and fixed in 3.7% formaldehyde in PBS for 10 minutes on ice. After rinsing once with PBS, the cells were permeabilized in 0.1% Triton X-100 in PBS, and rinsed twice with PBSA (0.5% bovine serum albumin [BSA] in PBS) followed by antibody staining. Antibodies and their dilutions used are as follows: rabbit polyclonal antibodies against Runx2 (1:200; Oncogene, Carlsbad, CA), rabbit polyclonal antibody raised against Runx1 (1:25, Geneka Biotechnology Inc., Montréal, Québec, Canada), tetra-acetylated-histone H4 (1:400, 06-866 Upstate Biotechnology, Waltham, MA), p300 (1:400, Santa Cruz Biotechnology, Carlsbad, CA) and a mouse monoclonal antibody against SC35 (1:200, Sigma-Aldrich, St. Louis, MO). The secondary antibodies used were either anti mouse Alexa 568 or anti rabbit Alexa 488 (1:800, Molecular Probes,

Eugene, OR). DNA was visualized by DAPI (4', 6-diamidino-2-phenylindole) staining. Immunostaining of cell preparations was recorded using an epifluorescence Zeiss Axioplan 2 (Zeiss Inc., Thorwood, NY) microscope attached to a CCD camera.

Exponentially growing Jurkat cells ($6X10^4$) were cytospun directly onto slides coated with Cell-Tak™ (BD Biosciences, Lexington, KY) and were then subjected to *in situ* immunofluorescence analysis as described above.

Quantitative Image Analysis.

We quantitated the relative DNA and protein distribution (mitotic partitioning) in each progeny nucleus. The amount of protein and DNA in each nucleus was measured using image pixel intensities. The relative protein or DNA distribution between progeny nuclei (the partition coefficient, PC) was then expressed as the ratio of nuclear signal intensity ($PC= I_1/I_2$,where I_1 and I_2 are integrated pixel intensities of each of the progeny nuclei, *i.e.*, total protein or DNA amount per nucleus; the designation of nucleus 1 versus nucleus 2 was randomly assigned.

We characterized Runx foci in G2 and telophase nuclei in terms of size, number and spatial organization. This analysis was carried out in three steps: image deconvolution, determination of the pixel intensity threshold, and image binarization. First, image deconvolution was accomplished by an unsharp mask algorithm. Pixel intensity for image thresholding was defined as the intranuclear pixel intensity level that maximizes the number of detectable foci. In our quantitative analysis, the image binarization is performed by assigning the value of '1' to pixels with grayscale values

higher than threshold; all other pixels are assigned the value of '0'. Quantitation of nuclear foci from the binary image included determining the number (connected components), the size in pixels (1 pixel = 0.028 μm^2) and the location of each of the foci (centroid image coordinates). The spatial organization of intranuclear foci is expressed as the coefficient of variation (CV) of nearest neighbor distances. For this purpose, the Euclidean nearest neighbor distance was determined for each focal point using the centroid coordinates. The mean (M) and standard deviation (SD) of foci nearest neighbor distances within a single nucleus were determined and used to compute the coefficient of variation (CV), where CV=SD/M. The image analysis was performed using the MATLAB® image processing toolbox (The Mathworks Inc., Natick, MA) and Metamorph Imaging Software (Universal Imaging Corp., Downingtown, PA).

Scatter plots were generated to illustrate the coincidence of pixel intensities between Runx and DNA images; each data point represents a corresponding pixel in the Runx and DNA images. The y-axis value reflects the pixel intensity from the Runx image whereas the x-axis reflects the pixel intensity from the DNA image. Data points above the red line are pixels that correspond to Runx foci. Intensity profiles for Runx and DNA images were generated using Metamorph Imaging Software, in which a pseudo-color map is applied to pixel intensities, i.e., red=255, blue=0.

Statistical Analysis

Statistical computations were performed in SAS® (The SAS Institute Inc., Cary, NC). Two-tail paired Student's t-test was used to compare differences between mean

DNA and Runx mitotic partition coefficients. In order to measure intracellular co-localization between proteins and DNA, the image cross-correlation analysis was employed using Pearson's coefficient (van Steensel et al., 1995). Analysis of variance (ANOVA) and Tukey's multiple comparison test (α=0.05) were performed to assess the significance of observed differences for protein (Runx2, H4, SC35 and p300)-DNA (DAPI) image correlations between mitotic phases, as well as for number of foci, average size of foci, and spatial distribution between telophase and interphase nuclei. Differences were considered statistically significant if p-value was less than 0.05.

RESULTS

Osteogenic and hematopoietic Runx proteins partition equally into progeny cells.

Runx transcription factors are required for lineage commitment and retention of phenotype (Speck et al., 1999; Westendorf and Hiebert, 1999). Stringent transcriptional and translational regulation of Runx proteins indicates that the maintenance of Runx cellular levels is critical for their biological activity. Temporal expression and regulation of Runx factors are documented during development and lineage commitment. We find that Runx protein levels remain constant during and following cell division (data not shown). To assess the cellular organization of the Runx regulatory proteins during mitosis, we examined hematopoietic Jurkat lymphoma and osteoblastic ROS 17/2.8 cells. These cells express Runx1 and Runx2, respectively, as well as Runx responsive phenotypic genes (Rodan, 1995; Speck et al., 1999; Westendorf and Hiebert, 1999). In addition, Runx1 and Runx2 in these cells exhibit characteristic punctate subnuclear distribution during interphase (Figure 4.1, top panels). We analyzed Runx proteins in telophase by *in situ* immunofluorescence microscopy. As shown in Figure 4.1 (bottom panels), Runx1 and Runx2 are present in both telophase nuclei. We next assessed the relative distribution of Runx proteins in progeny nuclei by measuring the ratio of the integrated pixel intensity between post-mitotic progeny nuclei. We find that both Runx proteins are equivalently distributed between progeny nuclei. Equal segregation of DNA, as assessed by DAPI staining, serves as a biological frame of reference and supports our conclusion that both Runx proteins are equivalently partitioned to progeny nuclei during mitosis.

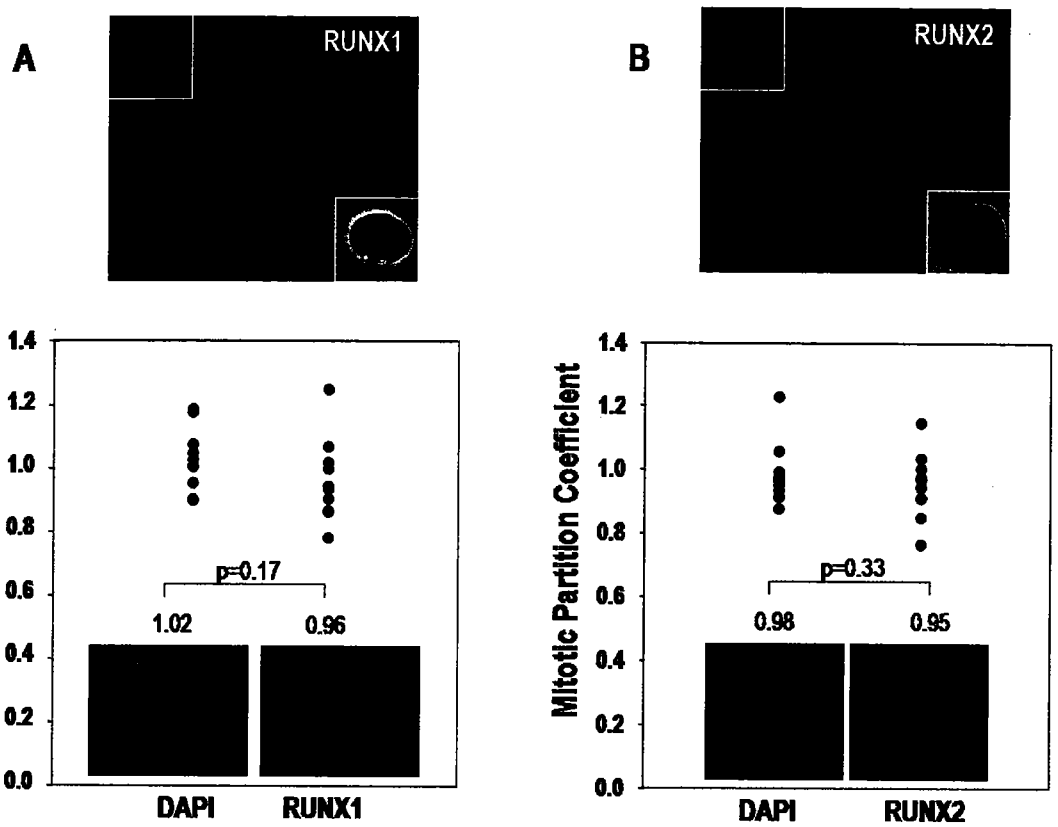

Figure 4.1: Runx proteins partition equivalently in progeny cells following cell division. Jurkat lymphoma cells (A) or ROS 17/2.8 osteosarcoma cells (B) were subjected to *in situ* immunofluorescence microscopy. Runx1 and Runx2 were detected by rabbit polyclonal antibodies followed by the incubation of cells with secondary antibodies conjugated with Alexa 488 flourochrome. Both Runx1 and Runx2 were distributed at punctate subnuclear foci throughout the interphase nucleus (top panels). A quantitative image analysis was applied to determine the relative levels of Runx in nuclei of the telophase cells (n=10; bottom panels). We defined a partition coefficient (PC) that reflects the ratio of integrated signal intensities between progeny nuclei. Both Runx proteins exhibited a partition coefficient equivalent to that of DNA demonstrating that these factors are equally segregated in progeny cells following cell division. Student's t-test was performed to assess significance of observed differences.

Runx proteins undergo dynamic alterations in distribution during mitosis and a subset of Runx foci remains associated with chromosomes.

Runx proteins persist throughout mitosis and are equally partitioned in telophase (Figure 4.1 and data not shown). We therefore examined the subcellular localization of Runx during successive mitotic stages by in situ immunofluorescence microscopy. Our results show that Runx proteins are distributed as punctate foci during all stages of mitosis (Figure 4.2, see insets). Concomitant with alterations in nuclear structure during mitosis, a sequential change in the distribution of Runx proteins is observed (see for example Figure 4.2). In contrast to interphase, these foci are no longer completely colocalized with chromosomes during prophase. As mitosis progresses through metaphase and anaphase, Runx foci predominantly exhibit an extra-chromosomal localization. During the anaphase to telophase transition Runx foci are redistributed, co-localizing with DNA at telophase (Figure 4.2). Interestingly, both microscopic observations (Figures 4.2 and 4.3) and image quantitation (Figure 4.3) show a subset of Runx foci associated with chromosomes throughout mitosis. We observe similar spatio-temporal redistribution of Runx foci during mitosis of normal diploid cells (data not shown). Specificity of the mitotic localization and chromosomal association of tissue specific Runx proteins is further indicated by displacement of sequence specific transcription factors (that include Oct1, cFos, SP1, AP2, HSF, etc) from the chromosomes (Martinez-Balbas et al., 1995). Thus Runx proteins are organized as punctate foci throughout mitosis and these foci are dynamically redistributed during mitotic progression, with consequent equal partitioning of the protein in progeny cells.

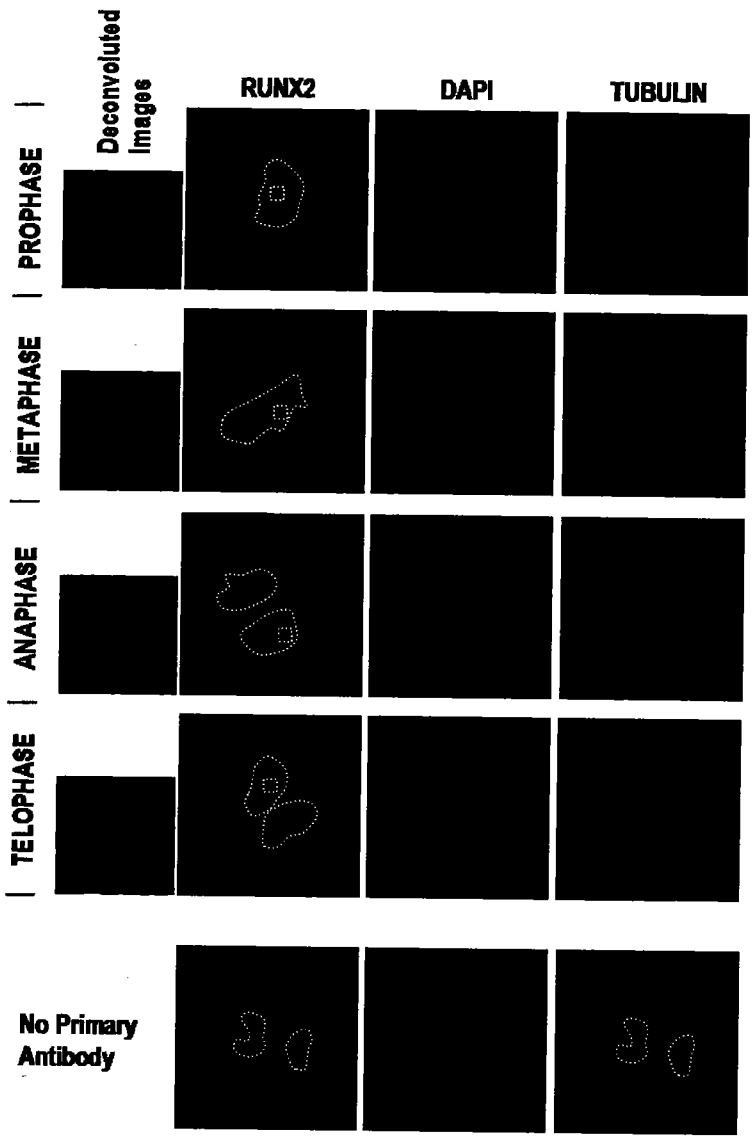

Figure 4.2: Runx foci dynamically redistribute during mitosis.
Endogenous Runx2 and tubulin were visualized by *in situ* immunofluorescence in synchronized ROS 17/2.8 cells at indicated stages of mitosis. Runx2 foci shown in deconvoluted images (marked by white boxes) in the left panel are distributed throughout the cell in prophase. This distribution of Runx2 foci changes to predominantly extra-chromosomal in metaphase and anaphase. In telophase, Runx2 foci appear to colocalize with DNA. Tubulin shows characteristic staining throughout mitosis and serves as a marker to identify mitotic stages. The DNA boundaries from DAPI images are drawn as white dotted lines. Specificity is demonstrated by in situ preparations in which the primary antibody incubation was omitted (bottom panel).

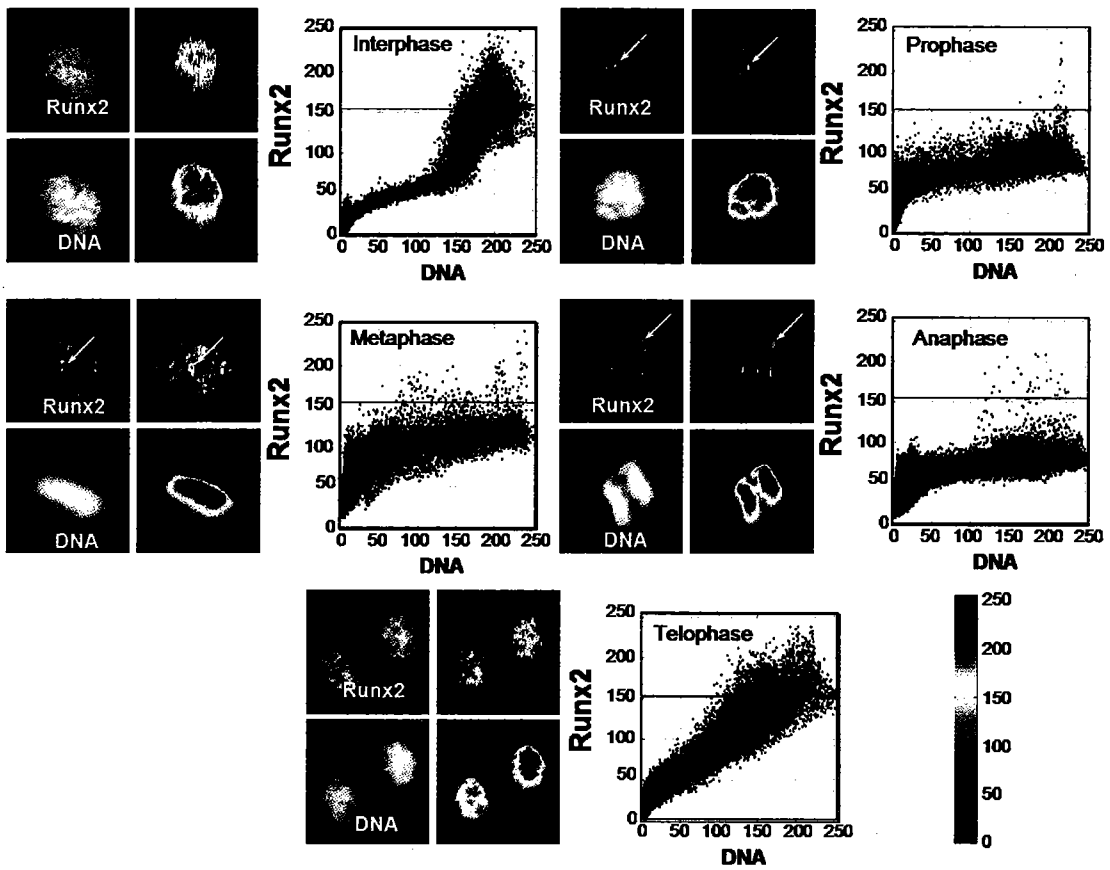

Figure 4.3: A subset of Runx2 foci associate with chromosomes throughout mitosis.
Images showing mitotic redistribution of Runx2 foci were subjected to quantitative image analysis. Intensity profiles (middle panel in each mitotic stage) of images shown on the left were generated using MetaMorph Imaging software. A scatter plot between the signal intensities of Runx2 (y-axis) and DNA (x-axis) indicates that Runx2 is associated with DNA in interphase and telophase while this association decreases during prophase-metaphase and anaphase. A subset of Runx2 foci (indicated by arrows) is associated with chromosomes during all stages of mitosis. The red line demarcates the level above which all pixels correspond to Runx foci. The bar at the bottom right represents the pseudocolor map for image intensity.

Post-mitotic restoration of Runx subnuclear distribution.

The organization of Runx proteins at subnuclear foci has been linked to transcriptional control (Stein et al., 2000b; Stein et al., 2000c). Hence, we determined the extent to which the punctate organization of Runx foci is restored in telophase nuclei. Runx2 was detected by *in situ* immunofluorescence microscopy. Using a quantitative approach the number and size as well as the spatial organization of subnuclear foci were assessed (Figure 4.4). We detect equal numbers of Runx2 foci in each of the telophase progeny nuclei, and this value is half the number of foci present in G2 (Figure 4.4A). These results are consistent with an equal mitotic partitioning of Runx proteins (Figure 4.1). Size and spatial organization of Runx2 foci in telophase nuclei remain equivalent to those in G2 nuclei (Figure 4.4A). It is well established that SC35 subnuclear speckles are associated with RNA processing [reviewed in (Shopland and Lawrence, 2000)]. Therefore, we assessed the parameters of subnuclear organization (i.e., number, size and spatial organization) for SC35. As shown in Figure 4.4B, we do not detect difference in foci number for SC35; yet these foci are significantly smaller in telophase than G2 nuclei and exhibit a different spatial organization. Thus, although it has been reported that splicing activity is detectable at this time, the interphase SC35 is not completely restored in telophase (Prasanth et al., 2003). Taken together, these findings demonstrate an equivalent partitioning of Runx2 foci into progeny nuclei with selective restoration of Runx2 subnuclear organization.

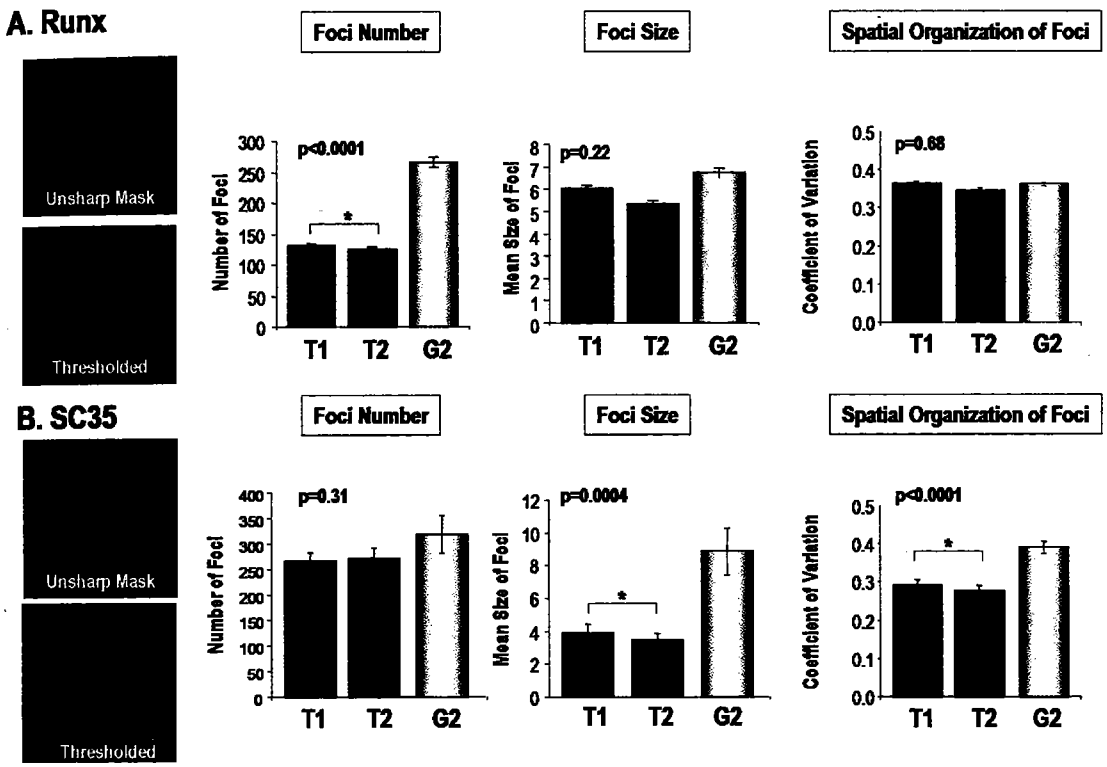

Figure 4.4: Runx2 foci are equally segregated to progeny nuclei with restoration of subnuclear organization during telophase.

We performed a quantitative image analysis on telophase and G2 nuclei to assess the number and size of Runx2 domains in parent and progeny cells. The analysis was carried out by image deconvolution (A, left panel for detail see Materials and Methods) followed by image thresholding and binarization to define Runx2 domains (A, right panel). The domain number (B), size (C) and spatial organization (D) were then calculated in each of the telophase (designated as T1 and T2) and G2 nuclei analyzed and mean values were displayed as bar graphs (n=10, nuclei). Asterisks indicate statistically significant differences between G2 and telophase nuclei. The error bars represent standard error of the mean (S.E.M.). We find double the number of Runx2 domains in G2 nuclei compared with telophase nuclei, while the domain size and spatial distribution remain the same. Conversely, we find equal number of SC35 foci, but these foci are smaller and exhibit a different spatial distribution than G2 nuclei.

Sequential redistribution of nuclear proteins involved in gene expression during cell division.

We assessed the sequential reorganization of Runx2 during mitosis relative to other nuclear proteins that are involved in transcription and RNA processing. We first examined the distribution of Runx co-regulatory protein p300 during cell division. In the interphase nucleus, p300 exhibits a punctate distribution and partially colocalizes with Runx2 (data not shown). During metaphase and anaphase, p300 foci, unlike Runx2, remain predominantly localized with the chromosomes (Figure 4.5A). The interphase subnuclear localization of p300 is restored in telophase as chromosomes de-condense. The extent that p300 is chromosomally associated may in part be cell type or reagent dependent (Kruhlak et al., 2001). As expected, the nucleosomal protein histone H4 remains tightly associated with chromosomes throughout mitosis (Figure 4.5B). In contrast, the SC35 RNA processing factor is not localized with chromosomes during mitosis (Figure 4.5A). These results show that a sequential re-organization of Runx2 and its co-regulatory protein p300 in progeny nuclei precedes reappearance of SC35 RNA processing speckles.

The extent to which each of these regulatory factors exhibits a spatio-temporal relationship with DNA during mitosis was quantitated using image cross-correlation analysis [(van Steensel et al., 1995), Figure 4.6]. Consistent with our microscopic observations (Figures 4.2 and 4.5), p300 and histone H4 show high correlation with DNA throughout mitosis. By comparison, Runx2 and DNA are highly co-localized only during

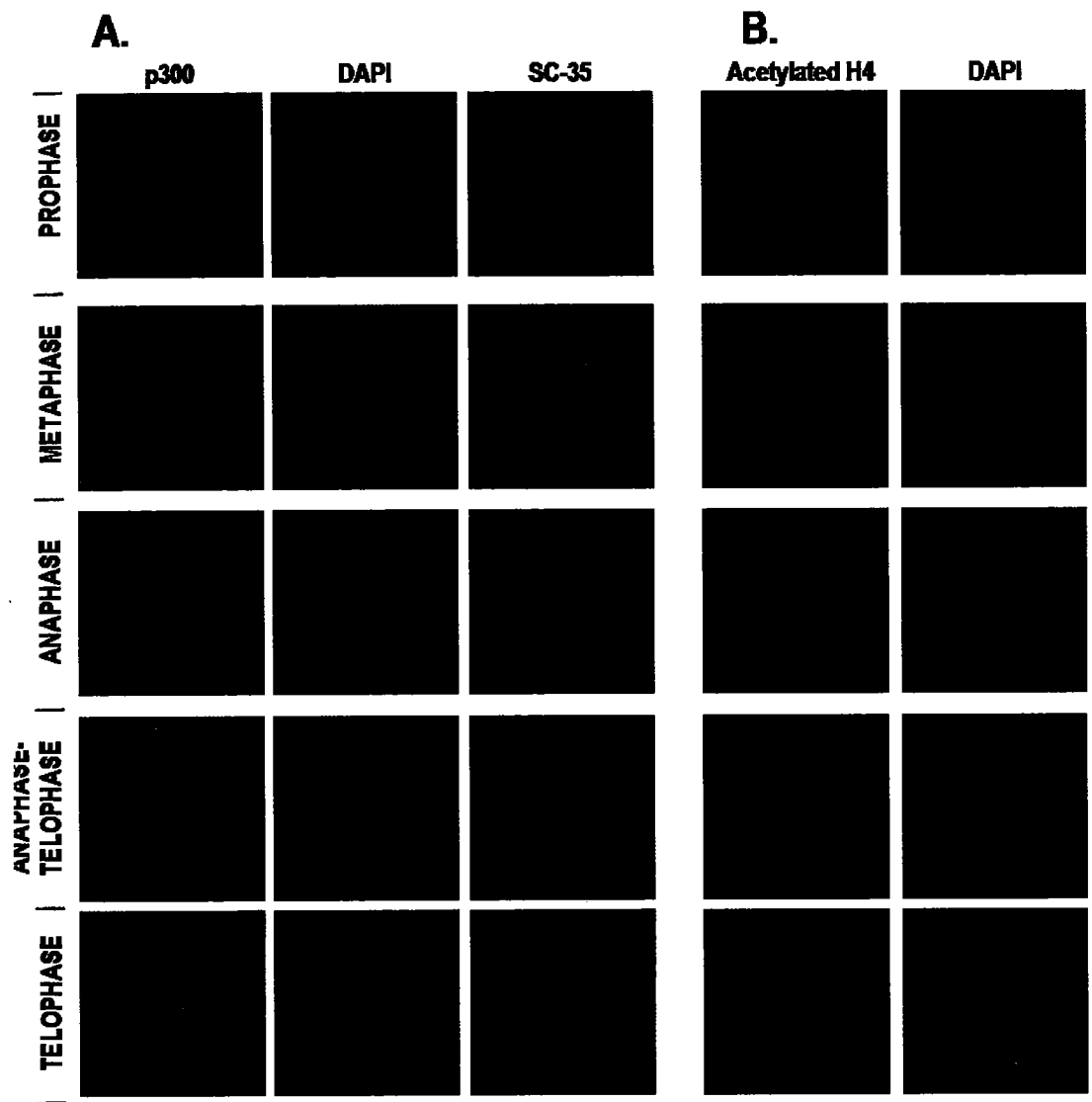

Figure 4.5: Chromatin modifying factor p300 and nucleosomal protein histone H4, but not RNA processing factor SC35, show colocalization with DNA during mitotic progression. Chromatin modifying factor p300 (A, left panel), RNA processing protein SC35 (A, middle panel) and tetra-acetylated histone H4 (B) were detected by *in situ* immunofluorescence in synchronized ROS 17/2.8 cells at indicated stages of mitosis. Histone H4 and p300 show a constitutive DNA localization throughout mitosis while SC35 is excluded from DNA.

interphase and telophase, as reflected by maximal correlation coefficient. The Runx2-DNA correlation gradually decreases in prophase and metaphase and increases in anaphase (Figure 4.6). In contrast, SC35 and DNA are weakly correlated during mitosis (Figure 4.6). Taken together, these findings demonstrate a sequential and selective reorganization of transcriptional regulators and RNA processing factors during progression of cell division.

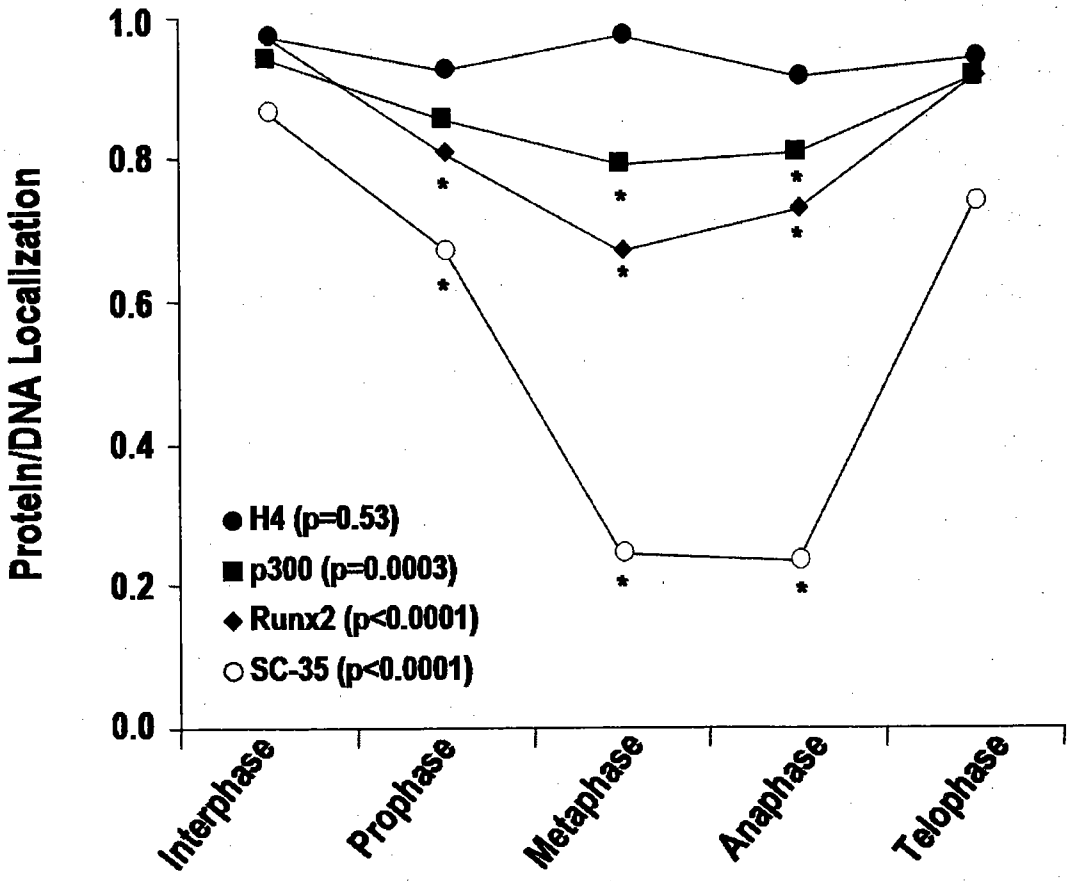

Figure 4.6: Sequential redistribution of nuclear proteins involved in RNA synthesis and processing following cell division.

The relationship between DNA and different nuclear proteins during mitosis was confirmed by Pearson correlation analysis. The correlation between images intensities reflects the colocalization of different nuclear proteins with DNA during mitotic progression. While histone H4 and p300 are colocalized to DNA throughout mitosis, SC 35 is excluded. Runx2, in comparison, shows a gradual decrease in chromosomal localization until cells enter anaphase. In telophase, Runx2 exhibits a restoration of interphase subnuclear distribution. Astericks indicates correlations which are significantly different from interphase.

CONCLUSION

Runx transcription factors provide a model for characterizing the distribution of regulatory proteins to progeny cells during mitosis. Runx proteins are distributed as transcriptionally active subnuclear foci throughout the interphase nucleus that support Runx dependent integration of regulatory signals e.g., BMP and Src signals (Harrington et al., 2002; Zaidi et al., 2002a; Zaidi et al., 2001b). In this study, we have demonstrated that Runx foci persist throughout mitosis and undergo a spatio-temporal redistribution that results in equal partitioning of the protein into each of the progeny nuclei. Loss of both amount and subnuclear organization of Runx proteins is associated with genetic disorders (Choi et al., 2001; Zhang et al., 2000a; McNeil et al., 1999). Equal partitioning and a complete restoration of subnuclear organization of Runx foci in telophase provides a mechanism for maintenance of cellular levels and activity of Runx proteins following mitosis. These findings are consistent with a requirement of Runx factors for post-mitotic transcriptional control and assembly of multi-component complexes to regulate Runx responsive genes. Furthermore, subnuclear organization of Runx foci precedes that of SC35 RNA processing speckles following cell division. Taken together, these findings demonstrate a spatio-temporal partitioning and reorganization of regulatory factors that render progeny cells equivalently competent for the resumption of tissue specific gene expression.

CHAPTER V:

Mitotic Retention of Phenotype by the Cell Fate Determining Transcription Factor Runx2

ABSTRACT

During cell division cessation of transcription is coupled with mitotic chromosome condensation. A fundamental biological question is how gene expression patterns are retained during mitosis to ensure the phenotype of progeny cells. We suggest that cell fate determining transcription factors provide an epigenetic mechanism for the retention of gene expression patterns during cell division. Runx proteins are lineage-specific transcription factors that are essential for hematopoietic, neuronal, gastrointestinal, and osteogenic cell fates. Here we show that Runx2 protein is stable during cell division and remains associated with chromosomes during mitosis through sequence-specific DNA binding. Using siRNA mediated silencing, mitotic cell synchronization, and expression profiling, we identify Runx2 regulated genes that are modulated post-mitotically. Novel target genes involved in cell growth and differentiation were validated by chromatin immunoprecipitation. Importantly, we find that during mitosis, when transcription is shut-down, Runx2 selectively occupies target gene promoters to control mitotic histone modifications. We conclude that Runx proteins have an active role in retaining phenotype during cell division to support lineage-specific control of gene expression in progeny cells.

INTRODUCTION

Lineage commitment and cell proliferation are critical for normal tissue development. Preservation of phenotype during clonal expansion of committed cells necessitates the faithful segregation of chromosomes and the conveyance of lineage-specific gene regulatory machinery to progeny cells. Mitosis involves nuclear reorganization, global chromosome condensation and transcription silencing, and occurs concomitant with protein degradation and/or displacement of many regulatory factors from chromosomes (Gottesfeld and Forbes, 1997; Martinez-Balbas et al., 1995; Muchardt et al., 1996; Prasanth et al., 2003). One fundamental question is how cells are programmed to sustain phenotypic gene expression patterns following cell division when transcriptional competency is restored in progeny cells.

Cell fate is determined in response to extracellular cues by lineage-specific master regulators that include the Runx family of transcription factors. In mammals, these proteins are required for development of hematopoietic (Runx1), osteogenic (Runx2), gastrointestinal and neuronal (Runx3) cell lineages (Choi et al., 2001; Komori et al., 1997; Wang et al., 1996a; Inoue et al., 2002; Li et al., 2002; Westendorf and Hiebert, 1999; Blyth et al., 2005). Runx factors integrate cell signaling pathways (e.g., TGF-Beta/BMP and Yes/Src) and recruit chromatin modifying enzymes (e.g., HDACs, HATs, SWI/SNF, SuVar139) to modulate promoter accessibility within a nucleosomal context (Zaidi et al., 2001a; Zaidi et al., 2003; Taniuchi and Littman, 2004; Vradii et al., 2005; Young et al., 2005; Sierra et al., 2003b; Westendorf and Hiebert, 1999). Runx proteins function as promoter bound scaffolds that organize the regulatory machinery for gene

expression within punctate subnuclear domains (Zaidi et al., 2005; Young et al., 2004). Pathological perturbations in the organization of these domains are linked with altered development and tumorigenesis (Westendorf and Hiebert, 1999; Javed et al., 2005; Barnes et al., 2003; Barnes et al., 2004; Blyth et al., 2001; Brubaker et al., 2003; Cameron and Neil, 2004; Ito, 2004; Neil et al., 1999; Vaillant et al., 1999; Otto et al., 2002; Ito, 2004). Temporal and spatial changes of these architecturally organized Runx domains occur during mitosis (Zaidi et al., 2003).

Osteogenic cell fate decisions and subsequent proliferation of osteoprogenitor cells is controlled by Runx2 (Afzal et al., 2005; Galindo et al., 2005; Lian et al., 2004; Pratap et al., 2004; Westendorf and Hiebert, 1999). A mechanism must be operative that ensures Runx2 dependent regulation of this osteogenic identity through multiple mitotic cell divisions. Here we have combined mitotic cell synchronization, expression profiling, chromatin immunoprecipitation, and RNA interference to investigate this mechanism. During mitosis Runx2 directly interacts with a novel set of cell fate and cell cycle related target genes that exhibit distinct Runx2 dependent modifications in histone acetylation and methylation. Our results indicate that Runx transcription factors reinforce cell fate through an epigenetic mechanism that retains phenotypic gene expression patterns following cell division.

MATERIALS AND METHODS

Cell Culture and Cell Synchronization.

Saos-2 osteosarcoma cells were maintained in McCoy's medium containing 15% fetal bovine serum (FBS) (Gibco Life Technology, Grand Island, NY) plus 2mM L-glutamine and a penicillin-streptomycin cocktail. Hela cells were maintained in DMEM plus 2mM L-glutamine penicillin-streptomycin cocktail. Ros cells were maintained in F12 plus 2mM L-glutamine penicillin streptomycin cocktail with 5% FBS. Cells were blocked in mitosis for biochemical fractionation and chromatin immunoprecipitation assays by adding 200ng/ml nocodazole for 24 hrs followed by shake-off of mitotic cells. For Block-release studies Saos-2 cells were synchronized by the addition of 200ng/ml of nocodazole for 24hrs. Cells were released by two washes in serum-free media followed by the addition of McCoy's medium containing 15% fetal bovine serum plus 2mM L-glutamine. Cell cycle analysis was performed by propidium iodide-stained cells subjected to fluorescence-activated cell sorting (FACS, UMass Medical Core Facility).

Expression Constructs

The following constructs have been previously reported: HA-Runx2 and Xpress-Runx2 (Zaidi et al., 2001a). The R166Q mutant of Runx2 was generated by PCR-based site-directed mutagenesis of the HA-Runx2 construct using the QuikChange ® Site-Directed Mutagenesis Kit. (Statagene, Cedar Creek, TX). The following primers where utilized for mutagenesis: Forward 5'-GAG ATT TGT GGG CCA GAG CGG ACG AGG-3' and reverse 5'-CCT CGT CCG CTC TGG CCC ACA AAT CTC-3'. Mutations were

confirmed by sequencing with the following primer: 5'-ATG CGC CCT AAA TCA CTG AG-3'

Electrophoretic Mobility Shift Assay

The upper strands (200 ng) of oligonucleotides including a Runx binding sequence were labeled with ^{32}P for 1 h at 37°C in a 50-µl volume using T4 Polynucleotide Kinase (New England BioLabs, Beverly, Mass.) as indicated by the manufacturer. The reaction was stopped by heat inactivation at 65°C for 1 h. Annealing was performed by addition of a twofold excess amount of bottom strand followed by boiling for 5 min and slow cooling to room temperature. The unincorporated nucleotides were removed using a quick-spin G 25 Sephadex column (Roche Molecular Biochemicals, Indianapolis, Ind.) according to the manufacturer's instructions. Electrophoretic mobility shift assay (EMSA) reaction mixtures were prepared using 50 fmol of probe, 50 mM KCl, 12 mM HEPES, 1 mM EDTA, 1 mM dithiothreitol, 12% glycerol, 2 µg of poly(dI-dC) · poly(dI-dC) and 0 to 4ul of IVTT protein extract protein using HA-Runx2 (R166Q) or wild-type HA-Runx2. Aliquots were loaded onto a 4% nondenaturing polyacrylamide gel. The gels were electrophoresed for 1.5 h at 200 V, dried, and exposed to film for autoradiography.

***In Situ* Immunofluorescence Microscopy.**

Saos-2 and Hela cells grown on gelatin-coated coverslips, were processed for *in situ* immunofluorescence using standard techniques. In brief, cells were rinsed twice with ice-cold PBS and fixed in 3.7% formaldehyde in PBS for 10 minutes on ice. After rinsing

once with PBS, the cells were permeabilized in 0.1% Triton X-100 in PBS, and rinsed twice with PBSA (0.5% bovine serum albumin [BSA] in PBS) followed by antibody staining. Antibodies and their dilutions used are as follows: rabbit polyclonal antibodies against Runx2 (1:200; M-70 Santa Cruz Biotechnology, Carlsbad, CA), rabbit polyclonal antibody raised against the HA-epitope (1:400; M-70 Santa Cruz Biotechnology, Carlsbad, CA), and mouse monoclonal raised against the Xpress-epitope (1:400; M-70 Invitrogen). The secondary antibodies used were either anti mouse Alexa 594 or anti rabbit Alexa 488 (1:800, Molecular Probes, Eugene, OR). DNA was visualized by DAPI (4', 6-diamidino-2-phenylindole) staining. Immunostaining of cell preparations was recorded using an epifluorescence Zeiss Axioplan 2 (Zeiss Inc., Thorwood, NY) microscope attached to a CCD camera.

siRNA Knockdown Experiments

Saos-2 cells at 30 to 50% confluency were transfected using Oligofectamine (Invitrogen Life Technologies) with small interfering RNA (siRNA) duplexes specific for human Runx2 obtained from (QIAGEN Inc. Stanford, Calif.). For gene profiling and histone modification studies oligos were utilized at 50nM and 25nM, respectively. The siRNA duplexes were r(GGUUCAACGAUCUGAGAUU)d(TT). The cells were also transfected with control siRNA duplexes specific for green fluorescent protein (GFP) or non-silencing siRNA (QIAGEN Inc.) using the same concentrations and vehicle alone as a control. Opti-MEM (a reduced serum medium from Invitrogen) was used to dilute the siRNA duplexes and Oligofectamine and for transfection. After treating the cells with

siRNA for 4 h, the cells were supplemented with McCoy's containing 45% FBS for a final concentration of 15% in the medium. The gene profiling siRNA experiment was carried out for 72 h, at which time the cells were harvested for total protein and RNA to analyze the knock-down effect of Runx2 siRNA on endogenous Runx2. For histone modification studies cells were treated with siRNA for 48 hrs, incubated for an additional 24hrs in the presence of the microtubule destabilizing agent Nocodazole (100ng/ml, Sigma-Aldrich), followed by shake-off to obtain mitotic cells; parallel plates were incubated with siRNA oligos for 72 hours without nocodazole treatment to obtain asynchronous cells.

Gene Expression Profiling

Gene expression profiling was performed using the osteogenic and cell cycle focused cDNA arrays according to the manufacturers GEArray™ instructions (SuperArray Bioscience Corporation, Frederick, MD). Briefly, total RNA was isolated from Saos-2 cells at the indicated time points for cell synchronization experiments and at 72 hours for the indicated treatments for siRNA experiments using Trizol reagent (Invitrogen, Carlsbad, CA). cDNA was generated from purified RNA using a reverse transcription reaction (Invitrogen Corporation, Carlsbad, CA) with primers provided with GEArray™ kits and P^{32}-α-dCTP. Radioactive reverse transcription cDNA products were directed hybridized to cDNA arrays for 16hrs at 60^{0C}, washed one with 1% Sodium-Dodecyl sulfate (SDS) and 2x Sodium Chloride-Sodium Citrate (SSC) pH 7.0 with rotation at 20rpm at 60^{0C} for 15 minutes, and once with 0.5% SDS and 0.1x SSC pH 7.0 with

rotation at 20rpm at 60^{0C} for 15 minutes. Arrays were exposed to BioMax film (Kodak) for 48hrs and digitized for quantitation. Digital images of gene arrays were quantified using ImageQuant TL software (GE Healthcare). Signals were background corrected and normalized to the average of four cyclophilin A cDNA spots. Exploratory analysis of gene expression patterns were performed using hierarchical cluster analysis of row-wise standardized data using dCHIP software (Li and Wong, 2001).

Chromatin Immunoprecipitation

Chromatin immunoprecipitation assays (ChIPs) were performed essentially as described (Hovhannisyan et al., 2003). Briefly, asynchronously growing or mitotic cells were crosslinked in DMEM with 1% Formaldehyde for 10 minutes. Crosslinking reaction was quenched by the addition of glycine at a final concentration of 250mM for 10minutes. Cells were scraped, pelleted and washed twice with PBS. Cell pellets were resuspended in 2.5ml of lysis buffer (150mM NaCl, 50mM Tris-HCl pH 8.0, 1% NP-40, 25uM MG-132, and 1X Complete® Protease inhibitor cocktail (Roche). After 10 minutes on ice cells were sonicated to a DNA fragment size of 500-1000 bp as determined by Agarose gel eletrophoresis with ethidium bromide staining. Cell debris was pre-clear by centrifugation at 15000rpm for 20minutes. Supernatant containing protein-DNA complexes was aliquoted into three tubes (1ml per antibody and 500ul for input DNA) were incubated for 16hours with 3ug Rabbit polyclonal antibody directed against Runx2 (M-70, Santa Cruz Biotechnology) and 3ug of Normal Rabbit IgG (Santa Cruz Biotechnology) or 4ul of Rabbit polyclonal antibodies directed against hyperacetylated

Histone H4 or dimethyl-K4 Histone H3 (#06-946 and #07-030, respectively Upstate Biotechnology) followed by 1hour with 50ul of Protein A/G conjugated Agarose beads. Protein A/G bead complexes were washed with the following buffers: low salt (20 mM Tris-Cl pH 8.1, 150 mM NaCl, 1% Triton X-100, 2 mM EDTA, 1X complete protease inhibitor), high salt (20 mM Tris-Cl pH 8.1, 500 mM NaCl, 1% Triton X-100, 2 mM EDTA), LiCl (10 mM Tris-Cl pH 8.1, 250 mM LiCl, 1% deoxycholate, 1% NP-40, 1mM EDTA) and twice in TE (10 mM Tris-Cl pH 8.1, 1 mM EDTA). Protein-DNA complexes were eluted in 1% SDS, 100 mM $NaHCO_3$. Crosslinks were reversed by incubation for 16hours in elution buffer and 300mM Sodium Acetate pH5.2. DNA was extracted, purified, precipitated and resuspended in TE for qPCR. ChIP enrichment was determined as a quantitative measure reflecting the percentage of input. Runx2 target gene ChIP data were normalized to the non-specific PHOX gene.

Western Blot Analysis:

Western blot analysis was performed as described previously in (Galindo et al., 2005). Briefly, amounts of total cellular protein were resolved in 8 or 10% SDS-PAGE and transferred to polyvinylidene difluoride membranes (Immobilon-P; Millipore Corp., Bedford, MA). Blots were incubated with a 1:2,000 dilution of each primary antibody for 1 hour. Mouse monoclonal antibodies specific for Lamin B1 (1:2000, Zymed Laboratories, Inc., San Francisco, CA) and Runx2 (Zhang et al., 2000a) were used. In addition, Rabbit polyclonal antibody against Histone H4 (1:1000) and Phospho-Ser10 Histone H3 were obtained from Upstate Biotechnology. Membranes were then

incubated with horseradish peroxidase conjugated secondary protein bands were visualized by a chemiluminescence detection kit (Perkin Elmer Life Sciences, Boston, MA).

RNA Analysis:

Total RNA was isolated from cells at the indicated time points using Trizol reagent (Invitrogen, Carlsbad, CA). Total RNA was purified using the DNA-Free RNA kit (Zymo Research Corporation, Orange CA). cDNA was generated from purified RNA using a reverse transcription reaction with random hexamer primers (Invitrogen Corporation, Carlsbad, CA). cDNA was then subjected to Real-Time PCR reaction using SYBR chemistry (Applied Biosystems, Inc., Foster City, CA). Primers used are shown in Supplementary Data. All primers for gene validation studies span exons which are contained in all known transcripts.

Statistical Analysis:

Analysis of variance (ANOVA) was carried out to assess the significance of Runx2 knockdown on histone modifications at target gene promoters. Data were obtained from duplicate ChIP assays using hyperacetylated Histone H4 and dimethylated-K4 Histone H3 antibodies from asynchronous and mitotic cells. qPCR measurements were made in duplicate for each of fourteen target genes and expressed as percentage input chromatin. A mixed models analysis was performed on log-transformed ChIP data using SAS/Analyst (Sas Institute Inc.,) with genes (14), antibodies (2), and cell cycle stage (2)

incorporated as fixed effects and qPCR well position as a random effect. Separate mixed models that were grouped by cell cycle stage were also analyzed. Multiple comparisons using Tukey HSD correction established p-values for pairwise comparisons of significant effects.

TABLE 5.1: Primer Sets

Promoter Primer Sets

GENE	*FORWARD SEQUENCE*	*REVERSE SEQUENCE*
CDC27	GGTGGAGAAGGATGCAGTGT	CCCCAAAAAGAGTGAACCAG
CDC46	CACCTGGACCCAATCATTTC	ACGGAGTCTCACCATCTTGC
CDC6	TGGCCTCTAAAGGAACCTGA	ATGGGGAGGGAATTATGACC
CDK4	TGGGAACAAGTGTGTTCTGG	GACGGATACAGGATTGCACA
CYCLIN B2	CTCCCAAAGTGCTGGGATTA	AAATGGGCAAAGGACATGAA
CYCLIN H	GAGTGTGTGGCTCTCCAAAA	TGAAAAGCCCACACAGGTAA
E2F-6	GTAGAGGCAGCCAGGACTTG	TTCCTCCTTCCTGTTTGACG
GADD45	TGCTTTCCACCTACAAGTTGC	CACCAGCTGAGAGACAACCA
P18/INK4	ATAGCTCGCCACACACACAC	AGATGATCCTGGCGGATTTT
P21/WAF	TGTCATTTTGGAGCCACAGA	AAGGGGAGGATTTGACGAGT
RPA3	CATCATCACCATCACCTGCT	TGCACTTGTATCGCAGCAA
SMAD 4	ACTCCCTCAAACAGGCCTTC	ACCACATCCGGGTAATTTCA
SMAD5	AGCATCGAGAAGAGCTCCAA	GAGTGGGACTGCCCATACAC
VEGF	TCACTGACTAACCCCGGAAC	GCCTGCAGACATCAAAGTGA
Runx2	AGAAAGTTTGCACCGCACTT	AAGCCACAGTGGTAGGCAGT

Exon-Exon Primer Sets			**Notes**
GENE	FORWARD SEQUENCE	REVERSE SEQUENCE	
CDC27	GAGTTTGGTGATTCAGCTTGC	AGGGAGACCAGAGGAAAGGA	EXON 4 and 5
CDC46	ACTTACTCGCCGAGGAGACA	CTGCCTTTCCCAGACGTGTA	EXON 9 and 10
CDC6	TGCTCTTGATCAGGCAGTTG	CCAAGAGCCCTGAAAGTGAC	EXON 10 and 11
CDK4	GAAACTCTGAAGCCGACCAG	ACATCTCGAGGCCAGTCATC	EXON 6 and 7
CYCLINB2	AACCAGAGCAGCACAAGTAGC	ACCCTTTGGAGCCAACTTTT	EXON 2 and 3
CYCLINH	CCTCCAGGGCTGGAATTACT	CTTCAGATCTGGGTGGTTCA	EXON 5 and 7
E2F6	GGAGCAGGGTCAGACCAGTA	TCTCAAATGCCATCAGTTGC	EXON 6 and 7
GADD45A	GGAGGAAGTGCTCAGCAAAG	ATCTCTGTCGTCGTCCTCGT	EXON 2 and 3
p18	ACGTCAATGCACAAAATGGA	CTCGGGATTTCCAAGTTTCA	EXON 3 and 4
p21	GACTCTCAGGGTCGAAAACG	GGATTAGGGCTTCCTCTTGG	EXON 2 and 3
RPA3	AGGGAGGCTGGAAAAGATTC	CCAACCACTTCCACAATTCC	EXON 3 and 5
SMAD4	ACATTGGATGGGAGGCTTCA	TTGTGAAGATCAGGCCACCT	EXON 1 and 2
SMAD5	TCTGCTTGGGTTTGTTGTCA	CTGCTGTCACTGAGGCATTC	EXON 5 and 6
VEGF	CCCACTGAGGAGTCCAACAT	TGCATTCACATTTGTTGTGC	EXON 3 and 4

RESULTS

Runx2 Protein is Stable During Mitosis and Associated with Mitotic Chromosomes.

Runx2, a tissue-specific transcription factor that confers cell fate and lineage-commitment, is localized to chromosomes at all stages of mitosis as determined by *in situ* immunofluorescence microscopy (Figure 5.1A). Biochemical fractionation validates the association of Runx2 with mitotic chromatin (Figure 5.1B). To assess whether Runx2 is metabolically stable during mitosis, we examined protein levels in synchronized cells. Mitotic cells were released into G1 in the presence or absence of the protein translation inhibitor cycloheximide. Progression into G1 was monitored by microscopy and FACS analysis and inhibition of translation was verified in parallel by metabolic labeling with ^{35}S methionine. As cells exit mitosis and enter G1, levels of Runx2 or Lamin B1 protein are unaffected by inhibition of translation (Figure 5.1C). Thus, Runx2 protein synthesized prior to division is not turned-over and is retained at the onset of the next G1-phase. The stability of Runx2 during mitosis and its association with mitotic chromosomes indicate a potentially novel regulatory function for this cell fate determinant.

Mitotic Chromosome Association of Runx2 Requires Sequence-Specific DNA Binding.

Loss-of-function mutations that abrogate the sequence-specific DNA binding of Runx proteins alter cell phenotype and result in cancer (e.g., Acute Myelogenous Leukemia) and other human disorders (e.g., Cleidocranial Dysplasia (CCD) and Familial Platelet Disorder) (Osato, 2004; Zhou et al., 1999). We hypothesized that the

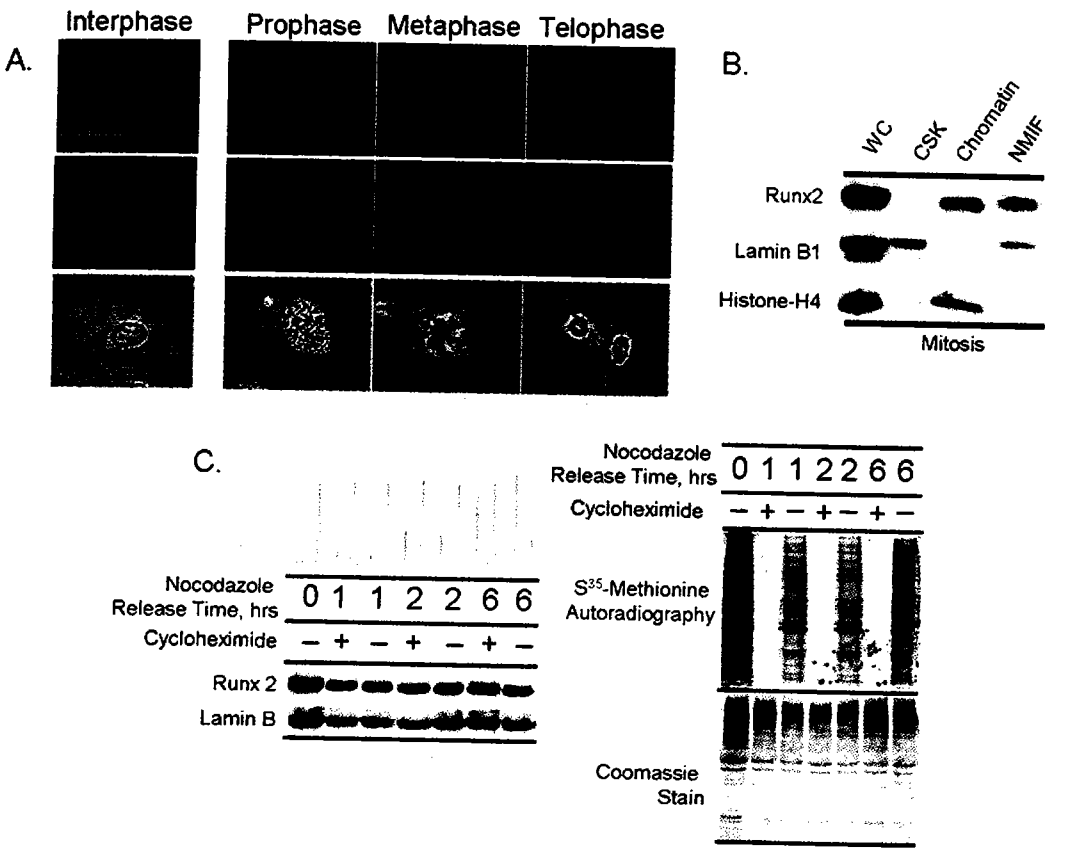

Figure 5.1: Runx2 is Stable and Associated with Chromosomes During Mitosis
A. Asynchronously growing Saos-2 cells were fixed in formaldehyde and prepared for in situ immunofluorescence analysis with staining for DNA using DAPI and Runx2 using a rabbit polyclonal antibody directed against the C-terminal region of the protein. Mitotic cells were identified by chromosome morphology. In mitosis Runx-2 is localized to chromosomes as well as the spindle assembly (data not shown). **B.** In ROS cells arrested in mitosis we assessed the localization of Runx2 by biochemical fractionation using standard techniques to generate soluble, chromatin associated, and insoluble protein fractions compared with whole cell protein levels. Proteins from each fraction were analyzed by western blot using antibodies against Runx2, as well as Lamin B1, and Histone H4 as controls. **C.** Stability of Runx2 protein in mitosis was established in a cycloheximide based cell synchronization. Saos cells were arrested at the G2/M boundary for 24hrs and allowed to release through mitosis into G1 by washing and re-feeding with fresh growth media. At 0 hrs protein was isolated for western analysis. Release was performed in the presence or absence of the protein translation inhibitor cycloheximide (50 ug/ml). Inhibition of protein translation was assessed in parallel by pulse labeling with ^{35}S-Methionine for 30 minutes prior to each time point. At 1, 2, and 6 hr timepoints protein samples were isolated for western analysis of Runx2 levels and the control Lamin B1 protein; in parallel protein was extracted from pulse labeled plates for autoradiography and Coommasse staining.

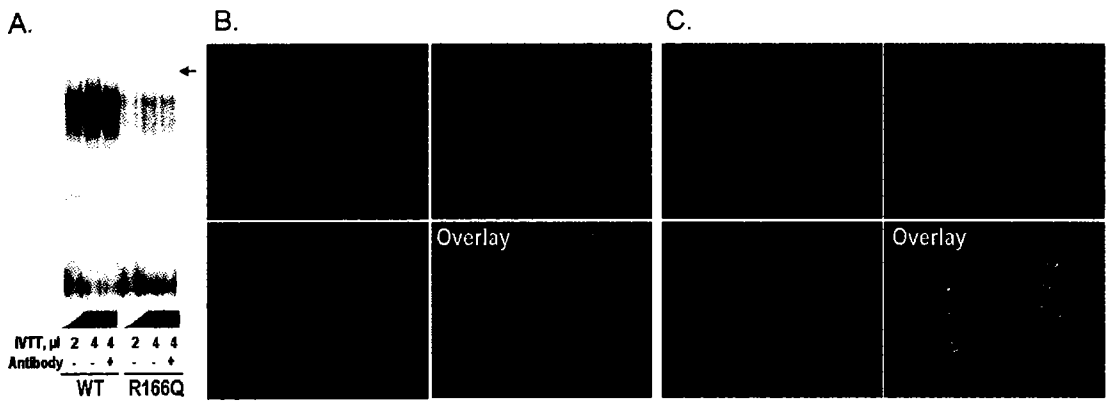

Figure 5.2. Runx2 Association with Mitotic Cells Requires Sequence Specific DNA Binding A point-mutation was introduced in the conserved Runt homology domain that results in an Arginine to Glutamine amino-acid substitution at amino-acid 166 in the MASNS-isoform of the mouse Runx2 protein [Runx2 (R166Q)]. **A.** To confirm the disruption of the Runx2 protein binding to its cognate recognition sequence electrophoretic mobility shift assays were performed using wild-type Runx2 and mutant Runx2 (R166Q), each generated in an IVTT reaction. Specificity of protein-DNA complexes was established by supershift using a rabbit polyclonal antibody against Runx2 (see arrow). Protein quantity used in the EMSA were equivalent as determined by western blot analysis. **B.** Co-localization studies were performed with wild-type Runx2 and mutant Runx2 (R166Q). Hela cells were co-transfected with wild-type Runx2 and mutant Runx2, which were N-terminally tagged with HA- and Xpress-epitopes, respectively. *In situ* immunofluorescence was performed with DNA staining by DAPI, and indirect immunolabeling with antibodies directed against HA and Xpress epitopes with appropriate secondary antibodies. Mitotic cells were identified by DNA morphology. **C.** Control colocalization experiments were performed using HA- and Xpress tagged wild-type proteins.

chromosomal association of Runx2 in mitosis involves sequence-specific protein-DNA interactions through its conserved Runt-homology domain. To test this concept we used site-directed mutagenesis to recapitulate a point-mutation observed in CCD that abrogates DNA binding (Figure 5.2A). Colocalization studies using indirect immunofluorescence microscopy reveal that the Runx2 DNA binding mutant is excluded from chromosomes during mitosis (Figure 5.2B). Thus, association of Runx2 protein with mitotic chromosomes requires sequence-specific DNA binding and provides evidence that Runx2 remains bound to its cognate regulatory elements within target genes.

Identification of Mitotically Regulated Runx2 Target Genes by Functional Genomics.

We applied a functional genomics strategy to identify mitotic targets of Runx2. Genes were selected that are sensitive to Runx2 siRNA, are mitotically controlled, and have Runx consensus motifs in their promoters. Using cDNA arrays comprising a total of 192 osteogenic and/or cell cycle regulatory genes, we discovered 31 genes that satisfy these three biological criteria (Figure 5.3A-C). Independent siRNA experiments analyzed by RT-PCR directly confirmed that Runx2 controls expression of selected genes (Figure 5.4A). Using chromatin immunoprecipitation assays we confirmed that at least 14 of these genes are direct Runx2 targets. Two of these genes have previously been established as Runx2 responsive (e.g., p21 and VEGF) and thus validate our approach (Westendorf et al., 2002; Zelzer et al., 2001) (Figure 5.4B). Functional classification of these target genes (Table 5.1)

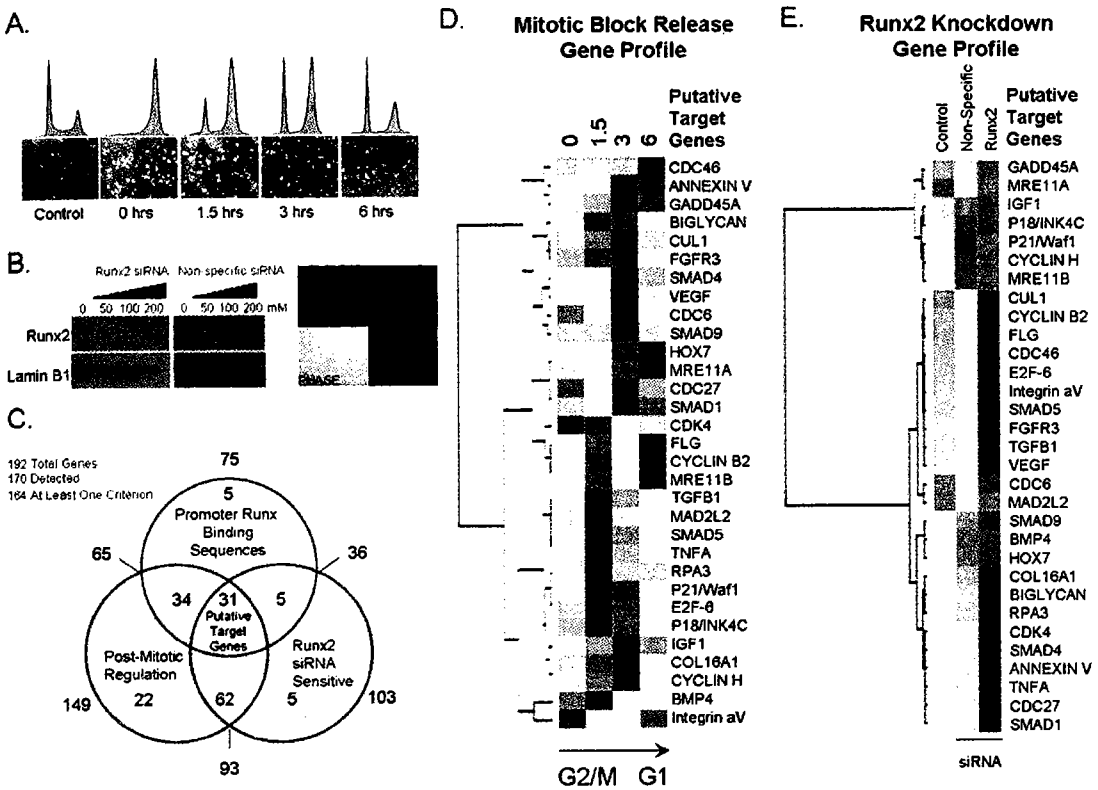

Figure 5.3: Runx2 Target Gene Identification

We applied a functional genomics strategy to identify mitotic target genes of Runx2. Genes were selected that exhibit alterations in steady state mRNA during progress from mitosis into G1, that are sensitive to Runx2 siRNA, and have that promoters with Runx consensus motifs. The first two criteria were assessed by cDNA-array based gene profiling and the final criterion was assessed through a bioinformatics analysis using TFSEARCH (Heinemeyer et al., 1998). **A.** Cells were synchronized at mitosis and released into G1 with RNA taken at 0, 1.5, 3, and 6hrs for analysis. **B.** siRNA knockdown of Runx2 levels was performed at various concentrations between 25nM (not shown), 50nM, 100nM, and 200nM. Knockdown samples were obtain after 72 hours of treatment with 50nM of specific Runx2 siRNA oligos, non-specific GFP targeted siRNA, and vehicle control. **C.** Using cDNA arrays comprising a total of 192 osteogenic and/or cell cycle regulatory genes from Superarray biosciences. A Venn diagram indicates the grouping of genes and we discovered thirty-one genes that satisfy all three criteria. Thirty-one target genes were analyzed by hierarchical clustering based on G2/M to G1 cell cycle expression data in **D.** and **E.** their expression in the Runx2 knockdown experiment. The colormap is applied to standardized gene expression data pure blue = -3, pure white = 0, and pure red = 3.

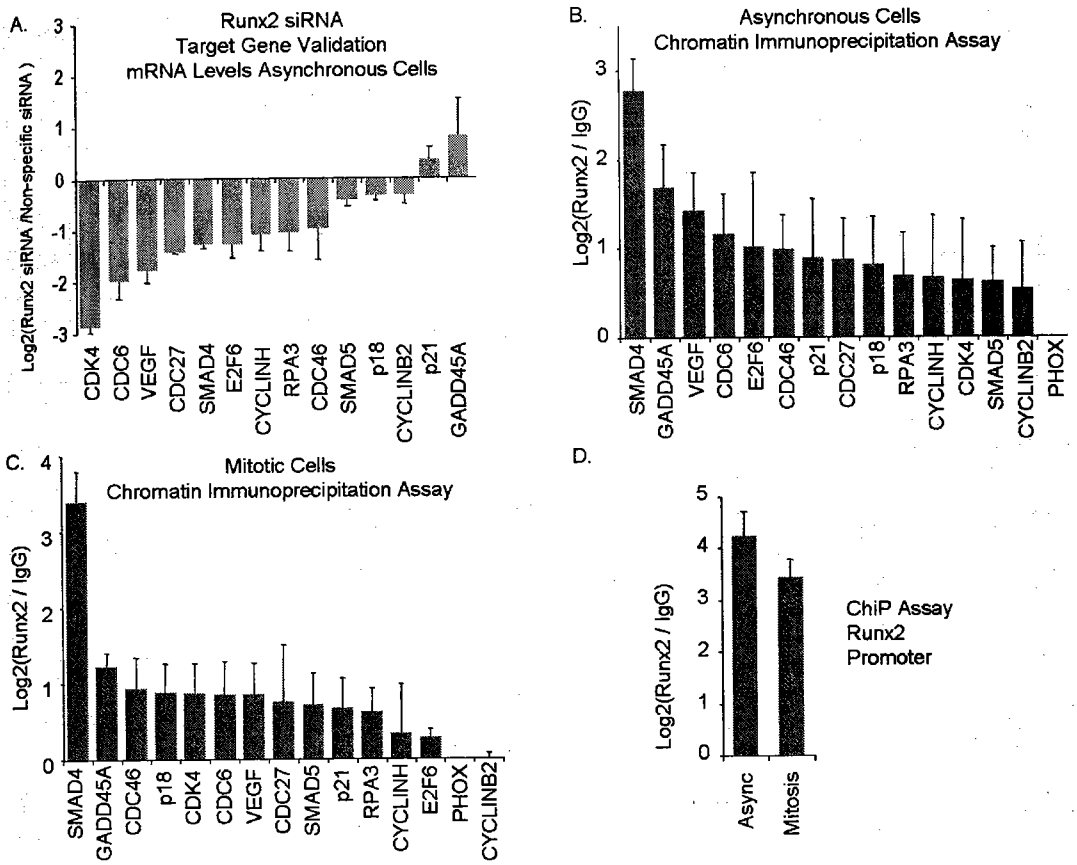

Figure 5.4: Target Gene Validation

Putative Runx2 target genes identified by gene expression profiling were examined by chromatin immunoprecipitations (ChIP). **A.** Fourteen genes were identified in a primary screen (data not shown) and characterized as bona-fide targets by qPCR analysis of ChIPs in two independent duplicate experiments. Samples were quantified relative to input and normalized to the non-specific immunoprecipitation of the PHOX gene promoter. Values represent the $\log_2$ difference between Runx2 specific signals and background levels established by ChIPs with control non-immune IgG. **B.** The responsiveness of the fourteen target genes to modulations in Runx2 levels were determined in independent siRNA experiments analyzed in duplicate by RT-qPCR with primer-sets designed against exon-exon junctions on each of the target genes. Gene expression data are normalized to 28s RNA and expressed as the $\log_2$ difference between Runx2 and non-specific siRNA. Error bars reflect standard error of the mean. **C.** Interaction of Runx2 with its novel target genes was assessed during mitosis by chromatin immunoprecipitations (ChIP) assays. ChIP studies for the fourteen target genes were performed with pure mitotic cells isolated by nocodazole-synchronization and mitotic shake-off in two independent experiments which were analyzed in duplicate by qPCR. Samples were quantified relative to input and normalized to the non-specific immunoprecipitation of the PHOX gene promoter. Values represent the $\log_2$ difference between Runx2 specific signals and background levels established by ChIPs with control non-immune IgG. **D.** The interaction of Runx2 with the promoter of its own gene was assessed by ChIP on asynchronous and mitotic cells.

TABLE 5.2: Target Gene Annotation

Gene Name	GenBank	Locus Link	Description
Cdc27	NM_001256	996	Anaphase promoting complex subunit 3, essential for cell division.
CDC46	NM_006739	4174	Also known as MCM5, forms a complex with MCM2 and is involved in DNA replication. May have a role in cell division
CDC6	NM_001254	990	Involved in the initiation of DNA replication. Also participates in checkpoint controls that ensure DNA replication is completed before mitosis is initiated.
Cdk4	NM_000075	1019	Probably involved in the control of the cell cycle.
Cyclin B2	NM_004701	9133	Essential for the control of the cell cycle at the G2/M (mitosis) transition.
Cyclin H	NM_001239	902	Involved in cell cycle control and in RNA transcription by RNA polymerase II. Its expression and activity are constant throughout the cell cycle.
E2F-6	NM_001952	1876	Inhibitor of E2F-dependent transcription lacks the transcriptional activation and pocket protein binding domains. Appears to regulate a subset of E2F-dependent genes whose products are required for entry into the cell cycle but not for normal cell cycle progression.
GADD45	NM_001924	1647	Binds to proliferating cell nuclear antigen. Might affect PCNA interaction with some CDK (cell division protein kinase) complexes; stimulates DNA excision repair in vitro and inhibits entry of cells into S phase.
p18/INK4C	NM_078626	1031	Interacts strongly with CDK6, weakly with CDK4. Inhibits cell growth and proliferation with a correlated dependence on endogenous retinoblastoma protein RB.
P21/Waf1/CIP1	NM_000389	1026	May be the important intermediate by which p53 mediates its role as an inhibitor of cellular proliferation in response to DNA damage. May bind to and inhibit cyclin-dependent kinase activity, preventing phosphorylation of critical cyclin-dependent kinase substrates and blocking cell cycle progression.
RPA3	NM_002947	6119	Absolutely required for simian virus 40 DNA replication in vitro. It participates in a very early step in initiation. RP-A is a single-stranded DNA-binding protein.
Smad4/DPC4	NM_005359	4089	Common mediator of signal transduction by TGF-beta (transforming growth factor) superfamily; SMAD4 is the common SMAD (co-SMAD). Promotes binding of the SMAD2/SMAD4/FAST-1 complex to DNA and provides an activation function required for SMAD1 or SMAD2 to stimulate transcription. May act as a tumor suppressor.
Smad5	NM_005903	4090	Transcriptional modulator activated by BMP (bone morphogenetic proteins) type 1 receptor kinase. SMAD5 is a receptor-regulated SMAD (R-SMAD).
VEGF	NM_003376	7422	Growth factor active in angiogenesis, vasculogenesis and endothelial cell growth. Induces endothelial cell proliferation, promotes cell migration, inhibits apoptosis, and induces permeabilization of blood vessels.

reveals that Runx2 exerts phenotype control at the transcriptional level to mediate cell cycle progression and signaling pathways that establish competency for lineage commitment.

Because our immunofluorescence microscopy studies indicate that Runx2 binds to mitotic chromosomes through the Runt homology sequence-specific DNA binding domain, we tested whether Runx2 associates with target genes at mitosis. Chromatin immunoprecipitation assays were performed on prometaphase cells. Our results show that within the condensed mitotic chromosomes, Runx2 retains association with the promoters of nearly all of target genes examined (Figure 5.4C). Furthermore, we have established that Runx2 protein binds to the Runx2 promoter during mitosis, suggesting a mitotic autoregulatory function (Figure 5.4D). Interestingly, in mitosis Runx2 does not associate with the Cyclin B2 target gene, which is involved in control of mitotic progression. Our findings suggest that Runx2 provides a critical regulatory function in progeny cells for post-mitotic gene expression in G1.

Runx2 Target Genes Exhibit Mitotic Specific Histone Modifications.

Recent work indicates that specific histone modifications may mark active genes in mitosis (Kouskouti and Talianidis, 2005b). We investigated whether promoters of Runx2 target genes exhibit mitotic specific epigenetic changes that could be indicative of post-mitotic transcriptional state. Acetylation of histone H4 and dimethylation of histone H3 on lysine 4 (K4), which are both linked with active gene

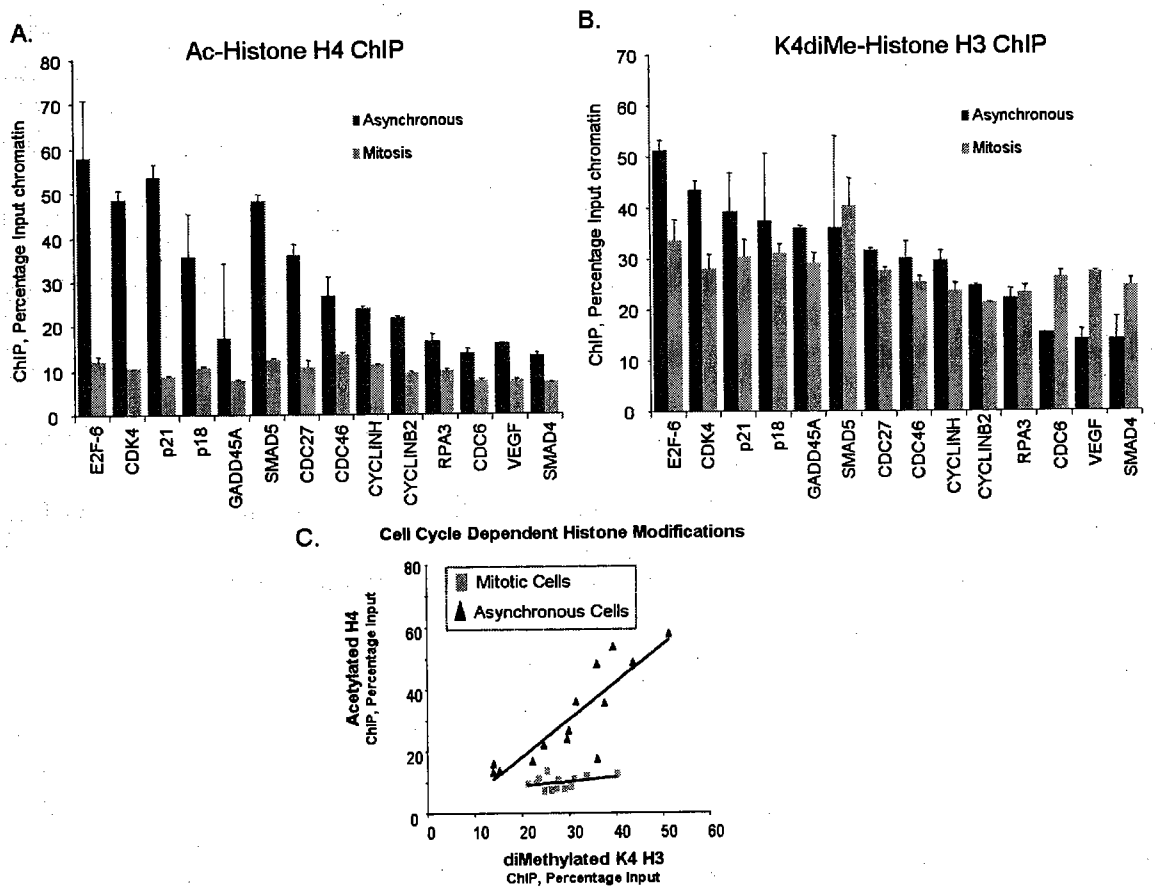

Figure 5.5. Runx2 is Associated with Epigenetically Modified Target Genes in Mitosis
ChIP analyses of histone modifications at the fourteen target genes were performed with asynchronous (dark gray bars) and pure mitotic cells (light gray bars) that were synchronized as described in Figure 4. Duplicate samples were analyzed by qPCR, quantified as a percentage of input and normalized ('median-shifted') for comparison with subsequent functional experiments in Figure 6. **A.** Histone H4 acetylation and **B.** histone H3 K4-dimethylation for the promoters of fourteen target genes promoters is shown. Ordinate is percentage input chromatin. **C.** A scatterplot of H4 acetylation (ordinate) versus H3 K4-dimethylation (abscissa) for all fourteen genes in asynchronous cells (black triangles) and mitotic cells (gray squares) is depicted. A least squares regression line is shown for each population.

expression, were examined in both asynchronous and mitotically synchronized cells (Figure 5.5). The majority of Runx2 responsive genes exhibit substantially decreased H4 acetylation in mitosis (Figure 5.5A). In contrast we observe a retention or selective increase in mitotic histone H3-K4 dimethylation compared with asynchronous cells (Figure 5.5B). Our data show that in general histone H4 acetylation is positively linked with histone H3 K4-dimethylation in asynchronous, but not mitotic cells (Figure 5.5C). The reduction of histone H4 acetylation may be coupled with the shut-down of transcription in mitosis. We propose that the persistence of basal levels of H4 acetylation and constitutive histone H3-K4 dimethylation at Runx target gene promoters during mitosis reflects a transcriptionally poised chromatin structure.

Runx2 affects post-translational histone modifications at target gene promoters during mitosis

Runx2 mediates activation and repression of gene transcription through interactions with a diverse set of chromatin modifying enzymes. Because Runx2 associates during mitosis with target gene promoters that exhibit distinct histone modifications, we mechanistically addressed whether Runx2 mediates these epigenetic alterations. We generated Runx2 deficient mitotic cells using RNA interference and determined the effect on H3-K4 dimethylation and H4 acetylation at Runx2 regulated promoters (Figure 5.6A). Quantitative chromatin immunoprecipitation analyses for the fourteen target genes revealed that depletion of Runx2 protein alters promoter histone modifications ($p=0.0005$); and that these effects are gene specific ($p=0.0001$). We

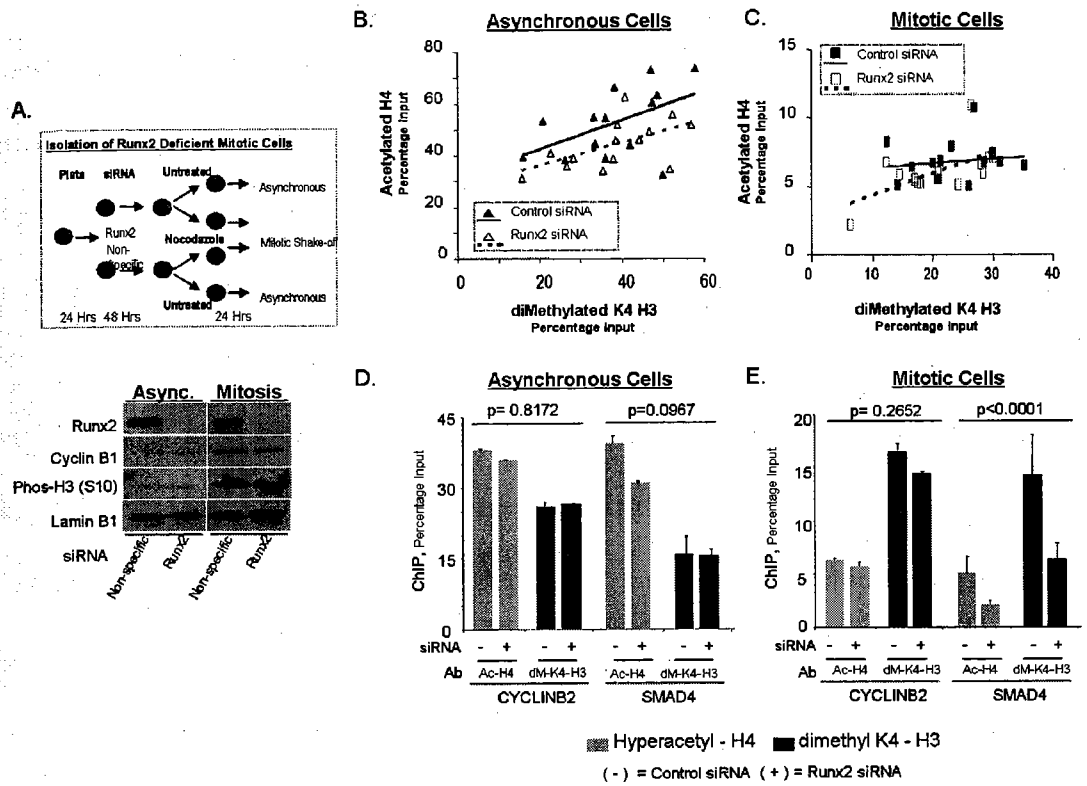

Figure 5.6: Runx2 Affects Mitotic Histone Modifications at Target Gene Promoters

A. The effects of Runx2 on promoter histone modifications were assessed by combining siRNA gene knockdown with mitotic cell synchronization. The schematic depicts the experimental strategy for obtaining Runx2 depleted mitotic cells. Histone modifications levels at target gene promoters in mitotic and asynchronous cells were assayed by chromatin immunoprecipitation and analyzed by qPCR. Protein was extracted in parallel plates to validate Runx2 knockdown. Cyclin B1 levels and histone H3 (S10) phosphorylation status were assessed as markers of mitosis and Lamin B1 was used as a loading control. Efficiency of siRNA transfection (>90%) was determined in parallel with flourophore conjugated non-silencing siRNA oligos (data not shown). The levels of hyperacetylated histone H4 and dimethylated histone H3 (K4) in control and Runx2 siRNA treated cells was determined in two separate ChIP assays each analyzed in duplicate by qPCR for the enrichment of fourteen target gene promoters (not shown). A scatterplot of H4 acetylation (ordinate) versus H3 K4-dimethylation (abscissa) for all fourteen genes in asynchronous cells (panel **B.**) and mitotic cells (panel **C.**) treated with control (black triangles) or Runx2 siRNA (open triangles). A least squares regression line is shown for each population: control (solid line) or Runx2 siRNA (broken line). A mixed model analysis of variance was employed to assess the significance of observed Runx2 siRNA effects compared with control for all fourteen genes, results from SMAD4 and CyclinB2 are shown. Multiple pairwise comparisons (Tukey's HSD) were evaluated to determine which effects differ significantly at a 0.05-level and to establish p-values; error bars are standard error (n=4). Column plots show ChIP results for SMAD4 and CYCLINB2 as percentage input chromatin (ordinate) in Runx2 and control siRNA treated (panel **D.**) asynchronous and (panel **E.**) mitotic cells.

find an overall reduction in levels of H4 acetylation, but not H3-K4 dimethylation, at Runx2 target gene promoters in asynchronous cells (Figure 5.6B). In contrast, during mitosis we find that loss of Runx2 significantly diminishes both H3-K4 dimethylation and H4 acetylation at target gene promoters (Figure 5.6C). We observe the greatest effect on histone modifications at the SMAD4 gene, which in response to Runx2 knockdown exhibits decreased H3-K4 dimethylation and H4 acetylation during mitosis ($p<0.0001$), but not in asynchronous cells (Figure 5.6D, E). These observations are consistent with high levels of Runx2 interaction with the SMAD4 promoter in mitosis and sensitivity of SMAD4 expression to Runx2 siRNA (Figure 5.4A, B). For comparison, we do not detect Runx2 dependent histone modifications at the cyclin B2 promoter, which does not bind Runx2 during mitosis (Figure 5.6D, E). Taken together our findings indicate that Runx2 contributes to the regulation of histone modifications at target gene promoters during mitosis (Figure 5.6F).

CONCLUSIONS

We have investigated the Runx2 transcription factor as a paradigm for understanding mechanisms by which phenotypic control of gene expression is sustained during mitotic division. Our results show that Runx2 interacts sequence-specifically with mitotic chromosomes at target gene promoters and influences histone H4 acetylation and histone H3 K4-dimethylation during mitosis. Runx2 is thought to function as a promoter-bound scaffold for the temporal recruitment of co-activators or repressors and associated chromatin modifying factors that establish histone modification patterns in mitosis. Loss-of-function DNA-binding mutations in Runx proteins eliminate mitotic chromosome association and are linked with alterations in cell phenotype in multiple human disorders. We propose that chromosomal association of Runx2 in mitosis supports epigenetic retention of phenotype during cell division to maintain lineage identity of progeny cells.

CHAPTER VI:

Mitotic occupancy and lineage-specific transcriptional control of ribosomal RNA genes by the Runx2 transcription factor

ABSTRACT

Regulation of ribosomal RNA expression supports the growth of cells and is tightly coupled with proliferation and differentiation. Transcription factors that govern cell identity must convey phenotypic information through successive cell divisions for regulatory events that determine cell cycle progression or exit in progeny cells. Runx proteins are master regulators that control cell fate during hematopoiesis (Runx1), osteogenesis (Runx2), as well as gastrointestinal and neuronal development (Runx3). Within the condensed mitotic chromosomes we find that Runx2 is retained in large discrete foci that are symmetrically positioned on sister chromatids. These chromosomal foci are associated with open chromatin at nucleolar organizing regions, co-localize with the RNA polymerase I transcription factor, UBF1, and transition into nucleoli during interphase. By chromatin immunoprecipitation analysis we demonstrate that during the M/G1, G0/G1, and G1/S transitions there are specific spatial and temporal changes in the binding of Runx2 throughout rDNA repeats. Reduction of Runx2 levels by siRNA activates rRNA transcription, while induction of Runx2 directly represses ribosomal biogenesis. Functional linkage between Runx2 and ribosomal gene expression is further demonstrated by enhanced ribosomal RNA synthesis in primary cells from Runx2 null mice. Runx2 repression of ribosomal gene expression is associated with growth inhibition and expression of lineage-specific genes. Our findings establish that Runx2 not only influences lineage commitment and cell proliferation by regulating RNA polymerase II transcription, but also acts as a cell cycle dependent suppressor of RNA

Polymerase I mediated rRNA synthesis. Thus, Runx2 provides an important mechanistic link between cell fate, proliferation and growth control.

INTRODUCTION

Cell identity is defined by the expression of tissue-specific proteins as well as proliferative capacity and cell size. Tissue-specific gene expression reflects cell fate determination and lineage commitment, which are controlled by master transcriptional regulators. Proliferative capacity is mediated by oncoproteins and tumor suppressors that regulate cell cycle progression and mitotic division. Cell proliferation in progeny cells is tightly coupled with growth, defined as the accumulation of cell mass and size, and requires ribosomal biogenesis. Phenotypic identity must be transmitted to progeny cells following mitosis, and it is imperative to elucidate the mechanism that accomplishes this fundamental biological process.

The Runx proteins are a unique class of transcription factors that establish lineage-commitment and phenotypic gene expression, as well as control proliferative potential of committed progenitors (Blyth et al., 2005). Runx factors are scaffolding proteins that integrate cell signals through the formation of gene regulatory complexes at subnuclear microenvironments (Zaidi et al., 2001a; Zaidi et al., 2003). At mitosis, these subnuclear domains and nucleoli reorganize concomitant with nuclear disassembly, chromatin condensation and transcriptional silencing (Swedlow and Hirano, 2003; Dimario, 2004; Hernandez-Verdun and Roussel, 2003; Gottesfeld and Forbes, 1997; Spector, 2003; Zaidi et al., 2005; Zaidi et al., 2003). We have shown that Runx proteins are present during mitosis and equally distributed between progeny cells (Zaidi et al., 2003). Hence, Runx proteins may have the inherent ability to maintain cell identity.

The essential roles of the mammalian Runx proteins in establishing phenotypic identity is evidenced by loss-of-function mutations that cause catastrophic defects in hematopoiesis (Runx1), osteogenesis (Runx2), or neuronal and gastro-intestinal development (Runx3) (Choi et al., 2001; Komori et al., 1997; Wang et al., 1996a; Inoue et al., 2002; Li et al., 2002; Westendorf et al., 2002). Furthermore, deregulation of Runx proteins in specific cellular contexts has been associated with tumor formation and metastases (Javed et al., 2005; Barnes et al., 2003; Brubaker et al., 2003; Yang et al., 2001; Blyth et al., 2001; Vaillant et al., 1999; Neil et al., 1999; Lund and van Lohuizen, 2002; Ito, 2004; Cameron and Neil, 2004). Runx1 is frequently rearranged in acute myelogenous leukemia, Runx2 is implicated in metastatic breast cancer and T-cell lymphomas and Runx3 is associated with gastric cancer (Barnes et al., 2003; Neil et al., 1999; Blyth et al., 2005; Li et al., 2002; Barnes et al., 2004; Javed et al., 2005). Runx2 normally attenuates osteoblast proliferation and promotes the development of the mature bone cell phenotype (Coffman, 2003; Westendorf et al., 2002; Pratap et al., 2003; Thomas et al., 2004; Lian et al., 2004; Galindo et al., 2005). Here we demonstrate that the lineage-specific Runx2 transcription factor controls ribosomal RNA synthesis through interphase and mitosis. Hence, we have discovered a heritable mechanism that coordinates ribosomal biogenesis, lineage commitment, and cell cycle progression. We conclude that Runx2 functions at a critical mechanistic juncture that regulates cell proliferation, growth and differentiation.

MATERIALS AND METHODS

Cell Culture and Synchronization

Saos-2 osteosarcoma cells were maintained in McCoy's medium containing 15% fetal bovine serum plus 2 mM L-glutamine and a penicillin-streptomycin cocktail. MC3T3 cells were maintained in α-MEM medium containing 10% fetal bovine serum plus 2 mM L-glutamine and a penicillin-streptomycin cocktail. Primary calvarial cells were isolated as described in (Owen et al., 1990) from mice homozygous for the wild-type Runx2 allele, the C-terminally truncated Runx2 allele (e.g., Runx2-ΔC) (Choi et al., 2001), and the Runx2 null allele (Komori et al., 1997) and were maintained in α-MEM medium containing 10% fetal bovine serum plus 2 mM L-glutamine and a penicillin-streptomycin cocktail. Human IMR-90 fibroblasts were maintained in Basal Eagle Medium containing 10% fetal bovine serum plus 2 mM L-glutamine and a penicillin-streptomycin cocktail.

MC3T3 and Saos-2 cells were blocked in mitosis for chromatin immunoprecipitation assays and block release studies by adding 100 ng/ml nocodazole for 18 or 24 hrs, respectively, followed by shake-off to detach mitotic cells. For block-release studies MC3T3 cells were synchronized in mitosis as described above and either processed for biochemical assays or washed once in serum-free medium, followed by replating in growth media to obtain subsequent time points in G1 for biochemical assays. The G0/G1 and G1/S synchronizations were obtained by serum deprivation and re-stimulation of MC3T3 cells. Quiescent cells (G0) were obtained by culturing for 48 hours in serum-free media and either processed for biochemical assays or stimulated to

reenter the cell cycle and traverse G1 and early S phase by the addition of serum containing growth media.

***In Situ* Immunofluorescence Microscopy.**

Cells grown on gelatin-coated coverslips as well as chromosome spread preparations, were processed for *in situ* immunofluorescence essentially as described (Zaidi et al., 2001a). In brief, cells or spreads were rinsed twice with PBS and fixed in 3.7% formaldehyde in PBS for 10 minutes. After rinsing once with PBS, the cells were permeabilized in 0.1% Triton X-100 in PBS, and rinsed twice with PBSA (0.5% bovine serum albumin [BSA] in PBS) followed by antibody staining. Antibodies and their dilutions used are as follows: rabbit polyclonal antibodies against Runx2 (1:200; M-70 Santa Cruz Biotechnology, Carlsbad, CA), Histone H3 Methylated on Lysine 9 (1:1000), Histone H3 Methylated on Lysine 4 (1:3000), or Histone H3 Phosphorylated on Serine 10 (1:1000); all histone antibodies were obtain from Upstate Biotechnology Charlottesville, VA, and mouse monoclonal antibodies directed against Runx2 (Zhang et al., 2000b) and UBF1 (1:400; F-9 Santa Cruz Biotechnology, Carlsbad, CA). The secondary antibodies used were either anti-mouse Alexa 594 or anti-rabbit Alexa 488 (1:800, Molecular Probes, Eugene, OR). DNA was visualized by DAPI (4', 6-diamidino-2-phenylindole) staining. Control samples for colocalization studies were incubated with and without Runx2 primary antibodies alone (mouse and rabbit) and both secondary antibodies (data not shown). Chromosome spreads were generated by incubating mitotic cells in 50 mM KCl solution for 15 minutes at room temperature following by centrifugation at 1000 rpm

for 10 minutes onto positively charged glass slides. DNAseI hypersensitive chromatin is labeled, essentially as described in Kerem et al (Kerem et al., 1984), with incorporation of Alexa488-dUTP (Molecular Probes, Eugene, OR) by DNA Polymerase I (10 units/ml) incorporation on DNAseI (2 units/ml) nicked chromosome spreads--5 minute incubation with both enzymes at room temperature. Staining of cell preparations and chromosome spreads was recorded as z-series stacks with a CCD camera attached to an epifluorescence Zeiss Axioplan 2 (Zeiss Inc., Thorwood, NY) microscope. Stacks were deconvoluted using MetaMorph Imaging Software (Universal Imaging).

Immunoelecton Microscopy

Immunelectron micrscopy was performed essentially as described in Nickerson JA et al. (Nickerson et al., 1990). Briefly, proliferating Saos-2 cells grown on Thermanox coverslips were washed in PBS, permeabilized in 0.1% Triton-X 100 in cytoskeletal buffer with AEBSF and VRC at 4°C, fixed in 4% paraformaldehyde (electron microscopy grade) in the same buffer, then antibody stained for Runx2 (1:100; M-70 Santa Cruz Biotechnology, Carlsbad, CA). Control sections were not exposed to the first antibody and others were stained for Lamin B1 for comparison (data not shown). The second antibody was linked to 5 nm gold beads. Cells were then fixed 2.5% Glutaraldehyde in 0.1M Cacodylate Buffer, pH7.4, at 4°C for 1 hour, then washed in the same buffer at 4°C. Cells were dehydrated in graded ethanol solutions with propylene oxide as the intermediate solvent, infiltrated, then embedded in Epon and cured at 60°C for 2 days. The coverslips were removed, thin sections were cut, stained with 1.4%

uranyl acetate in 40% ethanol, post stained with lead citrate, and imaged with a Philips CM-10 electron microscope. For whole mount analysis of nuclear matrix-intermediate filament preparations, Saos-2 cells were grown on gold grids coated with formvar and carbon before sterilization under ultraviolet light. Nuclear matrix intermediate filament preparations were made (He et al., 1990) and then fixed in formaldehyde, stained with an anti-Runx2 polyclonal antibody, incubated with a second antibody coupled to 5 nm gold beads, and critical point dried as described (Nickerson et al., 1990).

Chromatin Immunoprecipitation and Analysis

Chromatin immunoprecipitation assays (ChIPs) were performed essentially as described (Hovhannisyan et al., 2003). Briefly, asynchronously growing and mitotic cells were crosslinked with 1% Formaldehyde in DMEM for 10 minutes. Crosslinking reaction was quenched by the addition of glycine at a final concentration of 250 mM for 10 minutes. Cells were collected, pelleted and washed twice with PBS. Cell pellets were resuspended in 2.5 ml of lysis buffer (150 mM NaCl, 50 mM Tris-HCl pH 8.0, 1% NP-40, 25 uM MG-132, and 1X Complete® Protease inhibitor cocktail (Roche, Indianapolis, IN). After 10 minutes on ice, cells were sonicated to a DNA fragment size of approximately 500 bp as determined by agarose gel eletrophoresis with ethidium bromide staining. Cell debris was pre-cleared by centrifugation at 15000 rpm for 20 minutes. Supernatant containing protein-DNA complexes was aliquoted into four tubes (1 ml per antibody and 500 ul for input DNA) were incubated for 16 hours with 3 ug Rabbit polyclonal antibody directed against Runx2 (M-70, Santa Cruz Biotechnology), 3

ug of Mouse monoclonal antibody directed against UBF1 and 3 ug of IgG control (Santa Cruz Biotechnology) followed by 1 hour with 50 ul of Protein A/G conjugated Agarose beads. Protein A/G bead complexes were washed with the following buffers: low salt (20 mM Tris-Cl pH 8.1, 150 mM NaCl, 1% Triton X-100, 2 mM EDTA, 1X complete protease inhibitor), high salt (20 mM Tris-Cl pH 8.1, 500 mM NaCl, 1% Triton X-100, 2 mM EDTA), LiCl (10 mM Tris-Cl pH 8.1, 250 mM LiCl, 1% deoxycholate, 1% NP-40, 1mM EDTA) and twice in TE (10 mM Tris-Cl pH 8.1, 1 mM EDTA). Protein-DNA complexes were eluted in 1% SDS and 100 mM $NaHCO_3$. Crosslinks were reversed by incubation overnight in elution buffer and 300mM Sodium Acetate pH5.2. DNA then was extracted, purified, precipitated and resuspended in TE for qPCR using primers outline in Table 6.1.

ChIPs were performed on six pooled biological samples and duplicates were analyzed using a quantitative measure that reflects the amount of genomic DNA amplicon precipitated with a specific antibody (i.e., Runx2 or UBF) relative to the non-specific antibody (i.e., normal IgG) (Wells et al., 2003). Samples were normalized to a non-specific genomic DNA control; human cells (data not shown): PHOX promoter and mouse cells: IgH enhancer, Table 6.1. For determining the spatial occupancy profiles of Runx2 and UBF1 between different cell synchronies, we first computed the mean ChIP occupancy at each rDNA primer set location across each time course. For M/G1 this reflects an average of 0, 2, 4 and 8 hours post-mitotic release; for G0/G1 this reflects an average of 0, 3, 6, and 9 hours post serum stimulation; for G1/S this reflects an average of 12, 15 and 18 hours of the post serum stimulation. These time-averaged ChIP

occupancies were spatially standardized for each cell cycle transition (i.e., M/G1, G0/G1, and G1/S) by subtracting from each primer set the overall mean of all seven rDNA primer sets and dividing this value by overall standard deviation of all seven rDNA primer sets. The Pearson's correlation coefficient was computed to compare these spatial occupancy profiles between cell cycle transitions.

Western Blot Analysis:

Runx2 and cell cycle markers were analyzed by western blot analysis as described previously in Galindo et al (Galindo et al., 2005). Briefly, amounts of total cellular protein were resolved in SDS-PAGE and transferred to polyvinylidene difluoride membranes (Immobilon-P; Millipore Corp., Bedford, MA). Blots were incubated with a 1:2,000 dilution of each primary antibody for 1 hour. Rabbit polyclonal antibodies (Cdk2, CdK1, cyclin A, cyclin B1, cyclin E, and mouse monoclonal antibodies (cyclin D1) (Santa Cruz Biotechnology, Inc., CA). Mouse monoclonal antibodies specific for Lamin B1 (1:2000, Zymed Laboratories, Inc., San Francisco, CA), Tubulin (1:10000, Sigma) and Runx2 (1:2000, 22) were also used. Membranes were then incubated with horseradish peroxidase conjugated secondary protein bands were visualized by a chemiluminescence detection kit (Perkin Elmer Life Sciences, Boston, MA).

RNA Analysis:

Total RNA was isolated from cells at the indicated time points using Trizol reagent (Invitrogen, Carlsbad, CA). Total RNA was purified using the DNA-Free RNA

kit (Zymo Research Corporation, Orange CA). cDNA was generated from purified RNA using a reverse transcription reaction with random hexamer primers (Invitrogen Corporation, Carlsbad, CA). cDNA was then subjected to Real-Time PCR reaction using SYBR chemistry (Applied Biosystems, Inc., Foster City, CA). For analysis primers used are shown in Table I. Pre-rRNA synthesis was assessed using qPCR with primers flanking early rRNA processing sites and analyze relative to total rRNA levels with primers within the 28S coding region.

siRNA, Adenoviral Infection, and Transfection

IMR-90 cells were transduced with an adenovirus vector encoding mouse Runx2 protein under the control of a CMV promoter or a LacZ transgene for control. Briefly, viral particles were administered at 50 MOI in α-MEM with 1% FBS, incubated for 1 hour at 37°C. After infection, free virus was aspirated, and cells were washed twice in serum-free media. Transfection efficiency at 24 hours was approximately 100% as assessed by x-Gal staining and GFP fluorescence. Protein levels were monitored by western blot at 24 and 48 hours. Cell number was also monitored in parallel experiments through the use of a hemocytometer.

Saos-2 cells at 30 to 50% confluency were transfected using Oligofectamine (Invitrogen Life Technologies) with small interfering RNA (siRNA) duplexes specific for human Runx2 obtained from QIAGEN Inc. (Stanford, Calif.) at different concentrations 50 nM. The siRNA duplexes were r(GGUUCAACGAUCUGAGAUU)d(TT). The cells were also transfected with control siRNA duplexes specific for green fluorescent protein

(GFP) using the same concentrations and vehicle alone as a control. Opti-MEM (a reduced serum medium from Invitrogen) was used to dilute the siRNA duplexes and Oligofectamine and for transfection. After treating the cells with siRNA for 4 hours, the cells were supplemented with McCoy's containing 45% FBS for a final concentration of 15% in the medium. The siRNA experiment was carried out for 72 hours, at which time the cells were harvested for total protein and RNA to analyze the knock-down effect of Runx2 siRNA on endogenous Runx2 and its effect ribosomal RNA synthesis by qPCR.

MC3T3 cells at 30-40% confluency were transfected with 500 ng of MR170-BH reporter plasmid and 500 ng total plasmid DNA comprised either of 125 ng pcDNA-HA-Runx2 and 375 ng empty pcDNA, or 250 ng pcDNA-HA-Runx2 and 250 ng empty pcDNA. Control experiments were conducted with 1 ug GFP expression plasmid to monitor transfection efficiency by GFP fluorescence. MR170-BH is described in Budde and Grummt (Budde and Grummt, 1999) and contains a 170 bp minimal mouse rDNA promoter that drives expression of a unique pUC9 vector sequence fused to a RNA polymerase I transcriptional termination sequence. RNA and protein was harvested at 24 hours to assess reporter activity and Runx2 protein levels. Real time PCR primers were designed against the pUC9 transcribed sequence for assessment of reporter activity. Reporter activity as determined by qPCR was normalized to the control mitochondrial cytochrome c oxidase subunit II gene.

TABLE 6.1: Primers

Name		Sequence 5' to 3'	Species	Description	Accession Number
hrDNA1	Forward	TGTCAGGCGTTCTCGTCTC	Human	Ribosomal DNA Repeating Unit	U13369
	Reverse	GAGAGCACGACGTCACCAC			
hrDNA2	Forward	GGATGCGTGCATTTATCAGA	Human	Ribosomal DNA Repeating Unit	U13369
	Reverse	GTTGATAGGGCAGACGTTCG			
hrDNA3	Forward	CGCCGGTGAAATACCACTAC	Human	Ribosomal DNA Repeating Unit	U13369
	Reverse	CCAGTCAAACTCCCCACCT			
hrDNA4	Forward	GCCTTATTTGAGTGGCTTCC	Human	Ribosomal DNA Repeating Unit	U13369
	Reverse	CAGATCGGCCAGCTTTTACT			
hrDNA5	Forward	AAGCTGGCCGATCTGAATAA	Human	Ribosomal DNA Repeating Unit	U13369
	Reverse	TTCCCAAGTCTGGTTGATCC			
hrDNA6	Forward	CTCAGCCTCCCAAGTAGCTG	Human	Ribosomal DNA Repeating Unit	U13369
	Reverse	GATCGAGACCATCCTGGCTA			
hrDNA7	Forward	AGGTGTCCGTGTCCGTGT	Human	Ribosomal DNA Repeating Unit	U13369
	Reverse	GGACAGCGTGTCAGCAATAA			
mrDNA1	Forward	GCTTGTTTCTCCCGATTGC	Mouse	Ribosomal DNA Repeating Unit	BK000964
	Reverse	CGCGAACCACTGAGAAAAGT			
mrDNA2	Forward	GTCTCTCGGTCCCTTGTGAG	Mouse	Ribosomal DNA Repeating Unit	BK000964
	Reverse	ACGGGTCAGTCAGAGGAGAG			
mrDNA3	Forward	CGCCGGTGAAATACCACTAC	Mouse	Ribosomal DNA Repeating Unit	BK000964
	Reverse	CTGAGCTCGCCTTAGGACAC			
mrDNA4	Forward	ATCAGGAGGTCCCGCTAGTT	Mouse	Ribosomal DNA Repeating Unit	BK000964
	Reverse	ACGGCTTGACATCCAAACTC			
mrDNA5	Forward	TCCTTCCTTCCTCCCTTTTC	Mouse	Ribosomal DNA Repeating Unit	BK000964
	Reverse	AAGGTCACCCTGGCTTACAA			
mrDNA6	Forward	ACCCTCCTCTTCCACTGCTT	Mouse	Ribosomal DNA Repeating Unit	BK000964
	Reverse	GGCACCCAAAAACGAAAGTA			
mrDNA7	Forward	GCGGTTTTCTTTCATTGACC	Mouse	Ribosomal DNA Repeating Unit	BK000964
	Reverse	ACGACGCCTGGAAGTCATAC			
hpre-rRNA	Forward	CCGCGCTCTACCTTACCTAC	Human	Ribosomal DNA Repeating Unit	U13369
	Reverse	GAGCGACCAAAGGAACCATA			
h28s	Forward	GAACTTTGAAGGCCGAAGTG	Human	Ribosomal DNA Repeating Unit	U13369
	Reverse	ATCTGAACCCGACTCCCTTT			
mpre-rRNA	Forward	GCTTGTTTCTCCCGATTGC	Mouse	Ribosomal DNA Repeating Unit	BK000964
	Reverse	CGCGAACCACTGAGAAAAGT			
m28s	Forward	GAACTTTGAAGGCCGAAGTG	Mouse	Ribosomal DNA Repeating Unit	BK000964
	Reverse	ATCTGAACCCGACTCCCTTT			
mHistoneH4n	Forward	CCAGCTGGTGTTTCAGATTACA	Mouse	Replication Dependent Histone H4 Gene	AY158966
	Reverse	ACCCTTGCCTAGACCCTTTC			
mOsteopontin	Forward	TTTGCTTTTGCCTGTTTGC	Mouse	Principal phosphorylated glycoprotein of bone	NM_009263
	Reverse	CAGTCACTTTCACCGGGAGG			
hOsteopontin	Forward	ACACATATGATGGCCGAGGT	Human	Principal phosphorylated glycoprotein of bone	X13694
	Reverse	ATGGCCTTGTATGCACCATT			
MR170-BH	Forward	ATTCACTGGCCGTCGTTTTA	n/a	Mouse rDNA promoter/expression construct: unique pUC9 transcribed sequence	n/a
	Reverse	GGCCTCTTCGCTATTACGC			
Igγ Enhancer	Forward	TGGTGGGGCTGGACAGAGTGTTTC	Mouse	Enhancer element located in the intron upstream of the immunoglobulin gamma constant region	V01524
	Reverse	GCCGATCAGAACCAGAACACC			
Phox (GP91)	Forward	CCAATGATTATTAGCCAATTTCTG	Human	CYTOCHROME b(558), BETA SUBUNIT	M66390
	Reverse	CATGGTGGCAGAGGTTGAATGT			

RESULTS

Runx2 Foci Are Associated with Active Nucleolar Organizing Regions (NORs) of Mitotic Chromosomes.

A dynamic intracellular reorganization of the gene regulatory machinery takes place during mitosis. At the initiation of prophase, there is a global condensation of chromosomes, nuclear reorganization, disassembly of nucleoli, and a silencing of transcription. Our laboratory has previously demonstrated that the subnuclear localization of Runx2 is also disrupted during mitosis and restored in telophase, when transcription resumes (Zaidi et al., 2003). In contrast to transcription factors that are displaced from chromosomes and/or degraded during mitosis (Martinez-Balbas et al., 1995; Muchardt et al., 1996; Nuthall et al., 2002; Prasanth et al., 2003), Runx proteins remain stable and a subset is associated with mitotic chromatin (Zaidi et al., 2003).

Using immunofluorescence microscopy of metaphase chromosome spreads, we have made the striking observation that Runx2 is localized to large foci that are equivalently positioned on sister chromatids (Figure 6.1). These foci are distinct from CENP-A foci at centromeres and are observed using multiple antibodies directed against Runx2 as well as with a GFP-Runx2 fusion protein (data not shown). This unique focal organization of the lineage-specific Runx2 protein on mitotic chromosomes has not previously been documented for an RNA polymerase II transcription factor. Our findings suggest a novel regulatory function for Runx2 in post-mitotic gene regulation at early stages of G1, when cells commit to cell cycle exit or progression. These mitotic foci are also observed for a C-terminally truncated Runx2 mutant (ΔC) that retains the

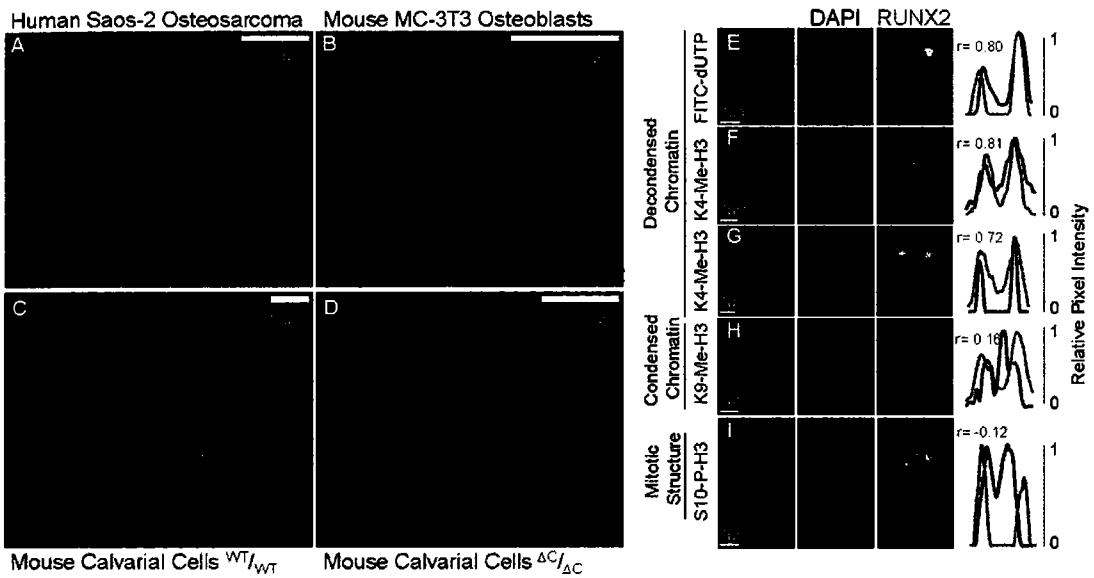

Figure 6.1: Runx2 Localizes in Pairwise Symmetric Foci in Open Chromatin on Mitotic Chromosomes

Mitotic chromosomes spreads were prepared for Human Saos-2 Osteosarcoma (A), Mouse MC3T3 (B), Primary Calvarial Cells from Mice homozygous for Wild-type Runx2 (C) and for the Runx2-ΔC allele (D), and processed for immunofluorescence microscopy using antibodies directed against the Runx2 protein. The right most column of row E through I shows the relative intensity of the Runx2 and the indicated co-labeled image pixels across the line scan shown in the overlay image. The Pearson's correlation coefficient, r was computed to compare the degree of colocalization between the two signals. Human chromosome showing localization of Runx2 with DAPI and DNAseI hypersensitive chromatin (row E, r=0.80), which is labeled by incorporation of FITC-dUTP by DNA Polymerase I incorporation on DNAseI nicked chromosome spreads. Spreads double labeled for Runx2 and either K4-methylated Histone H3 on human (row F, r=0.81) and mouse (row G, r=0.72) chromosomes, K9-methylated Histone H3 on human chromosomes (row H, r=0.16), or S10-phosphorylated Histone H3 on mouse chromosomes (row I, r=-0.12) along with DAPI staining for DNA.

phylogenetically conserved Runt-homology DNA binding domain (Figure 6.1). This result indicates that chromosomal association is independent of Runx2 C-terminal functions, including interphase subnuclear targeting, that we have previously shown are essential for normal tissue development (Choi et al., 2001). Furthermore, a Runx2 DNA binding mutant that occurs in cleidocranial dysplasia is excluded from mitotic chromosomes (data not shown). Thus the recruitment of Runx2 to its cognate motifs, which is known to support formation of open chromatin, must be necessary for its putative mitotic function. This idea is strengthened by the observation that Runx2 foci are in regions of open chromatin as determined by colocalization studies with antibodies against histone modifications and DNAseI hypersensitivity assays performed on mitotic chromosomes (Figure 6.1).

The size and pairwise symmetry nature of the mitotic Runx2 foci and their localization with decondensed chromatin suggest that Runx2 is clustered at gene-rich chromosomal loci to perform a novel regulatory function. From a cytogenetic perspective, our microscopic data localize Runx2 to pericentromeric regions of human and mouse chromosomes; in diploid human cells Runx2 foci are positioned on the acrocentric chromosomes (Figure 6.2). These regions are known to contain hundreds of copies of ribosomal genes that are organized in tandem head-to-tail repeats (Gonzalez and Sylvester, 2001). Our bioinformatics analyses of human and mouse rDNA loci reveal the presence of multiple Runx consensus elements (Figure 6.2). We therefore postulated that the in situ localization of Runx2 during mitosis reflects association with the chromosomal loci of rDNA genes. This hypothesis

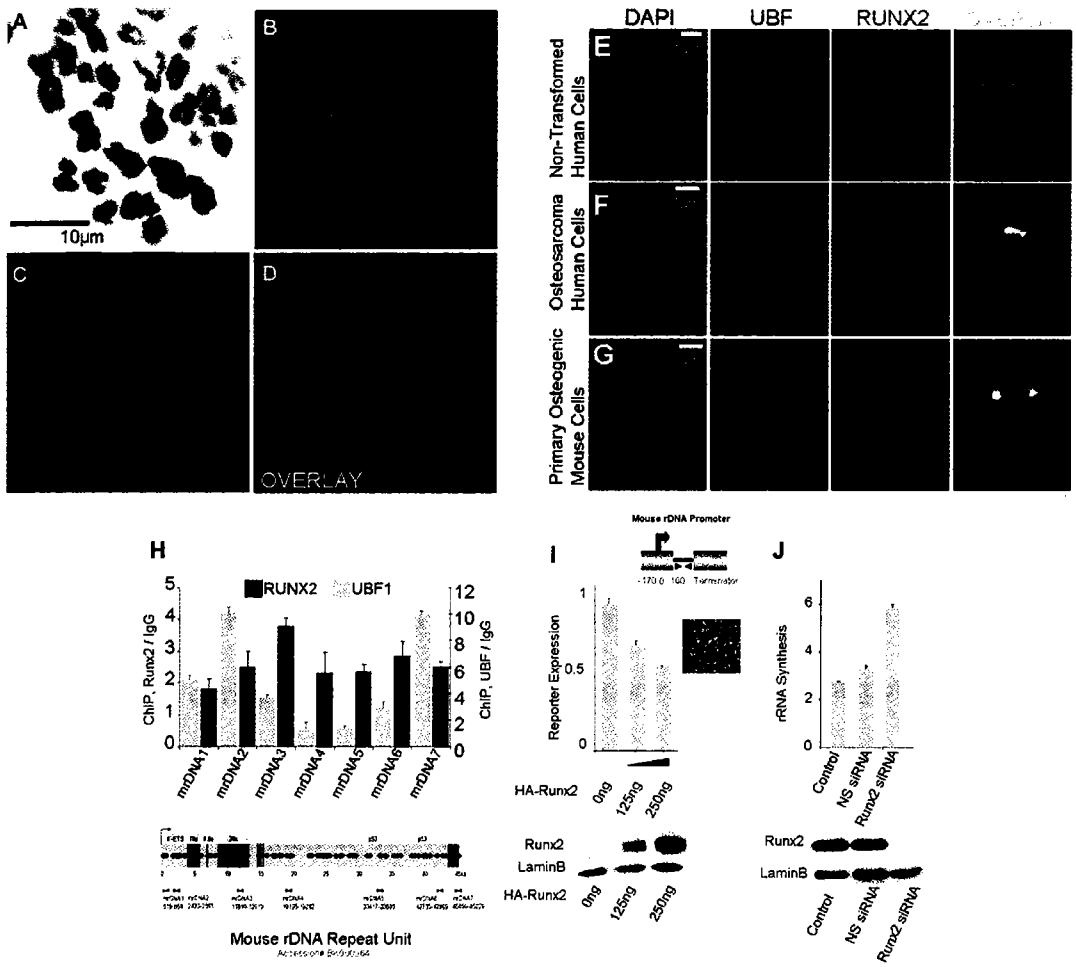

Figure 6.2: Runx2 Functionally Interacts with rDNA Loci

Mitotic chromosomes spreads were prepared for non-transformed human diploid MCF-10A cells (A-D and row E), human Saos-2 osteosarcoma (row F), primary calvarial cells (row G) from wild-type Runx2 mice, and processed for immunofluorescence microscopy using DAPI stain for DNA and antibodies directed against the Runx2 protein (green) and UBF1 (red). ChIP were performed on asynchronously growing Saos-2 (data not shown) and MC3T3 cells (H, top) using antibodies directed against Runx2, UBF1, and normal IgG as a control. Data of duplicate samples, which cover seven regions of the mouse rDNA repeat unit (hrDNA1-7) are shown as Runx2 or UBF1 versus IgG normalized to non-specific genomic DNA. Schematic of the mouse (H, bottom) rDNA repeat unit with Runx binding elements located with red diamonds. Primer locations for Chromatin immunoprecipitation assays (ChIP) are shown in blue and sequences are outlined in Table I. MC3T3 cells were transfected with a minimal mouse rDNA promoter construct, 500 ng with increasing concentrations of HA-Runx2. RNA polymerase I driven expression from the reporter was monitored in duplicate by Real time PCR with primers directed against unique transcribed sequences on the expression construct. Runx2 protein expression was monitored by western blot analysis along with Lamin B1 for control (I). Transfection efficiency was determined by independent transfection of GFP expression construct along with immunofluorescence microscopy. Where indicated Saos-2 cells were transfected with vehicle control, non-specific (NS) siRNA oligos or Runx2 siRNA oligos for 72 hrs (J). Runx2 protein expression was monitored by western blot analysis along with Lamin B1 for control. Pre-rRNA synthesis was monitored in duplicate by Real time PCR analysis using primers directed against unprocessed rRNA and 28s as a measure of total rRNA. Data is expressed as (Pre-rRNA versus 28s rRNA) x 100, see Table I for primer sequences.

challenges the current model that Runx proteins determine cell fate and cell cycle progression exclusively through control of RNA polymerase II transcribed genes.

The lineage-specific transcription factor Runx2 functionally associates with rDNA loci.

We directly examined whether Runx2 functionally interacts with rRNA genes during mitosis and interphase by immunofluorescence analysis, chromatin immunoprecipitations, and siRNA studies. The RNA polymerase I regulatory protein Upstream Binding Factor 1 (UBF1) has been shown to bind directly to rDNA repeats and its localization during mitosis is restricted to nucleolar organizing regions, which are mitotic precursors to interphase nucleoli (Mais et al., 2005; Gebrane-Younes et al., 1997; Suja et al., 1997; Rendon et al., 1994; Roussel et al., 1993; Zatsepina et al., 1993). In chromosome spreads from both human and mouse cells, we find that the Runx2 foci coincide with the focal pattern of UBF1 (Figure 6.2). We conclude that the large symmetrically positioned Runx2 foci are at nucleolar organizing regions that are enriched for spatially clustered rRNA genes.

To test at the molecular level whether Runx2 interacts with rDNA loci, we performed chromatin immunoprecipitations with interphase (Figure 6.2) and mitotic cells (Figure 6.5). We used antibodies directed against Runx2 and UBF1, and designed primer sets to amplify regions of the human and mouse rDNA repeats that are enriched in Runx elements (Figure 6.2). In actively proliferating cells, both Runx2 and UBF1 each interact with multiple distinct segments of the rDNA repeat unit, including the transcription

initiation regions (Figure 6.2). The interspersion of Runx2 and UBF1 binding events throughout the rDNA repeat unit indicates a proximity that is consistent with the in situ co-localization of the two proteins at nucleolar organizing regions.

The lineage-specific Runx transcription factors have not previously been implicated in the RNA polymerase I mediated biosynthesis of rRNAs. Interestingly, suppression of de novo ribosomal RNA synthesis accompanies cell differentiation in multiple lineages (Schwartz and Nilson, 1988; Donady et al., 1975; Maheshwari et al., 1993; Donady et al., 1973b), which more recently have been shown to be Runx dependent (Choi et al., 2001; Komori et al., 1997; Wang et al., 1996a; Inoue et al., 2002; Li et al., 2002; Flores et al., 1998). To establish whether Runx2 is rate-limiting for endogenous rRNA transcription, we depleted Runx2 levels using siRNA in proliferating cells and examined rRNA synthesis. Our results clearly show that reduction of Runx2 levels stimulates rRNA transcription (Figure 6.2). Additionally, forced expression of Runx2 inhibits expression from a minimal rRNA promoter (Figure 6.2). Taken together, our multiple lines of evidence indicate that Runx2 is a bona fide regulator of ribosomal biogenesis.

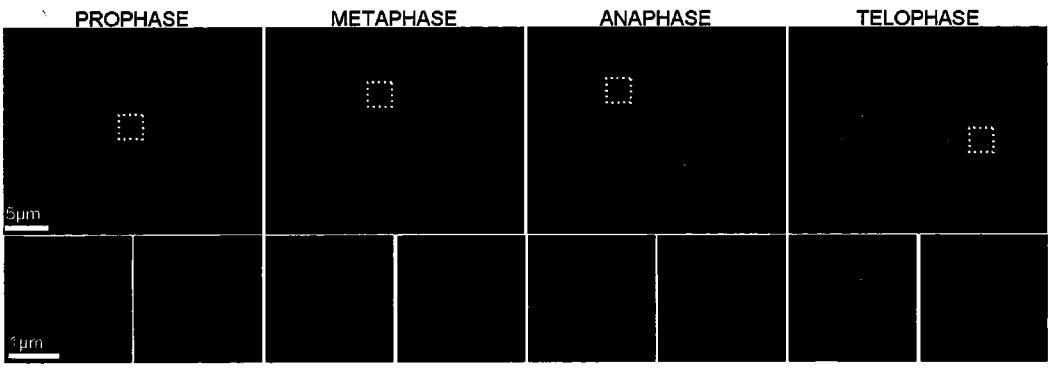

Figure 6.3: Runx2 Associates with Nucleolar Organizing Regions during Mitotic Progression

Asynchronously growing Saos-2 and Primary Mouse calvarial cells (data not shown) were fixed and processed for in situ immunofluorescence microscopy using antibodies directed against Runx2 (green) and UBF1 (red). Single image z-planes are shown from deconvoluted z-series stacks. Cells in the stages of mitosis: Prophase, Metaphase, Anaphase, and Telophase were identified by DNA morphology as visualized by DAPI staining. Overlay images of Runx2, UBF1 and DAPI staining are shown. The inset region in overlay images is reflected below with Runx2/DAPI overlay and UBF1/DAPI overlay images.

Runx2 remains associated with rDNA repeats during post-mitotic nucleolar formation.

During interphase the majority of Runx2 is organized in punctate subnuclear domains throughout the nucleus (Young et al., 2004; Zaidi et al., 2001a). Yet our data demonstrate the presence of Runx2 at nucleolar organizing regions of mitotic chromosomes that contain transcriptionally silent rDNA repeats. Combined with our finding that Runx2 controls rRNA biosynthesis, we predicted that Runx2 maintains its in situ localization with chromosomal NORs when they organize into nucleoli during progression from mitosis into G1.

Immunofluorescence microscopy of actively proliferating cells reveals that Runx2 colocalizes with UBF1 at NORs during multiple stages of mitosis (Figure 6.3). Significant overlap between Runx2 and UBF1 occurs during metaphase and anaphase when chromosomes are maximally condensed. When ribosomal biogenesis resumes in interphase, the rRNA transcriptional regulator UBF1 is present throughout each nucleolus and concentrates at foci, which have been shown to reflect sites of rRNA synthesis (Roussel et al., 1993; Cheutin et al., 2002) (Figure 6.4). Runx2 exhibits a punctate distribution throughout the nucleus, yet a subset of Runx2 foci is localized in the nucleolar periphery with UBF1 foci (Figure 6.4). The presence of Runx2 in nucleoli is evident at the ultrastructural level in whole cells and nuclear-matrix intermediate filament preparations (Figure 6.4). Our demonstration that Runx2 remains associated with mitotic NOR's and transition to nucleoli in interphase indicates a heritable and lineage-specific component to the regulation of rRNA synthesis.

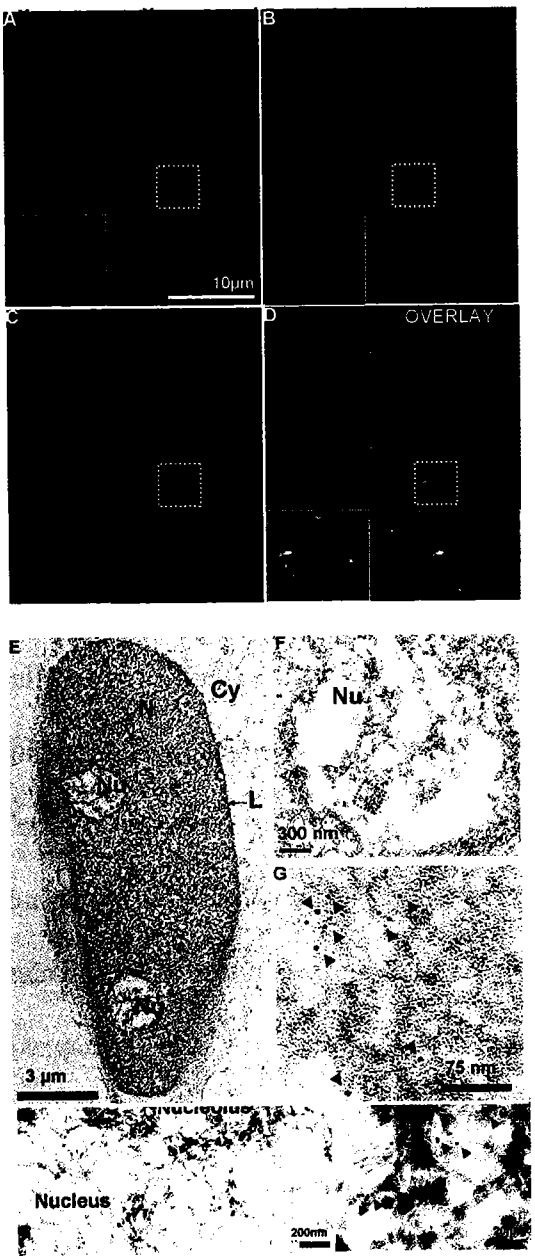

Figure 6.4: Runx2 is Localized to Nucleoli in Interphase Cells

Asynchronously growing Saos-2 cells were fixed and processed for in situ immunofluorescence microscopy using antibodies directed against Runx2 (green, B) and UBF1 (red, C); DNA was visualized by DAPI staining (blue, A). An interphase cell is shown with insets reflecting the localization of a Nucleolus. The overlay image shows Runx2 and UBF1 colocalization, and has two inset images of a nucleolus: one, on the lower-left, with the Runx2 and UBF1 overlay and a second, on the lower-right with Runx2, UBF1, and DAPI overlay (D). Proliferating Saos-2 cells were permeabilized in 0.5% Triton X-100 in cytoskeletal Buffer before fixation in formaldehyde and staining with an anti-Runx2 polyclonal antibody and a second antibody coupled to 5 nm gold beads as described (Nickerson et al., 1990). Samples were postfixed in glutaraldehyde, embedded in Epon, sectioned, and sections were counterstained with uranyl acetate-lead citrate (E-G). The inset in (E) outlining a nucleolus is shown in (F). The inner nucleolar region that is surrounded by the inset in (F) is shown in (G). Nuclear matrix intermediate filament preparations of Saos-2 cells were stained with an anti-Runx2 polyclonal antibody and a second antibody coupled to 5nm gold beads and processed for EM as whole-mount preparations. An inner region of the nucleus is shown with a portion of a nucleolus (H). The inner nucleolar region that is surrounded by the inset in (H) is shown in (I). Arrowheads in (G) and (I) indicate gold beads.

Runx2 exhibits alterations in spatial association with rDNA during cell cycle progression.

Ribosomal biogenesis is stringently regulated and occurs at a maximal rate in proliferating cells compared with quiescent and differentiated cells (Mauck and Green, 1973; Johnson et al., 1976; Grummt et al., 1976; Schwartz and Nilson, 1988; Donady et al., 1975; Maheshwari et al., 1993; Donady et al., 1973a). Key cell cycle transitions influencing rRNA synthesis rates are at the Mitosis to G1, the G0 to G1, and the G1 to S phase transitions (Voit et al., 1999; Voit and Grummt, 2001b; Klein and Grummt, 1999; Li et al., 2005; Pliss et al., 2005; Junera et al., 1995). To determine if Runx2 occupancy at ribosomal DNA is modulated during these transitions, we examined interaction of Runx2 with both coding and intergenic regulatory regions of the repeat unit during the cell cycle. Using chromatin immunoprecipitation analysis with synchronized cells, we find specific changes in the binding of Runx2 and UBF at the rDNA locus (Figure 6.5). For both proteins the occupancy increases during G0/G1 and G1/S, but not significantly during M/G1 (Figure 6.5). Because each of these transitions is characterized by an increase in ribosomal RNA expression (Figure 6.5), the extent of Runx2 or UBF occupancy can not completely account for the mechanism of regulation. This observation is consistent with the cell cycle dependent post-translational modifications that are known to regulate UBF function but not its localization with rDNA (Voit et al., 1999; Voit and Grummt, 2001a).

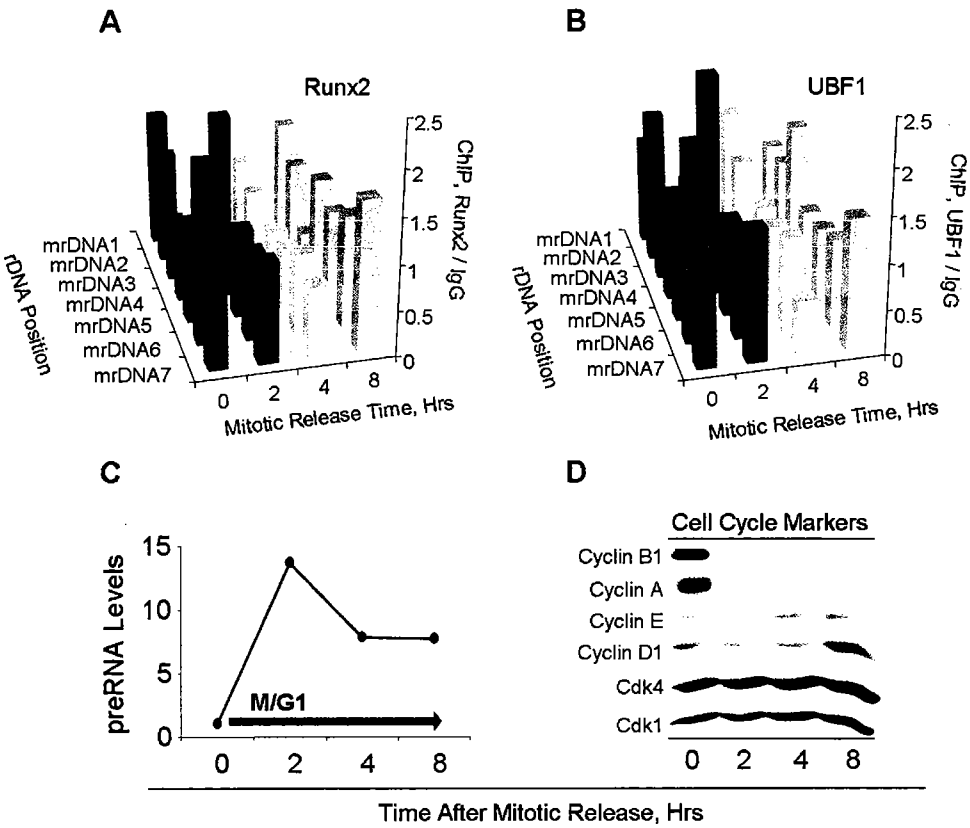

Figure 6.5: Cell cycle dependent alterations in Runx2 interactions with rDNA loci

MC3T3 cells were synchronized in mitosis (A-D) by a combination of nocodazole treatment and shake-off. Mitotic cells (0 Hrs) were taken directly for assays after shake-off. Cells in early G1 (2, 4, and 8 hrs) were obtained by washing and replating mitotic cells in fresh growth media. Cells were synchronized in G0 by serum starvation for 48 hrs. G0 synchronized cells were either processed for assays or restimulated with serum to obtain cells at the G0/G1 transition and the G1/S transition. At all time points in both synchronies cells were obtained for protein, RNA, and chromatin immunoprecipitation assays. ChIP was carried out using antibodies directed against Runx2 (A,E), UBF1 (B,F), and normal IgG as a control. ChIP DNA was analyzed by qPCR for seven regions (primer mrDNA1-7) of the mouse rDNA repeat along with a control non-specific genomic DNA reaction for normalization, see Table I for sequences. Data are shown as Runx2 or UBF1 versus IgG and normalized to non-specific genomic DNA. Pre-rRNA synthesis was monitored at each time point by qPCR (C,G). Cell synchronization was monitored by western blot of cell cycle proteins (D,I). The M/G1 transition was defined by monitoring Cyclin B1 levels. The G0/G1 transition was defined by monitoring the phosphorylation status of the Retinoblastoma protein. S-Phase was determined by monitoring DNA content by FACS analysis along with replication dependent histone H4/n expression by qPCR (H). ChIP data reflecting Runx2 and UBF occupancy at each rDNA primer set location were averaged across the M/G1 (0-8 hrs), G0/G1 (0-9 hrs), and G1/S transitions (12-18 hrs). To establish a standardized spatial occupancy profile for each cell cycle transition the time averaged ChIP data were then standardized between the seven rDNA primer sets. To illustrate Runx2 and UBF spatial occupancy in the context of the repetitive nature of the repeats three sets of standardized spatial occupancy profiles are plotted in series (J). To determine the degree of spatial dynamics between cell cycle stages the Pearson's correlation coefficient was computed comparing spatial occupancy profiles between each cell cycle transition (K). Pearson's correlation coefficients near one are consistent with a temporally static spatial profile.

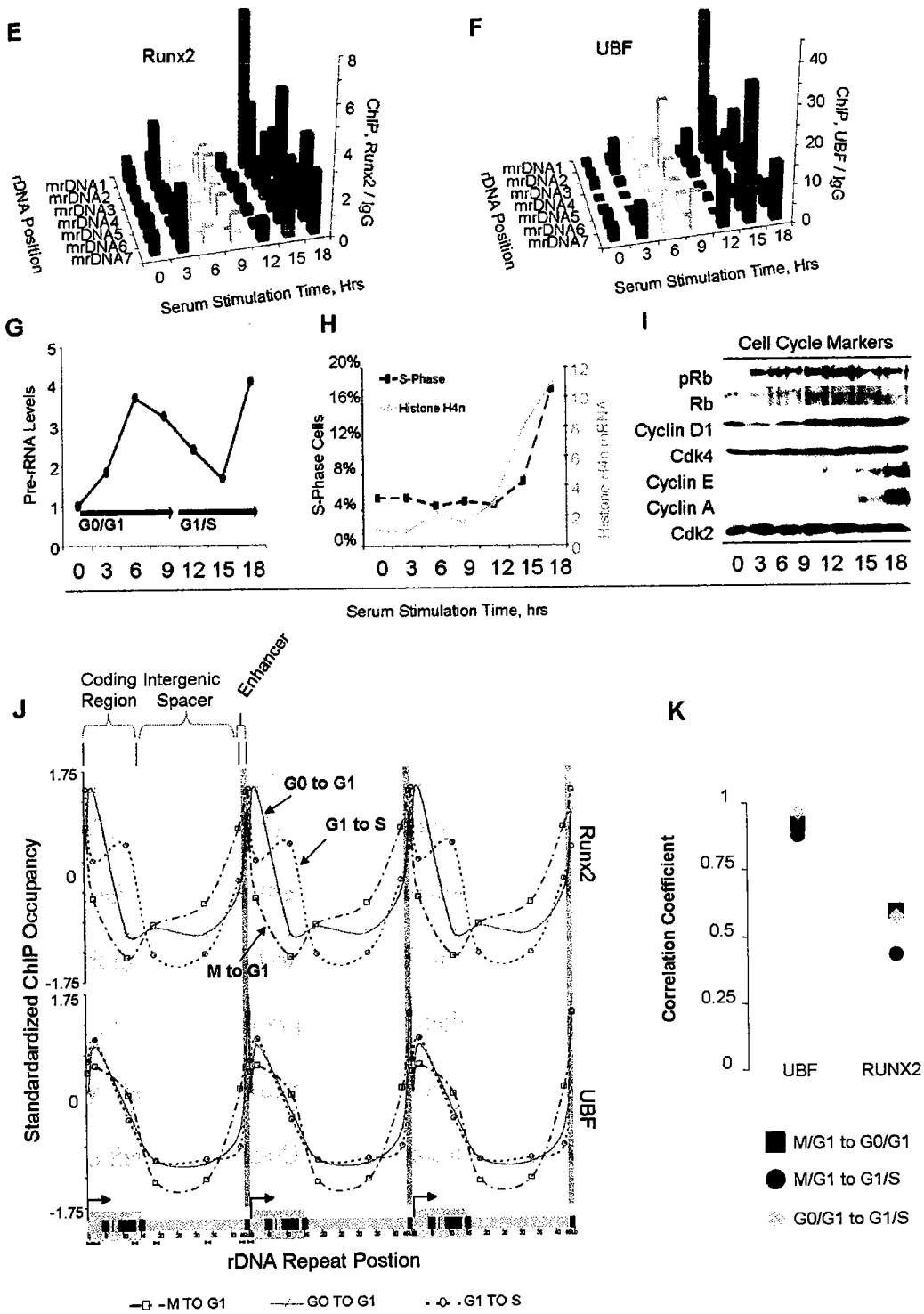

Figure 6.5: Cell cycle dependent alterations in Runx2 interactions with rDNA loci (cont.)

We next examined the spatial interactions of UBF1 and Runx2 with the rDNA repeat during cell cycle progression. The average occupancy of Runx2 and UBF1 proteins across the rDNA repeat unit was determined for the M/G1, G0/G1, and G1/S transitions using qPCR data from the complete set of chromatin immunoprecipitations. We find that the spatial organization of UBF is temporally static during these major changes in rRNA synthesis with preferential binding at the enhancer and transcriptional initiation regions (Figure 6.5). These results reflect the architectural role of UBF1 in organizing large-scale rDNA structure and suggest that this structure is maintained during cell cycle (Bazett-Jones et al., 1994; Wolffe, 1994; Mais et al., 2005; Stefanovsky et al., 2001). In contrast, the rDNA occupancy of Runx2 is spatially dynamic during progression of the cell cycle. Maximal Runx2 binding shifts from within the transcriptional initiation region during M/G1 and G1/S into the 5' transcribed region during G0/G1 (Figure 6.5). Additionally, Runx2 occupancy increases in intergenic regulatory regions during the M/G1 transition as well as in the transcription termination regions during the G1/S transition. Runx proteins are known to influence chromatin structure as an essential component of their gene regulatory function. We propose that Runx2 may facilitate lineage-specific and cell-cycle dependent alterations in rDNA organization that attenuates UBF1 activation of rRNA synthesis.

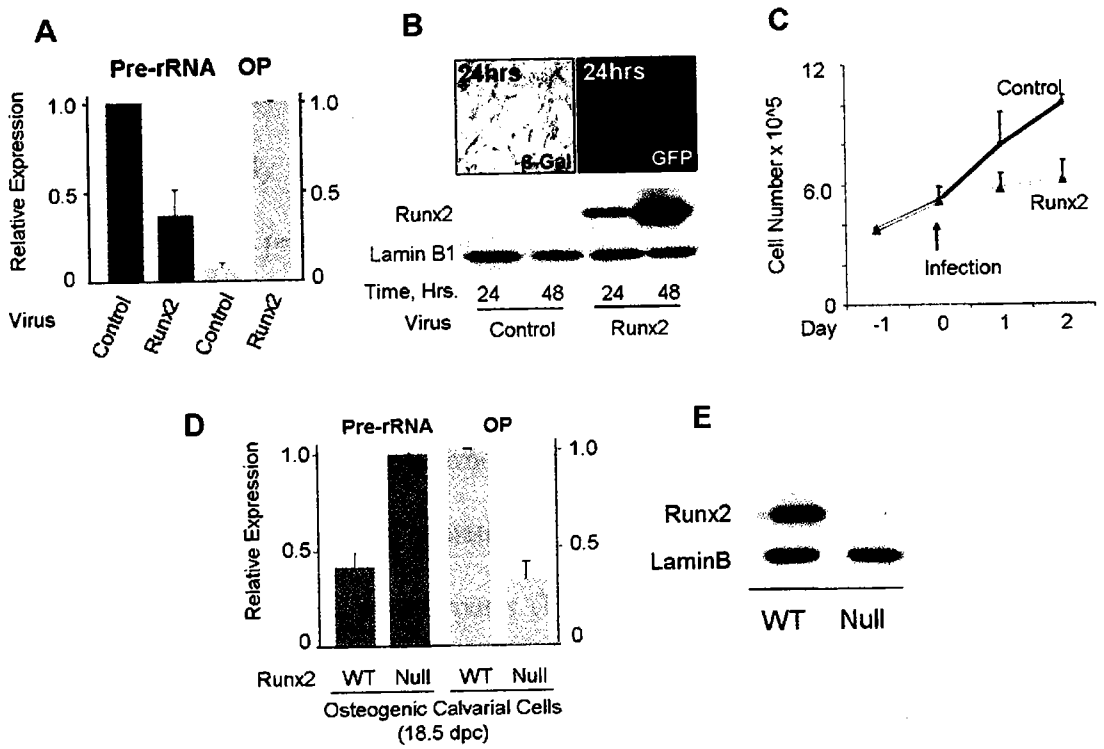

Figure 6.6: Repression of rRNA by Runx2 is coupled with inhibition of cell proliferation and induction of tissue-specific gene expression

Human IMR-90 fibroblasts where infected with adenoviral particles containing a CMV driven Runx2-IRES-GFP or control LacZ transgenes. At 48 hrs, pre-rRNA synthesis and the differentiation marker osteopontin (A) were analyzed in duplicate by qPCR, normalized to total rRNA and plotted relative to maximum between control and Runx2 infections. Runx2 protein levels (B) and Cell number (C) were monitored for up to 48 hrs post infection. Infection efficiency was monitored by LacZ staining and GFP protein expression (B). Primary calvarial cells were isolated from mouse embryos (17.5 dpc) homozygous for the wild-type Runx2 allele or the Runx2 null allele using standard procedures. Pre-rRNA synthesis and the differentiation marker osteopontin were analyzed in duplicate by qPCR, normalized to total rRNA and plotted relative to maximum between wild-type and null cells (D) and Runx2 protein was assessed by western analysis (E).

Runx2 repression of rRNA synthesis is associated with inhibition of cell proliferation and induction of lineage-specific gene expression

Our data clearly demonstrate that Runx2 functionally associates with rDNA repeats during cell cycle progression. To assess the biological consequences of modulating Runx2 levels, we examined rRNA synthesis in mesenchymal cells in which Runx2 is ectopically expressed or in Runx2 null cells (Figure 6.6). Upregulation of Runx2 decreases pre-rRNA synthesis with a concomitant suppression of cell proliferation. Consistent with Runx2 driven lineage progression, this induction stimulates expression of the phenotypic marker osteopontin, a Runx2 target gene (Figure 6.6) (Sato et al., 1998). Furthermore, osteogenic mesenchymal precursors in which Runx2 expression has been genetically ablated exhibit enhanced rRNA synthesis compared with wild-type counterparts (Figure 6.6). We also observe a reduction in osteopontin expression in Runx2 null cells that are compromised in capacity for lineage progression (Figure 6.6). We conclude that inhibition of rRNA synthesis and cell proliferation by Runx2 is intrinsically coupled with promotion of cell lineage commitment and retention of cell identity.

CONCLUSION

Here we report that Runx2 dynamically and functionally associates with ribosomal DNA loci during interphase and mitosis to regulate ribosomal rRNA synthesis. Our data indicate that the retention of Runx2 at nucleolar organizing regions on mitotic chromosomes provides a basis for conveying lineage-specific control of ribosomal RNA gene expression to progeny cells. This fundamental finding has major biomedical and biological ramifications.

It is currently appreciated that Runx proteins are fundamental gene regulatory factors that control essential aspects of metazoan development and are associated with human genetic disorders and cancer. The functional linkage between Runx2 control of rRNA synthesis, proliferation, and differentiation provides insight into the tissue-specific phenotype associated with Treacher Collins Syndrome (TCS). This syndrome is characterized by craniofacial bone defects and growth retardation that is causally linked with deregulated ribosome production (Valdez et al., 2004). Loss-of-function mutations in Runx2 cause Cleidocranial Dysplasia (CCD), which is predominantly characterized by craniofacial bone abnormalities including those observed in TCS (Otto et al., 2002). Because Runx2 controls bone development in tissues affected in TCS, the phenotypic penetrance of the disease can now be interpreted within the context of bone lineage-restricted regulation of ribosomal biogenesis by Runx2.

The pivotal contribution of Runx in establishing and maintaining phenotype has been attributed to combined roles in cell proliferation and differentiation. Our discovery that Runx2 regulates ribosomal biogenesis, which is intricately connected with cell

growth, represents a paradigm shifting finding. Thus, Runx2 coordinately controls growth, proliferation, and differentiation to establish cell identity. From a broader biological perspective lineage-specific control of ribosomal biogenesis may be a fundamental function of transcription factors that govern cell fate.

GENERAL DISCUSSION

Mechanisms controlling cell cycle progression, growth and differentiation, have been investigated in this thesis with the underlying goal to understand how the gene regulatory machinery that are central to these processes function in the context of nuclear organization. The Runx family of transcription factors is selected as a model system, based on three rationales: they (i.) have essential roles in cell fate determination to support animal development; (ii.) control the activation and repression of genes that mediate cell cycle progression and exit for differentiation; and (iii.) influence multiple aspects of nuclear architecture: including sequence-specific DNA binding at gene regulatory regions, organization of promoter chromatin structure, and are functionally compartmentalized in multiple foci throughout the nucleus.

The involvement of SWI/SNF chromatin remodeling complexes in Runx2-dependent osteoblast differentiation highlights the requirement for regulation at the level of chromatin structure in the establishment of cell phenotypic properties. Using primary cells that are homozygous for the Runx2 null allele, this work reveals that Runx2 is required for BMP2 mediated induction of the osteoblast differentiation and confirms the findings of others (Lee et al., 2000; Franceschi and Xiao, 2003). This thesis extends this concept by demonstrating that, BMP2 and Runx2 are not sufficient for osteogenic differentiation in the presence of a dominant negative SWI/SNF chromatin remodeling complex, which indicates that chromatin remodeling activity is critical for the induction of osteoblast differentiation by Runx2. These results are consistent with the observation that chromatin remodeling and activation of the bone-specific osteocalcin (OC) promoter

require promoter binding of Runx proteins (Javed et al., 1999; Montecino et al., 1996). Since, Runx proteins are not competent to remodel chromatin (Gutierrez et al., 2002), but interact with a host of chromatin remodeling factors (Gutierrez et al., 2002; Javed et al., 1999), these results predict that Runx2 recruits chromatin remodeling activity to skeletal gene promoters to support osteoblast differentiation. From the developmental perspective Runx2 null mice do not produce a mineralized skeleton (Komori et al., 1997). Furthermore, it is known that approximately one-out-of-ten, mice heterozygous for either the Brg1 or BAF155 null allele exhibit craniofacial defects (Bultman et al., 2000; Kim et al., 2001). Together these results indicate that the coordination of SWI/SNF mediated chromatin alterations by Runx2 proteins is critical component of osteoblast differentiation and skeletal development.

Several chromatin modifying enzymes and signaling factors interact with the Runx2 C-terminus. Knock-in studies from our laboratory reveal that this portion of the protein is essential for osteoblast differentiation and skeletal development (Choi et al., 2001). Follow-up studies reveal that this portion of the protein is also required for the inhibition of proliferation in osteoprogenitor cells (Pratap et al., 2003). The development of novel quantitative image analysis strategies (*i.e., intranuclear informatics*) in this thesis has facilitated the description and definition of nuclear organization in quantitative terms that are utilized for comparative analyses. Such work has revealed that a quantitative 'signature' of nuclear organization can be uniquely defined for regulatory proteins and, as an example, serve as a basis for statistical classification of biological function. Application of intranuclear informatics in this thesis has lead to the discovery

that the C-terminal portion of Runx2 provides a molecular determinant for the nuclear organization of Runx2 foci. Multivariate statistical analyses reveal that the subnuclear organization of Runx2 point mutants (i.e., Y428A and Y433A) is similar to that of the Runx2-ΔC mutant. These mutant proteins are functionally compromised and are incompetent for integrating physiological signals, which include BMP/TGFβ and Src/YAP signaling. These observations directly link Runx2 function with its organization in the nucleus. Consistent with this idea, intranuclear informatics studies further reveal that the organization of Runx2 proteins is conserved in progeny cells following mitotic division.

Mitotic cell division reflects a natural perturbation in nuclear structure and function. Chapters 4, 5, and 6 of this thesis comprise a series of studies that initiated with the examination of Runx2 during mitosis. At the outset, two basic questions were addressed: (i) what is fate of Runx2 foci? and (ii.) how progeny cells sustain competency for Runx2 dependent gene expression following mitotic division? Initial experiments were conducted with both Runx1 protein (in Jurkat T-cell lymphoma cells) and Runx2 proteins in (Rat Osteosarcoma Cells). These studies revealed that in both contexts, Runx proteins were equally partitioned to daughter cells following mitosis. Studies were continued that focus on Runx2 protein and revealed retention of the protein throughout all stages of mitosis. The focal organization of Runx2 was intact, but redistributed; a subset associated with mitotic chromosomes and another subset appeared associated with the mitotic apparatus. Localization of Runx2 with the mitotic apparatus promoted a follow-up study, which ultimately revealed the direct association of Runx2 with tubulin

and a working model for microtubule directed trafficking of the Runx2 protein (Pockwinse et al., 2005). The sequential reorganization of Runx2 proteins was assessed relative to other nuclear proteins that are involved in transcription and RNA processing. These results show that a sequential re-organization of Runx2 and its co-regulatory protein p300 in progeny nuclei precedes reappearance of SC35 RNA processing speckles. Image cross correlation analyses were developed to quantitatively define the temporal reorganization following mitosis. This strategy demonstrated in quantitative terms a sequential and selective reorganization of transcriptional regulators and RNA processing factors during progression of cell division that render progeny cells equivalently competent to support Runx2 mediated gene expression. It is well appreciated that during development asymmetric cell divisions are a primary mechanism for developing diversity in cell lineage (Roegiers and Jan, 2004). A compelling question that is relevant to the competency of progeny cells to support Runx2 mediated gene regulation, is if and how Runx2 protein is partitioned during asymmetric cell divisions.

The association of Runx2 with mitotic chromosomes was a striking observation. Because mitosis is a time when transcription is silenced and most transcription factors, including RNA polymerase II, are excluded from chromosomes the association of Runx2 with mitotic chromosomes suggested a novel regulatory role. A series of follow-up studies, comprising chapter 5 and 6, were carried out to determine the functional significance of this association. Site-directed mutagenesis was performed to establish that mitotic chromosome localization of Runx2 requires an intact DNA-binding domain, indicating that the association involves sequence-specific DNA binding.

Immunolocalization studies performed on chromosome spreads revealed that mitotic Runx2 foci are located in regions of chromatin that are hypersensitive to DNase I digestion and enriched in histone H3 that is methylated on lysine 4; this indicates that Runx2 is associated with regions containing transcriptionally competent genes (these observations became the underlying basis for chapter 6) and led to the hypothesis that Runx2 retains its association with target genes during mitosis. To test this hypothesis, a functional genomics strategy was designed that utilized RNAi technology, mitotic cell synchronization, and focused expression profiling with the goal of identifying Runx2 regulated genes that are modulated post-mitotically. This integrated approach identified more than thirty novel target genes involved in cell growth and differentiation, all of which were subsequently tested for Runx2 association by chromatin immunoprecipitation assays on proliferating cells. Fourteen genes were confirmed as bona fide Runx2 targets and were functionally validated in independent siRNA experiments. Importantly, ChIP assays were carried out on pure mitotic cells and revealed that Runx2 remains bound to these target gene promoters. This was the first demonstration of a cell fate determining transcription retaining association with genes during mitosis, and these findings suggested a mechanism for the retention of lineage-specific gene expression patterns during mitosis. Further experiments were carried out to reveal that these fourteen genes exhibit mitotic specific histone modifications that are indicative of the post-mitotic transcriptional state. Importantly, functional studies revealed that Runx2 proteins control both basal histone H4 acetylation as well as dimethylation of histone H3 lysine 4 at target gene promoters during mitosis. Taken together these observations indicate that the

Runx2 proteins have an active role in retaining phenotype during cell division to support lineage-specific control of gene expression in progeny cells. This work suggests that cell-fate determining transcription factors program cells to sustain phenotypic gene expression patterns following cell division when transcriptional competency is restored in progeny cells.

As a whole, these results have far-reaching implications to understanding the complex roles of Runx proteins in development and cancer. Runx proteins exhibit a complex phenotype with respect to tumorigenesis that includes properties of both tumor suppressors as well as oncoproteins (Cameron and Neil, 2004). Insight into the underlying mechanisms that give rise to this complexity was gained by examining the biological functions of Runx2 target genes identified in this work, notably, DNA repair, protein stability, cell cycle control, signaling competency, and lineage-specific differentiation. These results support the hypothesis that the multifaceted contributions of Runx proteins to oncogenesis are, in part, a consequence of a direct and broad-based influence on gene expression patterns. Preliminary analyses comparing the sensitivity of target genes to perturbations in Runx2 levels between non-transformed fibroblasts and tumor cell lines indicated that the directionality of control (i.e., activation or repression) by Runx2 is context dependent. It will be interesting to determine if this dependency correlates with the different tumorigenic properties of Runx proteins, to specific post-translation modifications, and/or with cell-type specific expression of co-regulatory proteins.

A number of experimental observations made during the study of Runx2 in mitosis have become the basis for a follow-up project in our laboratory. In the course of the work described in Chapters 4 through 6, it was discovered that Runx2 electrophoretic mobility is altered in mitosis and migrates at a higher molecular weight. Metabolic labeling studies with ^{32}P ortho-phosphate conducted by the author revealed that Runx2 is hyperphosphorylated in mitosis. These observations have been extended by Arun Rajgopal, a postdoctoral fellow in the Stein laboratory, to reveal that Runx2 is a target of the master mitotic kinase, Cdk1-CyclinB. A manuscript describing this work is in preparation and functional studies are being carried out to understand the significance of these results. Preliminary evidence indicates that this phosphorylation may be coupled with a mitotic specific interaction of Runx2 with the peptidyl-prolyl isomerase, Pin1. Interestingly, Pin1 modulates the mitotic structure and function of RNA polymerase II by interacting with the CTD and stabilizing the Cdk1-CyclinB phosphorylation(Albert et al., 1999; Xu et al., 2003). It will be interesting to understand the role of this hyper-phosphorylation in the mitotic control of target genes by Runx2.

By far the most serendipitous finding that has emerged in this thesis is that Runx2 controls RNA polymerase I driven ribosomal genes expression. Immunolocalization of Runx2 foci on mitotic chromosome spreads revealed several large foci with pairwise symmetry on sister chromatids on a subset of chromosomes. Further work identified that these foci were located at regions of active chromatin, and studies with diploid human cells localized these foci to the short-arm of human acrocentric chromosomes where nucleolar organization regions are known to reside. Colocalization studies revealed that

Runx2 chromosomal foci co-localize with the RNA polymerase I transcription factor, Upstream Binding Factor (UBF1). Furthermore, a bioinformatics analysis identified the presence of multiple Runx binding elements within regulatory regions of rRNA genes, and chromatin immunoprecipitation (ChIP) analysis established that Runx2 directly associates with ribosomal RNA genes. Reduction of Runx2 levels in human Saos-2 cells by siRNA activated rRNA transcription, indicating that ribosomal gene production is indeed Runx2 responsive. Both immunofluorescence as well as immunoelectron microscopy determined that a subset of Runx2 is localized to nucleoli where ribosomal genes reside and ribosomal biogenesis occurs. Cell synchronization strategies and ChIP assays were employed to demonstrate that the association of Runx2 with rDNA is a cell cycle regulated process. Functional linkage between Runx2 and ribosomal gene expression was further substantiated by demonstrating enhanced ribosomal RNA synthesis in primary cells isolated from the calvarial tissue of Runx2 null mice compared with wild-type Runx2 counterparts. Notably, induction of Runx2 in uncommitted mesenchymal cells directly repressed ribosomal biogenesis, and this repression of ribosomal gene expression by Runx2 is associated with cell growth inhibition and expression of osteoblast-specific genes. Taken together, this work reveals that Runx2 not only controls osteoblast lineage commitment, but also acts as a suppressor of cell growth by inhibiting rRNA synthesis. On a molecular level, this work extends knowledge of the regulatory functions of Runx proteins in RNA Polymerase II mediated transcription to include also RNA polymerase I. It is reasonable to predict that Runx proteins will also likely engage in RNA Polymerase III transcription. In this regard, Myc proteins provide

a precedence in that they have been shown to control transcription from all three polymerases (Oskarsson and Trumpp, 2005). These findings elucidate a model by which ribosomal biogenesis is coordinately controlled by the Runx2 transcription factor to support osteoblast differentiation and skeletal development. From a broader biological perspective lineage-specific control of ribosomal biogenesis may be a fundamental function of transcription factors that govern cell fate.

REFERENCES

Afzal,F., Pratap,J., Ito,K., Ito,Y., Stein,J.L., van Wijnen,A.J., Stein,G.S., Lian,J.B., and Javed,A. (2005). Smad function and intranuclear targeting share a Runx2 motif required for osteogenic lineage induction and BMP2 responsive transcription. J. Cell. Physiol. *204*, 63-72.

Agalioti,T., Lomvardas,S., Parekh,B., Yie,J., Maniatis,T., and Thanos,D. (2000). Ordered recruitment of chromatin modifying and general transcription factors to the IFN-beta promoter. Cell *103*, 667-678.

Ahrens,M., Ankenbauer,T., Schroder,D., Hollnagel,A., Mayer,H., and Gross,G. (1993). Expression of human bone morphogenetic proteins-2 or -4 in murine mesenchymal progenitor C3H10T1/2 cells induces differentiation into distinct mesenchymal cell lineages. DNA Cell Biol. *12*, 871-880.

Albert,A., Lavoie,S., and Vincent,M. (1999). A hyperphosphorylated form of RNA polymerase II is the major interphase antigen of the phosphoprotein antibody MPM-2 and interacts with the peptidyl-prolyl isomerase Pin1. J. Cell Sci. *112 (Pt 15)*, 2493-2500.

Arney,K.L. and Fisher,A.G. (2004). Epigenetic aspects of differentiation. J. Cell Sci. *117*, 4355-4363.

Balint,E., Lapointe,D., Drissi,H., van der Meijden,C., Young,D.W., van Wijnen,A.J., Stein,J.L., Stein,G.S., and Lian,J.B. (2003). Phenotype discovery by gene expression profiling: mapping of biological processes linked to BMP-2-mediated osteoblast differentiation. J. Cell. Biochem. *89*, 401-426.

Bangs,P., Burke,B., Powers,C., Craig,R., Purohit,A., and Doxsey,S. (1998). Functional analysis of Tpr: identification of nuclear pore complex association and nuclear localization domains and a role in mRNA export. J Cell Biol. *143*, 1801-1812.

Barnes,G.L., Hebert,K.E., Kamal,M., Javed,A., Einhorn,T.A., Lian,J.B., Stein,G.S., and Gerstenfeld,L.C. (2004). Fidelity of Runx2 activity in breast cancer cells is required for the generation of metastases associated osteolytic disease. Cancer Res. *64*, 4506-4513.

Barnes,G.L., Javed,A., Waller,S.M., Kamal,M.H., Hebert,K.E., Hassan,M.Q., Bellahcene,A., van Wijnen,A.J., Young,M.F., Lian,J.B., Stein,G.S., and Gerstenfeld,L.C. (2003). Osteoblast-related transcription factors Runx2 (Cbfa1/AML3) and MSX2 mediate the expression of bone sialoprotein in human metastatic breast cancer cells. Cancer Res. *63*, 2631-2637.

Barseguian,K., Lutterbach,B., Hiebert,S.W., Nickerson,J., Lian,J.B., Stein,J.L., van Wijnen,A.J., and Stein,G.S. (2002). Multiple subnuclear targeting signals of the leukemia-related AML1/ETO and ETO repressor proteins. Proc. Natl. Acad. Sci. U. S. A *99*, 15434-15439.

Bazett-Jones,D.P., Leblanc,B., Herfort,M., and Moss,T. (1994). Short-range DNA looping by the Xenopus HMG-box transcription factor, xUBF. Science *264*, 1134-1137.

Berezney,R. (2002). Regulating the mammalian genome: the role of nuclear architecture. Adv. Enzyme Regul. *42*, 39-52.

Berezney,R. and Jeon,K.W. (1995). Structural and functional organization of the nuclear matrix. (New York: Academic Press).

Berger,S.L. (2001). An embarrassment of niches: the many covalent modifications of histones in transcriptional regulation. Oncogene *20*, 3007-3013.

Berube,N.G., Smeenk,C.A., and Picketts,D.J. (2000). Cell cycle-dependent phosphorylation of the ATRX protein correlates with changes in nuclear matrix and chromatin association. Hum. Mol Genet. *9*, 539-547.

Blagosklonny,M.V. and Pardee,A.B. (2002). The restriction point of the cell cycle. Cell Cycle *1*, 103-110.

Blyth,K., Cameron,E.R., and Neil,J.C. (2005). The runx genes: gain or loss of function in cancer. Nat. Rev. Cancer *5*, 376-387.

Blyth,K., Terry,A., Mackay,N., Vaillant,F., Bell,M., Cameron,E.R., Neil,J.C., and Stewart,M. (2001). Runx2: a novel oncogenic effector revealed by in vivo complementation and retroviral tagging. Oncogene *20*, 295-302.

Brubaker,K.D., Vessella,R.L., Brown,L.G., and Corey,E. (2003). Prostate cancer expression of runt-domain transcription factor Runx2, a key regulator of osteoblast differentiation and function. Prostate *56*, 13-22.

Budde,A. and Grummt,I. (1999). p53 represses ribosomal gene transcription. Oncogene *18*, 1119-1124.

Buendia,B., Courvalin,J.C., and Collas,P. (2001). Dynamics of the nuclear envelope at mitosis and during apoptosis. Cell Mol. Life Sci. *58*, 1781-1789.

Bultman,S., Gebuhr,T., Yee,D., La Mantia,C., Nicholson,J., Gilliam,A., Randazzo,F., Metzger,D., Chambon,P., Crabtree,G., and Magnuson,T. (2000). A

Brg1 null mutation in the mouse reveals functional differences among mammalian SWI/SNF complexes. Mol. Cell *6*, 1287-1295.

Burke,B. and Ellenberg,J. (2002). Remodelling the walls of the nucleus. Nat. Rev. Mol. Cell Biol. *3*, 487-497.

Burstone,M.S. (1962). Alkaline phosphatase, naphthol AS-BI phosphate method. In Enzyme Histochemistry and Its Application on the Study of Neoplasm, M.S.Burstone, ed. (New York: Academic Press), pp. 275-276.

Cameron,E.R. and Neil,J.C. (2004). The Runx genes: lineage-specific oncogenes and tumor suppressors. Oncogene *23*, 4308-4314.

Capco,D.G. and Penman,S. (1983). Mitotic architecture of the cell: the filament networks of the nucleus and cytoplasm. J. Cell Biol. *96*, 896-906.

Carrington,W.A., Lynch,R.M., Moore,E.D., Isenberg,G., Fogarty,K.E., and Fay,F.S. (1995). Superresolution three-dimensional images of fluorescence in cells with minimal light exposure. Science *268*, 1483-1487.

Cheutin,T., O'Donohue,M.F., Beorchia,A., Vandelaer,M., Kaplan,H., Defever,B., Ploton,D., and Thiry,M. (2002). Three-dimensional organization of active rRNA genes within the nucleolus. J. Cell Sci. *115*, 3297-3307.

Chiba,H., Muramatsu,M., Nomoto,A., and Kato,H. (1994). Two human homologues of *Saccharomyces cerevisiae SW12/SNF2* and *Drosophila brahma* are transcriptional coactivators cooperating with the estrogen receptor and the retinoic acid receptor. Nucl. Acids Res. *22*, 1815-1820.

Choi,J.-Y., Pratap,J., Javed,A., Zaidi,S.K., Xing,L., Balint,E., Dalamangas,S., Boyce,B., van Wijnen,A.J., Lian,J.B., Stein,J.L., Jones,S.N., and Stein,G.S. (2001). Subnuclear targeting of Runx/Cbfa/AML factors is essential for tissue-specific differentiation during embryonic development. Proc. Natl. Acad. Sci. , USA *98*, 8650-8655.

Clark,P.J. and Evans,F.C. (1954). Distance to nearest neighbor as a measure of spatial relationships in populations. Ecology *35*, 445-453.

Coffman,J.A. (2003). Runx transcription factors and the developmental balance between cell proliferation and differentiation. Cell Biol. Int. *27*, 315-324.

Cook,P.R. (1999). The organization of replication and transcription. Science *284*, 1790-1795.

Cooper,S. (2004). Control and maintenance of mammalian cell size. BMC. Cell Biol. *5*, 35.

Cremer,T. and Cremer,C. (2001). Chromosome territories, nuclear architecture and gene regulation in mammalian cells. Nat. Rev. Genet. *2*, 292-301.

de la Serna,I., Carlson,K.A., Hill,D.A., Guidi,C.J., Stephenson,R.O., Sif,S., Kingston,R.E., and Imbalzano,A.N. (2000). Mammalian SWI-SNF complexes contribute to activation of the hsp70 gene. Mol. Cell Biol. *20*, 2839-2851.

de la Serna,I., Carlson,K.A., and Imbalzano,A.N. (2001). Mammalian SWI/SNF complexes promote MyoD-mediated muscle differentiation. Nat. Genet. *27*, 187-190.

DeFranco,D.B. (2002). Navigating Steroid Hormone Receptors through the Nuclear Compartment. Mol. Endocrinol. *16*, 1449-1455.

Dimario,P.J. (2004). Cell and molecular biology of nucleolar assembly and disassembly. Int. Rev. Cytol. *239*, 99-178.

Donady,J.J., Seecof,R.L., and Dewhurst,S. (1975). Actinomycin D-sensitive periods in the differentiation of Drosophila neurons and muscle cells in vitro. Differentiation *4*, 9-14.

Donady,J.J., Seecof,R.L., and Fox,M.A. (1973b). Differentiation of Drosophila cells lacking ribosomal DNA, in vitro. Genetics *73*, 429-434.

Donady,J.J., Seecof,R.L., and Fox,M.A. (1973a). Differentiation of Drosophila cells lacking ribosomal DNA, in vitro. Genetics *73*, 429-434.

Donnelly,K.P. (1978). Simulations to determine the variance and edge effect of total nearest-neighbor distance. In Simulation studies in archaelogy, I.Hodder, ed. (London: Cambridge University Press), pp. 91-95.

Drissen,R., Palstra,R.J., Gillemans,N., Splinter,E., Grosveld,F., Philipsen,S., and de,L.W. (2004). The active spatial organization of the beta-globin locus requires the transcription factor EKLF. Genes Dev. *18*, 2485-2490.

Dundr,M. and Misteli,T. (2001). Functional architecture in the cell nucleus. Biochem J *356*, 297-310.

Dyck,J.A., Maul,G.G., Miller,W.H., Chen,J.D., Kakizuka,A., and Evans,R.M. (1994). A novel macromolecular structure is a target of the promyelocyte-retinoic acid receptor oncoprotein. Cell *76*, 333-343.

Fan,H. and Penman,S. (1971). Regulation of synthesis and processing of nucleolar components in metaphase-arrested cells. J. Mol Biol. *59*, 27-42.

Flores,G.V., Daga,A., Kalhor,H.R., and Banerjee,U. (1998). Lozenge is expressed in pluripotent precursor cells and patterns multiple cell types in the Drosophila eye through the control of cell-specific transcription factors. Development *125*, 3681-3687.

Francastel,C., Schubeler,D., Martin,D.I., and Groudine,M. (2000). Nuclear compartmentalization and gene activity. Nat. Rev. Mol Cell Biol. *1*, 137-143.

Franceschi,R.T. and Xiao,G. (2003). Regulation of the osteoblast-specific transcription factor, Runx2: Responsiveness to multiple signal transduction pathways. J. Cell Biochem. *88*, 446-454.

Galindo,M., Pratap,J., Young,D.W., Hovhannisyan,H., Im,H.J., Choi,J.Y., Lian,J.B., Stein,J.L., Stein,G.S., and van Wijnen,A.J. (2005). The bone-specific expression of RUNX2 oscillates during the cell cycle to support a G1 related anti-proliferative function in osteoblasts. J. Biol. Chem. *280*, 20274-20285.

Gebrane-Younes,J., Fomproix,N., and Hernandez-Verdun,D. (1997). When rDNA transcription is arrested during mitosis, UBF is still associated with non-condensed rDNA. J Cell Sci. *110*, 2429-2440.

Gerhart,J., Wu,M., and Kirschner,M. (1984). Cell cycle dynamics of an M-phase-specific cytoplasmic factor in Xenopus laevis oocytes and eggs. J. Cell Biol. *98*, 1247-1255.

Gonzalez,I.L. and Sylvester,J.E. (2001). Human rDNA: evolutionary patterns within the genes and tandem arrays derived from multiple chromosomes. Genomics *73*, 255-263.

Gottesfeld,J.M. and Forbes,D.J. (1997). Mitotic repression of the transcriptional machinery. Trends Biochem. Sci. *22*, 197-202.

Grummt,I., Smith,V.A., and Grummt,F. (1976). Amino acid starvation affects the initiation frequency of nucleolar RNA polymerase. Cell *7*, 439-445.

Guidi,C.J., Sands,A.T., Zambrowicz,B.P., Turner,T.K., Demers,D.A., Webster,W., Smith,T.W., Imbalzano,A.N., and Jones,S.N. (2001). Disruption of Ini1 leads to peri-implantation lethality and tumorigenesis in mice. Mol. Cell Biol. *21*, 3598-3603.

Guo,B., Odgren,P.R., van Wijnen,A.J., Last,T.J., Nickerson,J., Penman,S., Lian,J.B., Stein,J.L., and Stein,G.S. (1995). The nuclear matrix protein NMP-1 is the transcription factor YY1. Proc. Natl. Acad. Sci. USA *92*, 10526-10530.

Gupta,S., Luong,M.X., Bleuming,S.A., Miele,A., Luong,M., Young,D., Knudsen,E.S., van Wijnen,A.J., Stein,J.L., and Stein,G.S. (2003). The tumor suppressor pRB functions as a co-repressor of the CCAAT displacement protein (CDP/cut) to regulate cell cycle controlled histone H4 transcription. J. Cell Physiol. *196*, 541-546.

Gutierrez,S., Javed,A., Tennant,D., van Rees,M., Montecino,M., Stein,G.S., Stein,J.L., and Lian,J.B. (2002). CCAAT/enhancer-binding proteins (C/EBP) b and d Activate osteocalcin gene transcription and synergize with Runx2 at the C/EBP element to regulate bone-specific expression. J. Biol. Chem. *277*, 1316-1323.

Gutierrez, S., Javed, A., Tennant, D., van Rees, M., van Wijnen, A. J., Stein, J. L., Stein, G. S., and Lian, J. B. C/EBP is a potent activator of osteocalcin gene transcription. J.Bone Miner.Res. 15, S497. 2000.
Ref Type: Abstract

Hanai,J., Chen,L.F., Kanno,T., Ohtani-Fujita,N., Kim,W.Y., Guo,W.-H., Imamura,T., Ishidou,Y., Fukuchi,M., Shi,M.J., Stavnezer,J., Kawabata,M., Miyazono,K., and Ito,Y. (1999). Interaction and functional cooperation of PEBP2/CBF with smads. Synergistic induction of the immmunoglobulin germline ca promoter. J. Biol. Chem. *274*, 31577-31582.

Harrington,K.S., Javed,A., Drissi,H., McNeil,S., Lian,J.B., Stein,J.L., van Wijnen,A.J., Wang,Y.-L., and Stein,G.S. (2002). Transcription factors RUNX1/AML1 and RUNX2/Cbfa1 dynamically associate with stationary subnuclear domains. J. Cell Sci. *115*, 4167-4176.

Hassan,A.H., Neely,K.E., Vignali,M., Reese,J.C., and Workman,J.L. (2001). Promoter targeting of chromatin-modifying complexes. Front Biosci. *6*, D1054-D1064.

He,D.C., Nickerson,J.A., and Penman,S. (1990). Core filaments of the nuclear matrix. J Cell Biol. *110*, 569-580.

Heinemeyer,T., Wingender,E., Reuter,I., Hermjakob,H., Kel,A.E., Kel,O.V., Ignatieva,E.V., Ananko,E.A., Podkolodnaya,O.A., Kolpakov,F.A., Podkolodny,N.L., and Kolchanov,N.A. (1998). Databases on transcriptional regulation: TRANSFAC, TRRD and COMPEL. Nucleic Acids Res. *26*, 362-367.

Hendzel,M.J., Wei,Y., Mancini,M.A., Van Hooser,A., Ranalli,T., Brinkley,B.R., Bazett-Jones,D.P., and Allis,C.D. (1997). Mitosis-specific phosphorylation of histone H3 initiates primarily within pericentromeric heterochromatin during G2 and spreads in an ordered fashion coincident with mitotic chromosome condensation. Chromosoma *106*, 348-360.

Hernandez-Verdun,D. and Roussel,P. (2003). Regulators of nucleolar functions. Prog. Cell Cycle Res. *5*, 301-308.

Horn,P.J. and Peterson,C.L. (2002). Molecular biology. Chromatin higher order folding--wrapping up transcription. Science *297*, 1824-1827.

Hovhannisyan,H., Cho,B., Mitra,P., Montecino,M., Stein,G.S., van Wijnen,A.J., and Stein,J.L. (2003). Maintenance of open chromatin and selective genomic occupancy at the cell-cycle-regulated histone H4 promoter during differentiation of HL-60 promyelocytic leukemia cells. Mol. Cell. Biol. *23*, 1460-1469.

Htun,H., Barsony,J., Renyi,I., Gould,D.L., and Hager,G.L. (1996). Visualization of glucocorticoid receptor translocation and intranuclear organization in living cells with a green fluorescent protein chimera. Proc. Natl. Acad. Sci. U. S. A. *93*, 4845-4850.

Iborra,F.J. and Cook,P.R. (2002). The interdependence of nuclear structure and function. Curr. Opin. Cell Biol. *14*, 780-785.

Imbalzano,A.N. and Xiao,H. (2004). Functional properties of ATP-dependent chromatin remodeling enzymes. Adv. Protein Chem. *67*, 157-179.

Inoue,K., Ozaki,S., Shiga,T., Ito,K., Masuda,T., Okado,N., Iseda,T., Kawaguchi,S., Ogawa,M., Bae,S.C., Yamashita,N., Itohara,S., Kudo,N., and Ito,Y. (2002). Runx3 controls the axonal projection of proprioceptive dorsal root ganglion neurons. Nat. Neurosci. *5*, 946-954.

Ito,Y. (2004). Oncogenic potential of the RUNX gene family: 'overview'. Oncogene *23*, 4198-4208.

Ito,Y. and Miyazono,K. (2003). RUNX transcription factors as key targets of TGF-beta superfamily signaling. Curr. Opin. Genet. Dev. *13*, 43-47.

Javed,A., Barnes,G.L., Pratap,J., Antkowiak,T., Gerstenfeld,L.C., van Wijnen,A.J., Stein,J.L., Lian,J.B., and Stein,G.S. (2005). Impaired intranuclear trafficking of Runx2 (AML3/CBFA1) transcription factors in breast cancer cells inhibits osteolysis in vivo. Proc. Natl. Acad. Sci. , USA *102*, 1454-1459.

Javed,A., Guo,B., Hiebert,S., Choi,J.-Y., Green,J., Zhao,S.-C., Osborne,M.A., Stifani,S., Stein,J.L., Lian,J.B., van Wijnen,A.J., and Stein,G.S. (2000). Groucho/TLE/R-Esp proteins associate with the nuclear matrix and repress RUNX (CBFa/AML/PEBP2a) dependent activation of tissue-specific gene transcription. J. Cell Sci. *113*, 2221-2231.

Javed,A., Gutierrez,S., Montecino,M., van Wijnen,A.J., Stein,J.L., Stein,G.S., and Lian,J.B. (1999). Multiple Cbfa/AML sites in the rat osteocalcin promoter are required for basal and vitamin D responsive transcription and contribute to chromatin organization. Mol. Cell. Biol. *19*, 7491-7500.

Jenuwein,T. and Allis,C.D. (2001). Translating the histone code. Science *293*, 1074-1080.

Johansen,K.M. (1996). Dynamic remodeling of nuclear architecture during the cell cycle. J. Cell Biochem. *60*, 289-296.

Johnson,L.F., Levis,R., Abelson,H.T., Green,H., and Penman,S. (1976). Changes in RNA in relation to growth of the fibroblast. IV. Alterations in theproduction and processing of mRNA and rRNA in resting and growing cells. J. Cell Biol. *71*, 933-938.

Junera,H.R., Masson,C., Geraud,G., and Hernandez-Verdun,D. (1995). The three-dimensional organization of ribosomal genes and the architecture of the nucleoli vary with G1, S and G2 phases. J. Cell Sci. *108 (Pt 11)*, 3427-3441.

Karpuj,M.V., Garren,H., Slunt,H., Price,D.L., Gusella,J., Becher,M.W., and Steinman,L. (1999). Transglutaminase aggregates huntingtin into nonamyloidogenic polymers, and its enzymatic activity increases in Huntington's disease brain nuclei. Proc. Natl. Acad. Sci. U. S. A *96*, 7388-7393.

Kastan,M.B. and Bartek,J. (2004). Cell-cycle checkpoints and cancer. Nature *432*, 316-323.

Katagiri,T., Yamaguchi,A., Komaki,M., Abe,E., Takahashi,N., Ikeda,T., Rosen,V., Wozney,J.M., Fujisawa-Sehara,A., and Suda,T. (1994). Bone morphogenetic protein-2 converts the differentiation pathway of C2C12 myoblasts into the osteoblast lineage. J. Cell Biol. *127*, 1755-1766.

Kerem,B.S., Goitein,R., Diamond,G., Cedar,H., and Marcus,M. (1984). Mapping of DNAase I sensitive regions on mitotic chromosomes. Cell *38*, 493-499.

Khavari,P.A., Peterson,C.L., Tamkun,J.W., Mendel,D.B., and Crabtree,G.R. (1993). BRG1 contains a conserved domain of the SWI2/SNF2 family necessary for normal mitotic growth and transcription. Nature *366*, 170-174.

Kim,J.K., Huh,S.O., Choi,H., Lee,K.S., Shin,D., Lee,C., Nam,J.S., Kim,H., Chung,H., Lee,H.W., Park,S.D., and Seong,R.H. (2001). Srg3, a mouse homolog of yeast SWI3, is essential for early embryogenesis and involved in brain development. Mol. Cell Biol. *21*, 7787-7795.

Klein,J. and Grummt,I. (1999). Cell cycle-dependent regulation of RNA polymerase I transcription: the nucleolar transcription factor UBF is inactive in mitosis and early G1. Proc. Natl. Acad. Sci. U. S. A *96*, 6096-6101.

Klochendler-Yeivin,A., Fiette,L., Barra,J., Muchardt,C., Babinet,C., and Yaniv,M. (2000). The murine SNF5/INI1 chromatin remodeling factor is essential for embryonic development and tumor suppression. EMBO Rep. *1*, 500-506.

Kobayashi,H., Gao,Y., Ueta,C., Yamaguchi,A., and Komori,T. (2000). Multilineage differentiation of Cbfa1-deficient calvarial cells in vitro. Biochem Biophys. Res. Commun. *273*, 630-636.

Kohwi,Y. and Kohwi-Shigematsu,T. (1995). [Biological significance of nuclear matrix attachment regions (MAR) and tissue specific MAR-DNA binding proteins]. Seikagaku *67*, 1115-1127.

Komori,T. (2002). Runx2, a multifunctional transcription factor in skeletal development. J Cell Biochem. *87*, 1-8.

Komori,T., Yagi,H., Nomura,S., Yamaguchi,A., Sasaki,K., Deguchi,K., Shimizu,Y., Bronson,R.T., Gao,Y.-H., Inada,M., Sato,M., Okamoto,R., Kitamura,Y., Yoshiki,S., and Kishimoto,T. (1997). Targeted disruption of *Cbfa1* results in a complete lack of bone formation owing to maturational arrest of osteoblasts. Cell *89*, 755-764.

Kosak,S.T. and Groudine,M. (2004). Form follows function: The genomic organization of cellular differentiation. Genes Dev. *18*, 1371-1384.

Kouskouti,A. and Talianidis,I. (2005b). Histone modifications defining active genes persist after transcriptional and mitotic inactivation. EMBO J. *24*, 347-357.

Kouskouti,A. and Talianidis,I. (2005a). Histone modifications defining active genes persist after transcriptional and mitotic inactivation. EMBO J. *24*, 347-357.

Kowenz-Leutz,E. and Leutz,A. (1999). A C/EBP beta isoform recruits the SWI/SNF complex to activate myeloid genes. Mol. Cell *4*, 735-743.

Kozubek,S., Lukasova,E., Jirsova,P., Koutna,I., Kozubek,M., Ganova,A., Bartova,E., Falk,M., and Pasekova,R. (2002). 3D Structure of the human genome: order in randomness. Chromosoma *111*, 321-331.

Kruhlak,M.J., Hendzel,M.J., Fischle,W., Bertos,N.R., Hameed,S., Yang,X.J., Verdin,E., and Bazett-Jones,D.P. (2001). Regulation of global acetylation in mitosis through loss of histone acetyltransferases and deacetylases from chromatin. J Biol. Chem. *276*, 38307-38319.

Kundu,M., Javed,A., Jeon,J.P., Horner,A., Shum,L., Eckhaus,M., Muenke,M., Lian,J.B., Yang,Y., Nuckolls,G.H., Stein,G.S., and Liu,P.P. (2002). Cbfbeta interacts with Runx2 and has a critical role in bone development. Nat. Genet. *32*, 639-644.

Lachner,M., O'Sullivan,R.J., and Jenuwein,T. (2003). An epigenetic road map for histone lysine methylation. J. Cell Sci. *116*, 2117-2124.

Lamond,A.I. and Spector,D.L. (2003). Nuclear speckles: a model for nuclear organelles. Nat. Rev. Mol. Cell Biol. *4*, 605-612.

Lee,K.S., Kim,H.J., Li,Q.L., Chi,X.Z., Ueta,C., Komori,T., Wozney,J.M., Kim,E.G., Choi,J.Y., Ryoo,H.M., and Bae,S.C. (2000). Runx2 is a common target of transforming growth factor beta1 and bone morphogenetic protein 2, and cooperation between runx2 and smad5 induces osteoblast-specific gene expression in the pluripotent mesenchymal precursor cell line C2C12. Mol. Cell Biol. *20*, 8783-8792.

Lemon,B. and Tjian,R. (2000). Orchestrated response: a symphony of transcription factors for gene control. Genes Dev. *14*, 2551-2569.

Li,C. and Wong,W.H. (2001). Model-based analysis of oligonucleotide arrays: expression index computation and outlier detection. Proc. Natl. Acad. Sci. U. S. A *98*, 31-36.

Li,J., Santoro,R., Koberna,K., and Grummt,I. (2005). The chromatin remodeling complex NoRC controls replication timing of rRNA genes. EMBO J. *24*, 120-127.

Li,Q.L., Ito,K., Sakakura,C., Fukamachi,H., Inoue,K., Chi,X.Z., Lee,K.Y., Nomura,S., Lee,C.W., Han,S.B., Kim,H.M., Kim,W.J., Yamamoto,H., Yamashita,N., Yano,T., Ikeda,T., Itohara,S., Inazawa,J., Abe,T., Hagiwara,A., Yamagishi,H., Ooe,A., Kaneda,A., Sugimura,T., Ushijima,T., Bae,S.C., and Ito,Y. (2002). Causal relationship between the loss of RUNX3 expression and gastric cancer. Cell *109*, 113-124.

Lian,J.B., Javed,A., Zaidi,S.K., Lengner,C., Montecino,M., van Wijnen,A.J., Stein,J.L., and Stein,G.S. (2004). Regulatory controls for osteoblast growth and differentiation: role of Runx/Cbfa/AML factors. Crit Rev. Eukaryot. Gene Expr. *14*, 1-41.

Lian,J.B. and Stein,G.S. (2003). The Temporal and Spatial Subnuclear Organization of Skeletal Gene Regulatory Machinery: Integrating Multiple Levels of Transcriptional Control. Calcif. Tissue Int. *72*, 631-637.

Lisby,M. and Rothstein,R. (2004). DNA damage checkpoint and repair centers. Curr. Opin. Cell Biol. *16*, 328-334.

Louvet,E., Junera,H.R., Le,P.S., and Hernandez-Verdun,D. (2005). Dynamics and compartmentation of the nucleolar processing machinery. Exp. Cell Res. *304*, 457-470.

Lund,A.H. and van Lohuizen,M. (2002). RUNX: a trilogy of cancer genes. Cancer Cell *1*, 213-215.

Lutterbach,B. and Hiebert,S.W. (2000). Role of the transcription factor AML-1 in acute leukemia and hematopoietic differentiation. Gene *245*, 223-235.

Ma,H., Samarabandu,J., Devdhar,R.S., Acharya,R., Cheng,P.C., Meng,C., and Berezney,R. (1998). Spatial and temporal dynamics of DNA replication sites in mammalian cells. J. Cell Biol. *143*, 1415-1425.

Ma,H., Siegel,A.J., and Berezney,R. (1999). Association of chromosome territories with the nuclear matrix. Disruption of human chromosome territories correlates with the release of a subset of nuclear matrix proteins. J. Cell Biol. *146*, 531-542.

Maheshwari,Y., Rao,M., Sykes,D.E., Tyner,A.L., and Weiser,M.M. (1993). Changes in ribosomal protein and ribosomal RNA synthesis during rat intestinal differentiation. Cell Growth Differ. *4*, 745-752.

Mais,C., Wright,J.E., Prieto,J.L., Raggett,S.L., and McStay,B. (2005). UBF-binding site arrays form pseudo-NORs and sequester the RNA polymerase I transcription machinery. Genes Dev. *19*, 50-64.

Mancini,M.A., Shan,B., Nickerson,J.A., Penman,S., and Lee,W.-H. (1994). The retinoblastoma gene product is a cell cycle-dependent, nuclear matrix-associated protein. Proc. Natl. Acad. Sci. USA *91*, 418-422.

Marmorstein,R. and Berger,S.L. (2001). Structure and function of bromodomains in chromatin-regulating complexes. Gene *272*, 1-9.

Martinez-Balbas,M.A., Dey,A., Rabindran,S.K., Ozato,K., and Wu,C. (1995). Displacement of sequence-specific transcription factors from mitotic chromatin. Cell *83*, 29-38.

Masui,Y. (1992). Towards understanding the control of the division cycle in animal cells. Biochem. Cell Biol. *70*, 920-945.

Masui,Y. and Wang,P. (1998). Cell cycle transition in early embryonic development of Xenopus laevis. Biol. Cell *90*, 537-548.

Mauck,J.C. and Green,H. (1973). Regulation of RNA synthesis in fibroblasts during transition from resting to growing state. Proc. Natl. Acad. Sci. U. S. A *70*, 2819-2822.

McNeil,S., Guo,B., Stein,J.L., Lian,J.B., Bushmeyer,S., Seto,E., Atchison,M.L., Penman,S., van Wijnen,A.J., and Stein,G.S. (1998). Targeting of the YY1 transcription factor to the nucleolus and the nuclear matrix in situ: the C-terminus is a principal determinant for nuclear trafficking. J. Cell. Biochem. *68*, 500-510.

McNeil,S., Zeng,C., Harrington,K.S., Hiebert,S., Lian,J.B., Stein,J.L., van Wijnen,A.J., and Stein,G.S. (1999). The t(8;21) chromosomal translocation in acute myelogenous leukemia modifies intranuclear targeting of the AML1/CBFalpha2 transcription factor. Proc. Natl. Acad. Sci. U. S. A. *96*, 14882-14887.

Merriman,H.L., van Wijnen,A.J., Hiebert,S., Bidwell,J.P., Fey,E., Lian,J., Stein,J., and Stein,G.S. (1995). The tissue-specific nuclear matrix protein, NMP-2, is a member of the AML/CBF/PEBP2/runt domain transcription factor family: interactions with the osteocalcin gene promoter. Biochemistry *34*, 13125-13132.

Misteli,T. (2001). Protein dynamics: implications for nuclear architecture and gene expression. Science *291*, 843-847.

Mitchison,T.J. and Salmon,E.D. (2001). Mitosis: a history of division. Nat. Cell Biol. *3*, E17-E21.

Moen,P.T., Jr., Johnson,C.V., Byron,M., Shopland,L.S., de,I.S., I, Imbalzano,A.N., and Lawrence,J.B. (2004). Repositioning of muscle-specific genes relative to the periphery of SC-35 domains during skeletal myogenesis. Mol. Biol. Cell *15*, 197-206.

Montecino,M., Lian,J., Stein,G., and Stein,J. (1996). Changes in chromatin structure support constitutive and developmentally regulated transcription of the bone-specific osteocalcin gene in osteoblastic cells. Biochemistry *35*, 5093-5102.

Muchardt,C., Reyes,J.-C., Bourachot,B., Legouy,E., and Yaniv,M. (1996). The hbrm and BRG-1 proteins, components of the human SNF/SWI complex, are phosphorylated and excluded from the condensed chromosomes during mitosis. EMBO J. *15*, 3394-3402.

Muchardt,C. and Yaniv,M. (1993). A human homologue of *Saccharomyces cerevisiae SNF2/SWI2* and *Drosophila brm* genes potentiates transcriptional activation by the glucocorticoid receptor. EMBO J. *12*, 4279-4290.

Muller,W.G., Walker,D., Hager,G.L., and McNally,J.G. (2001). Large-scale chromatin decondensation and recondensation regulated by transcription from a natural promoter. J. Cell Biol. *154*, 33-48.

Nasmyth,K. (2002). Segregating sister genomes: the molecular biology of chromosome separation. Science *297*, 559-565.

Neil,J., Stewart,M., Terry,A., O'Hara,M., Hu,M., Blyth,K., Baxter,E., Onions,D., and Cameron,E. (1999). Identification of murine CBF alpha1, a runt domain transcription factor, as a putative Myc collaborator in T cell lymphoma. Leukemia *13 Suppl 1*, S83-S86.

Nickerson,J.A., He,D.C., Krochmalnic,G., and Penman,S. (1990). Immunolocalization in three dimensions: immunogold staining of cytoskeletal and nuclear matrix proteins in resinless electron microscopy sections. Proc. Natl. Acad. Sci. USA *87*, 2259-2263.

Nickerson,J.A. and Penman,S. (1992a). Localization of nuclear matrix core filament proteins at interphase and mitosis. Cell Biol. Int. Rep. *16*, 811-826.

Nickerson,J.A. and Penman,S. (1992b). The nuclear matrix: structure and involvement in gene expression. In Molecular and Cellular Approaches to the Control of Proliferation and Differentiation, G.S.Stein and J.B.Lian, eds. (New York: Academic Press), pp. 343-380.

Nielsen,J.A., Hudson,L.D., and Armstrong,R.C. (2002). Nuclear organization in differentiating oligodendrocytes. J Cell Sci. *115*, 4071-4079.

Noordmans,H.J., van der,K.K., van Driel,R., and Smeulders,A.W. (1998). Randomness of spatial distributions of two proteins in the cell nucleus involved in mRNA synthesis and their relationship. Cytometry *33*, 297-309.

Norman,G.R. (2000). Biostatistics: The Bare Essentials. (Hamilton, Ontario: Decker, Inc.).

Nuthall,H.N., Joachim,K., Palaparti,A., and Stifani,S. (2002). A role for cell cycle-regulated phosphorylation in Groucho-mediated transcriptional repression. J. Biol. Chem. *277*, 51049-51057.

O'Farrell,P.H. (2001). Triggering the all-or-nothing switch into mitosis. Trends Cell Biol. *11*, 512-519.

Ogawa,E., Maruyama,M., Kagoshima,H., Inuzuka,M., Lu,J., Satake,M., Shigesada,K., and Ito,Y. (1993). PEBP2/PEA2 represents a family of transcription factors homologous to the products of the Drosophila runt gene and the human AML1 gene. Proc. Natl. Acad. Sci. USA *90*, 6859-6863.

Ohyama,K., Chung,C.H., Chen,E., Gibson,C.W., Misof,K., Fratzl,P., and Shapiro,I.M. (1997). p53 influences mice skeletal development. J. Craniofac. Genet. Dev. Biol. *17*, 161-171.

Osato,M. (2004). Point mutations in the RUNX1/AML1 gene: another actor in RUNX leukemia. Oncogene *23*, 4284-4296.

Oskarsson,T. and Trumpp,A. (2005). The Myc trilogy: lord of RNA polymerases. Nat. Cell Biol. *7*, 215-217.

Otto,F., Kanegane,H., and Mundlos,S. (2002). Mutations in the RUNX2 gene in patients with cleidocranial dysplasia. Hum. Mutat. *19*, 209-216.

Otto,F., Thornell,A.P., Crompton,T., Denzel,A., Gilmour,K.C., Rosewell,I.R., Stamp,G.W.H., Beddington,R.S.P., Mundlos,S., Olsen,B.R., Selby,P.B., and Owen,M.J. (1997). *Cbfa1*, a candidate gene for cleidocranial dysplasia syndrome, is essential for osteoblast differentiation and bone development. Cell *89*, 765-771.

Owen,T.A., Aronow,M., Shalhoub,V., Barone,L.M., Wilming,L., Tassinari,M.S., Kennedy,M.B., Pockwinse,S., Lian,J.B., and Stein,G.S. (1990). Progressive development of the rat osteoblast phenotype in vitro: reciprocal relationships in expression of genes associated with osteoblast proliferation and differentiation during formation of the bone extracellular matrix. J. Cell. Physiol. *143*, 420-430.

Pardee,A.B. (1989). G1 events and regulation of cell proliferation. Science *246*, 603-608.

Paredes,R., Gutierrez,J., Gutierrez,S., Allison,L., Puchi,M., Imschenetzky,M., van Wijnen,A., Lian,J., Stein,G., Stein,J., and Montecino,M. (2002). Interaction of the 1alpha,25-dihydroxyvitamin D3 receptor at the distal promoter region of the bone-specific osteocalcin gene requires nucleosomal remodelling. Biochem. J. *363*, 667-676.

Pedersen,T.A., Kowenz-Leutz,E., Leutz,A., and Nerlov,C. (2001). Cooperation between C/EBPalpha TBP/TFIIB and SWI/SNF recruiting domains is required for adipocyte differentiation. Genes Dev. *15*, 3208-3216.

Pederson,T. (2001). Protein mobility within the nucleus--what are the right moves? Cell *104*, 635-638.

Peterson,C.L. and Logie,C. (2000). Recruitment of chromatin remodeling machines. J. Cell Biochem. *78*, 179-185.

Peterson,C.L. and Tamkun,J.W. (1995). The SWI-SNF complex: a chromatin remodeling machine? Trends Biochem. Sci. *20*, 143-146.

Peterson,C.L. and Workman,J.L. (2000). Promoter targeting and chromatin remodeling by the SWI/SNF complex. Curr. Opin. Genet. Dev. *10*, 187-192.

Petrini,J.H. and Stracker,T.H. (2003). The cellular response to DNA double-strand breaks: defining the sensors and mediators. Trends Cell Biol. *13*, 458-462.

Pliss,A., Koberna,K., Vecerova,J., Malinsky,J., Masata,M., Fialova,M., Raska,I., and Berezney,R. (2005). Spatio-temporal dynamics at rDNA foci: global switching between DNA replication and transcription. J. Cell Biochem. *94*, 554-565.

Pockwinse, S., Rajigopa A, Young, D., Lian, J. B., van Wijnen, A. J., Stein, J. L., and Stein, G. S. Runx2 association with microtubules. Journal of Cellular Biochemistry . 2005.
Ref Type: Generic

Pombo,A. and Cook,P.R. (1996). The localization of sites containing nascent RNA and splicing factors. Exp. Cell Res. *229*, 201-203.

Pombo,A., Cuello,P., Schul,W., Yoon,J.B., Roeder,R.G., Cook,P.R., and Murphy,S. (1998). Regional and temporal specialization in the nucleus: a transcriptionally-active nuclear domain rich in PTF, Oct1 and PIKA antigens associates with specific chromosomes early in the cell cycle. EMBO J. *17*, 1768-1778.

Pombo,A., Jones,E., Iborra,F.J., Kimura,H., Sugaya,K., Cook,P.R., and Jackson,D.A. (2000). Specialized transcription factories within mammalian nuclei. Crit Rev. Eukaryot. Gene Expr. *10*, 21-29.

Prasanth,K.V., Sacco-Bubulya,P.A., Prasanth,S.G., and Spector,D.L. (2003). Sequential entry of components of gene expression machinery into daughter nuclei. Mol Biol. Cell *14*, 1043-1057.

Pratap,J., Galindo,M., Zaidi,S.K., Vradii,D., Bhat,B.M., Robinson,J.A., Choi,J.-Y., Komori,T., Stein,J.L., Lian,J.B., Stein,G.S., and van Wijnen,A.J. (2003). Cell growth regulatory role of Runx2 during proliferative expansion of pre-osteoblasts. Cancer Res. *63*, 5357-5362.

Pratap, J., Galindo, M., Zaidi, S. K., Vradii, D., Robinson, J. A., Bhat, B. M., Choi, J., Komori, T., Stein, J. L., Stein, G. S., and van Wijnen, A. J. Cell growth regulatory role of Runx2 during proliferative expansion of pre-osteoblasts. J.Bone Miner.Res. 17[Suppl 1], S151. 2002.
Ref Type: Abstract

Pratap, J., Vashi, S., Zhang, J., Languino, L., van Wijnen, A. J., Stein, J. L., Lian, J. B., and Stein, G. S. Runx2 regulates transcription of gelatinases (MMP9) in metastatic cancer cell lines and functionally related to cell migration. J.Bone Miner.Res. 19[Suppl 1], S123. 2004.
Ref Type: Abstract

Rendon,M.C., Bolivar,J., Ortiz,M., and Valdivia,M.M. (1994). Immunodetection of the ribosomal transcription factor UBF at the nucleolus organizer regions of fish cells. Cell Struct. Funct. *19*, 153-158.

Reyes,J.-C., Muchardt,C., and Yaniv,M. (1997). Components of the human SWI/SNF complex are enriched in active chromatin and are associated with the nuclear matrix. J. Cell Biol. *137*, 263-274.

Roberts,C.W., Galusha,S.A., McMenamin,M.E., Fletcher,C.D., and Orkin,S.H. (2000). Haploinsufficiency of Snf5 (integrase interactor 1) predisposes to malignant rhabdoid tumors in mice. Proc. Natl. Acad. Sci. U. S. A *97*, 13796-13800.

Rodan,G.A. (1995). Osteopontin overview. Ann. N. Y. Acad. Sci. *760*, 1-5.

Roegiers,F. and Jan,Y.N. (2004). Asymmetric cell division. Curr. Opin. Cell Biol. *16*, 195-205.

Roix,J.J., McQueen,P.G., Munson,P.J., Parada,L.A., and Misteli,T. (2003). Spatial proximity of translocation-prone gene loci in human lymphomas. Nat. Genet. *34*, 287-291.

Roussel,P., Andre,C., Masson,C., Geraud,G., and Hernandez-Verdun,D. (1993). Localization of the RNA polymerase I transcription factor hUBF during the cell cycle. J. Cell Sci. *104 (Pt 2)*, 327-337.

Salma,N., Xiao,H., Mueller,E., and Imbalzano,A.N. (2004). Temporal recruitment of transcription factors and SWI/SNF chromatin-remodeling enzymes during adipogenic induction of the peroxisome proliferator-activated receptor gamma nuclear hormone receptor. Mol. Cell Biol. *24*, 4651-4663.

Sato,M., Morii,E., Komori,T., Kawahata,H., Sugimoto,M., Terai,K., Shimizu,H., Yasui,T., Ogihara,H., Yasui,N., Ochi,T., Kitamura,Y., Ito,Y., and Nomura,S.

(1998). Transcriptional regulation of osteopontin gene in vivo by PEBP2alphaA/CBFA1 and ETS1 in the skeletal tissues. Oncogene *17*, 1517-1525.

Schotta,G., Lachner,M., Peters,A.H., and Jenuwein,T. (2004). The indexing potential of histone lysine methylation. Novartis. Found. Symp. *259*, 22-37.

Schubeler,D., MacAlpine,D.M., Scalzo,D., Wirbelauer,C., Kooperberg,C., van,L.F., Gottschling,D.E., O'Neill,L.P., Turner,B.M., Delrow,J., Bell,S.P., and Groudine,M. (2004). The histone modification pattern of active genes revealed through genome-wide chromatin analysis of a higher eukaryote. Genes Dev. *18*, 1263-1271.

Schwartz,E.L. and Nilson,L. (1988). Multiple mechanisms for the inhibition of rRNA synthesis during HL-60 leukemia cell differentiation. J. Cell Physiol *136*, 526-530.

Selvamurugan,N., Kwok,S., Alliston,T., Reiss,M., and Partridge,N.C. (2004b). Transforming growth factor-beta 1 regulation of collagenase-3 expression in osteoblastic cells by cross-talk between the Smad and MAPK signaling pathways and their components, Smad2 and Runx2. J. Biol. Chem. *279*, 19327-19334.

Selvamurugan,N., Kwok,S., Alliston,T., Reiss,M., and Partridge,N.C. (2004a). Transforming growth factor-beta 1 regulation of collagenase-3 expression in osteoblastic cells by cross-talk between the Smad and MAPK signaling pathways and their components, Smad2 and Runx2. J. Biol. Chem. *279*, 19327-19334.

Shen,J., Montecino,M.A., Lian,J.B., Stein,G.S., van Wijnen,A.J., and Stein,J.L. (2002). Histone acetylation in vivo at the osteocalcin locus is functionally linked to vitamin D dependent, bone tissue-specific transcription. J. Biol. Chem. *277*, 20284-20292.

Shiels,C., Islam,S.A., Vatcheva,R., Sasieni,P., Sternberg,M.J., Freemont,P.S., and Sheer,D. (2001). PML bodies associate specifically with the MHC gene cluster in interphase nuclei. J Cell Sci. *114*, 3705-3716.

Shopland,L.S., Johnson,C.V., Byron,M., McNeil,J., and Lawrence,J.B. (2003). Clustering of multiple specific genes and gene-rich R-bands around SC-35 domains: evidence for local euchromatic neighborhoods. J. Cell Biol. *162*, 981-990.

Shopland,L.S. and Lawrence,J.B. (2000). Seeking common ground in nuclear complexity. J Cell Biol. *150*, F1-F4.

Si,X., Yang,L., and Jin,Y. (1999). Effects of human BMP2 gene transfection on NIH3T3 cells in vitro. Zhonghua Kou Qiang. Yi. Xue. Za Zhi. *34*, 103-105.

Sierra,J., Villagra,A., Paredes,R., Cruzat,F., Gutierrez,S., Arriagada,G., Olate,J., Imschenetzky,M., van Wijnen,A.J., Lian,J.B., Stein,G.S., Stein,J.L., and Montecino,M. (2003a). Regulation of the bone-specific osteocalcin gene by p300 requires Runx2/Cbfa1 and the vitamin D3 receptor but not p300 intrinsic histone acetyl transferase activity. Mol Cell Biol. *23*, 3339-3351.

Sierra,J., Villagra,A., Paredes,R., Cruzat,F., Gutierrez,S., Javed,A., Arriagada,G., Olate,J., Imschenetzky,M., van Wijnen,A.J., Lian,J.B., Stein,G.S., and Stein,J.L. (2003b). Regulation of the bone-specific osteocalcin gene by p300 requires Runx2/Cbfa1 and the vitamin D3 receptor but not p300 intrinsic histone acetyltransferase activity. Mol Cell Biol. *23*, 3339-3351.

Sif,S. (2004). ATP-dependent nucleosome remodeling complexes: enzymes tailored to deal with chromatin. J. Cell Biochem. *91*, 1087-1098.

Sif,S., Saurin,A.J., Imbalzano,A.N., and Kingston,R.E. (2001). Purification and characterization of mSin3A-containing Brg1 and hBrm chromatin remodeling complexes. Genes Dev. *15*, 603-618.

Sinclair,D.F. (1985). On tests of spatial randomness using mean nearest neighbor distance. Ecology *66*, 1084-1085.

Soutoglou,E. and Talianidis,I. (2002). Coordination of PIC assembly and chromatin remodeling during differentiation-induced gene activation. Science *295*, 1901-1904.

Speck,N.A., Stacy,T., Wang,Q., North,T., Gu,T.L., Miller,J., Binder,M., and Marin-Padilla,M. (1999). Core-binding factor: a central player in hematopoiesis and leukemia. Cancer Res. *59*, 1789s-1793s.

Spector,D.L. (2003). The dynamics of chromosome organization and gene regulation. Annu. Rev. Biochem *72*, 573-608.

Spilianakis,C.G. and Flavell,R.A. (2004). Long-range intrachromosomal interactions in the T helper type 2 cytokine locus. Nat. Immunol. *5*, 1017-1027.

Spilianakis,C.G., Lalioti,M.D., Town,T., Lee,G.R., and Flavell,R.A. (2005). Interchromosomal associations between alternatively expressed loci. Nature *435*, 637-645.

Stefanovsky,V.Y., Pelletier,G., Bazett-Jones,D.P., Crane-Robinson,C., and Moss,T. (2001). DNA looping in the RNA polymerase I enhancesome is the result

of non-cooperative in-phase bending by two UBF molecules. Nucleic Acids Res. *29*, 3241-3247.

Stein,G.S., Baserga,R., Giordano,A., and Denhardt,D. (1998). Cell Cycle and Growth Control. (New York: Wiley-Liss).

Stein,G.S., Lian,J.B., Montecino,M., van Wijnen,A.J., Stein,J.L., Javed,A., and Zaidi,K. (2002). Involvement of nuclear architecture in regulating gene expression in bone cells. In Principles of Bone Biology, J.P.Bilezikian, L.G.Raisz, and G.A.Rodan, eds. (San Diego: Academic Press), pp. 169-188.

Stein,G.S., Montecino,M., van Wijnen,A.J., Stein,J.L., and Lian,J.B. (2000a). Nuclear structure - gene expression interrelationships: implications for aberrant gene expression in cancer. Cancer Res. *60*, 2067-2076.

Stein,G.S., van Wijnen,A.J., Stein,J.L., Lian,J.B., Montecino,M., Choi,J.-Y., Zaidi,K., and Javed,A. (2000b). Intranuclear trafficking of transcription factors: implications for biological control. J. Cell Sci. *113*, 2527-2533.

Stein,G.S., van Wijnen,A.J., Stein,J.L., Lian,J.B., Montecino,M., Zaidi,S.K., and Javed,A. (2000c). Subnuclear organization and trafficking of regulatory proteins: implications for biological control and cancer. J. Cell Biochem. *35*, 84-92.

Stein,G.S., Zaidi,S.K., Braastad,C.D., Montecino,M., van Wijnen,A.J., Choi,J.-Y., Stein,J.L., Lian,J.B., and Javed,A. (2003). Functional architecture of the nucleus: organizing the regulatory machinery for gene expression, replication and repair. Trends Cell Biol. *13*, 584-592.

Stenoien,D., Sharp,Z.D., Smith,C.L., and Mancini,M.A. (1998). Functional subnuclear partitioning of transcription factors. J. Cell. Biochem. *70*, 213-221.

Stenoien,D.L., Nye,A.C., Mancini,M.G., Patel,K., Dutertre,M., O'Malley,B.W., Smith,C.L., Belmont,A.S., and Mancini,M.A. (2001). Ligand-mediated assembly and real-time cellular dynamics of estrogen receptor alpha-coactivator complexes in living cells. Mol Cell Biol. *21*, 4404-4412.

Stenoien,D.L., Simeoni,S., Sharp,Z.D., and Mancini,M.A. (2000). Subnuclear dynamics and transcription factor function. J. Cell Biochem. *Suppl 35*, 99-106.

Suja,J.A., Gebrane-Younes,J., Geraud,G., and Hernandez-Verdun,D. (1997). Relative distribution of rDNA and proteins of the RNA polymerase I transcription machinery at chromosomal NORs. Chromosoma *105*, 459-469.

Swedlow,J.R. and Hirano,T. (2003). The making of the mitotic chromosome: modern insights into classical questions. Mol. Cell *11*, 557-569.

Tanabe,H., Habermann,F.A., Solovei,I., Cremer,M., and Cremer,T. (2002). Non-random radial arrangements of interphase chromosome territories: evolutionary considerations and functional implications. Mutat. Res. *504*, 37-45.

Tang,L., Guo,B., van Wijnen,A.J., Lian,J.B., Stein,J.L., Stein,G.S., and Zhou,G.W. (1998). Preliminary crystallographic study of the glutathione S-transferase fused with the nuclear matrix targeting signal of the transcription factor AML-1/CBFa2. J. Struct. Biol. *123*, 83-85.

Tang,Q.Q. and Lane,M.D. (1999). Activation and centromeric localization of CCAAT/enhancer-binding proteins during the mitotic clonal expansion of adipocyte differentiation. Genes Dev. *13*, 2231-2241.

Taniuchi,I. and Littman,D.R. (2004). Epigenetic gene silencing by Runx proteins. Oncogene *23*, 4341-4345.

Telfer,J.C. and Rothenberg,E.V. (2001). Expression and function of a stem cell promoter for the murine CBFalpha2 gene: distinct roles and regulation in natural killer and T cell development. Dev. Biol. *229*, 363-382.

Thomas,D.M., Carty,S.A., Piscopo,D.M., Lee,J.S., Wang,W.F., Forrester,W.C., and Hinds,P.W. (2001). The retinoblastoma protein acts as a transcriptional coactivator required for osteogenic differentiation. Molec. Cell *8*, 303-316.

Thomas,D.M., Johnson,S.A., Sims,N.A., Trivett,M.K., Slavin,J.L., Rubin,B.P., Waring,P., McArthur,G.A., Walkley,C.R., Holloway,A.J., Diyagama,D., Grim,J.E., Clurman,B.E., Bowtell,D.D., Lee,J.S., Gutierrez,G.M., Piscopo,D.M., Carty,S.A., and Hinds,P.W. (2004). Terminal osteoblast differentiation, mediated by runx2 and p27KIP1, is disrupted in osteosarcoma. J. Cell Biol. *167*, 925-934.

Tolhuis,B., Palstra,R.J., Splinter,E., Grosveld,F., and de,L.W. (2002). Looping and interaction between hypersensitive sites in the active beta-globin locus. Mol. Cell *10*, 1453-1465.

Tracey,W.D. and Speck,N.A. (2000). Potential roles for RUNX1 and its orthologs in determining hematopoietic cell fate. Semin. Cell Dev. Biol. *11*, 337-342.

Tumbar,T. and Belmont,A.S. (2001). Interphase movements of a DNA chromosome region modulated by VP16 transcriptional activator. Nat. Cell Biol. *3*, 134-139.

Vaillant,F., Blyth,K., Terry,A., Bell,M., Cameron,E.R., Neil,J., and Stewart,M. (1999). A full-length *Cbfa1* gene product perturbs T-cell development and promotes lymphomagenesis in synergy with MYC. Oncogene *18*, 7124-7134.

Valdez,B.C., Henning,D., So,R.B., Dixon,J., and Dixon,M.J. (2004). The Treacher Collins syndrome (TCOF1) gene product is involved in ribosomal DNA gene transcription by interacting with upstream binding factor. Proc. Natl. Acad. Sci. U. S. A *101*, 10709-10714.

van Steensel,B., Jenster,G., Damm,K., Brinkmann,A.O., and van Driel,R. (1995). Domains of the human androgen receptor and glucocorticoid receptor involved in binding to the nuclear matrix. J. Cell. Biochem. *57*, 465-478.

van,D.R., Fransz,P.F., and Verschure,P.J. (2003). The eukaryotic genome: a system regulated at different hierarchical levels. J. Cell Sci. *116*, 4067-4075.

Verschure,P.J., van Der Kraan,I., Manders,E.M., and van Driel,R. (1999). Spatial relationship between transcription sites and chromosome territories. J. Cell Biol. *147*, 13-24.

Verschure,P.J., van,d.K., I, Manders,E.M., Hoogstraten,D., Houtsmuller,A.B., and van,D.R. (2003). Condensed chromatin domains in the mammalian nucleus are accessible to large macromolecules. EMBO Rep. *4*, 861-866.

Voit,R. and Grummt,I. (2001a). Phosphorylation of UBF at serine 388 is required for interaction with RNA polymerase I and activation of rDNA transcription. Proc. Natl. Acad. Sci. U. S. A *98*, 13631-13636.

Voit,R. and Grummt,I. (2001b). Phosphorylation of UBF at serine 388 is required for interaction with RNA polymerase I and activation of rDNA transcription. Proc. Natl. Acad. Sci. U. S. A *98*, 13631-13636.

Voit,R., Hoffmann,M., and Grummt,I. (1999). Phosphorylation by G1-specific cdk-cyclin complexes activates the nucleolar transcription factor UBF. EMBO J. *18*, 1891-1899.

Vradii, D., Doan, D. N., Wagner, S., Nickerson, J. A., Lian, J. B., Stein, J. L., van Wijnen, A. J., Imbalzano, A. N., and Stein, G. S. Brg1, the ATPase subunit of SWI/SNF chromatin remodeling complex, is required for myeloid differentiation to granulocytes. 2005.
Ref Type: Unpublished Work

Wagner,B., Krochmalnic,G., and Penman,S. (1986). Resinless section electron microscopy of HeLa cell mitotic architecture. Proc. Natl. Acad. Sci. USA *83*, 8996-9000.

Wang,E.A., Israel,D.I., Kelly,S., and Luxenberg,D.P. (1993). Bone morphogenetic protein-2 causes commitment and differentiation in C3H10T1/2 and 3T3 cells. Growth Factors *9*, 57-71.

Wang,Q., Stacy,T., Binder,M., Marin-Padilla,M., Sharpe,A.H., and Speck,N.A. (1996a). Disruption of the *Cbfa2* gene causes necrosis and hemorrhaging in the central nervous system and blocks definitive hematopoiesis. Proc. Natl. Acad. Sci. U. S. A. *93*, 3444-3449.

Wang,W., Cote,J., Xue,Y., Zhou,S., Khavari,P.A., Biggar,S.R., Muchardt,C., Kalpana,G.V., Goff,S.P., Yaniv,M., Workman,J.L., and Crabtree,G.R. (1996b). Purification and biochemical heterogeneity of the mammalian SWI- SNF complex. EMBO J. *15*, 5370-5382.

Wei,X., Samarabandu,J., Devdhar,R.S., Siegel,A.J., Acharya,R., and Berezney,R. (1998). Segregation of transcription and replication sites into higher order domains. Science *281*, 1502-1505.

Wells,J., Yan,P.S., Cechvala,M., Huang,T., and Farnham,P.J. (2003). Identification of novel pRb binding sites using CpG microarrays suggests that E2F recruits pRb to specific genomic sites during S phase. Oncogene *22*, 1445-1460.

Westendorf,J.J. and Hiebert,S.W. (1999). Mammalian runt-domain proteins and their roles in hematopoiesis, osteogenesis, and leukemia. J Cell Biochem. *Suppl 32-33*, 51-58.

Westendorf,J.J., Zaidi,S.K., Cascino,J.E., Kahler,R., van Wijnen,A.J., Lian,J.B., Yoshida,M., Stein,G.S., and Li,X. (2002). Runx2 (Cbfa1, AML-3) interacts with histone deacetylase 6 and represses the p21(CIP1/WAF1) promoter. Mol. Cell Biol. *22*, 7982-7992.

Wolffe,A.P. (1994). Architectural transcription factors. Science *264*, 1100-1101.

Workman,J.L. and Kingston,R.E. (1998). Alteration of nucleosome structure as a mechanism of transcriptional regulation. Annu. Rev Biochem *67*, 545-579.

Xu,Y.X., Hirose,Y., Zhou,X.Z., Lu,K.P., and Manley,J.L. (2003). Pin1 modulates the structure and function of human RNA polymerase II. Genes Dev. *17*, 2765-2776.

Yang,J., Fizazi,K., Peleg,S., Sikes,C.R., Raymond,A.K., Jamal,N., Hu,M., Olive,M., Martinez,L.A., Wood,C.G., Logothetis,C.J., Karsenty,G., and Navone,N.M. (2001). Prostate cancer cells induce osteoblast differentiation through a Cbfa1-dependent pathway. Cancer Res. *61*, 5652-5659.

Yergeau,D.A., Hetherington,C.J., Wang,Q., Zhang,P., Sharpe,A.H., Binder,M., Marin-Padilla,M., Tenen,D.G., Speck,N.A., and Zhang,D.E. (1997). Embryonic

lethality and impairment of haematopoiesis in mice heterozygous for an AML1-ETO fusion gene. Nat. Genet. *15*, 303-306.

Young,D.W., Pratap,J., Javed,A., Weiner,B., Ohkawa,Y., van Wijnen,A., Montecino,M., Stein,G.S., Stein,J.L., Imbalzano,A.N., and Lian,J.B. (2005). SWI/SNF chromatin remodeling complex is obligatory for BMP2-induced, Runx2-dependent skeletal gene expression that controls osteoblast differentiation. J. Cell Biochem. *94*, 720-730.

Young,D.W., Zaidi,S.K., Furcinitti,P.S., Javed,A., van Wijnen,A.J., Stein,J.L., Lian,J.B., and Stein,G.S. (2004). Quantitative signature for architectural organization of regulatory factors using intranuclear informatics. J. Cell Sci. *117*, 4889-4896.

Zaidi,S.K., Javed,A., Choi,J.-Y., van Wijnen,A.J., Stein,J.L., Lian,J.B., and Stein,G.S. (2001a). A specific targeting signal directs Runx2/Cbfa1 to subnuclear domains and contributes to transactivation of the osteocalcin gene. J. Cell Sci. *114*, 3093-3102.

Zaidi, S. K., Sullivan, A. J., Ito, Y., van Wijnen, A. J., Stein, J. L., Stein, G. S., and Lian, J. B. The Yes-associated protein (YAP) is a suppressor of Runx2/Cbfa1 dependent activation of the bone specific osteocalcin gene. J.Bone Miner.Res. 16, S205. 2001b.
Ref Type: Abstract

Zaidi,S.K., Sullivan,A.J., Medina,R., Ito,Y., van Wijnen,A.J., Stein,J.L., Lian,J.B., and Stein,G.S. (2004). Tyrosine phosphorylation controls Runx2-mediated subnuclear targeting of YAP to repress transcription. EMBO J. *23*, 790-799.

Zaidi,S.K., Sullivan,A.J., van Wijnen,A.J., Stein,J.L., Stein,G.S., and Lian,J.B. (2002b). Integration of Runx and Smad regulatory signals at transcriptionally active subnuclear sites. Proc. Natl. Acad. Sci. , USA *99*, 8048-8053.

Zaidi,S.K., Sullivan,A.J., van Wijnen,A.J., Stein,J.L., Stein,G.S., and Lian,J.B. (2002a). Integration of Runx and Smad Regulatory Signals at Transcriptionally Active Subnuclear Sites. Proc. Natl. Acad. Sci. , USA *99*, 8048-8053.

Zaidi,S.K., Young,D.W., Choi,J.Y., Pratap,J., Javed,A., Montecino,M., Stein,J.L., van Wijnen,A.J., Lian,J.B., and Stein,G.S. (2005). The dynamic organization of gene-regulatory machinery in nuclear microenvironments. EMBO Rep. *6*, 128-133.

Zaidi,S.K., Young,D.W., Pockwinse,S.H., Javed,A., Lian,J.B., Stein,J.L., van Wijnen,A.J., and Stein,G.S. (2003). Mitotic partitioning and selective

reorganization of tissue specific transcription factors in progeny cells. Proc. Natl. Acad. Sci. , USA *100*, 14852-14857.

Zatsepina,O.V., Voit,R., Grummt,I., Spring,H., Semenov,M.V., and Trendelenburg,M.F. (1993). The RNA polymerase I-specific transcription initiation factor UBF is associated with transcriptionally active and inactive ribosomal genes. Chromosoma *102*, 599-611.

Zelzer,E., Glotzer,D.J., Hartmann,C., Thomas,D., Fukai,N., Soker,S., and Olsen,B.R. (2001). Tissue specific regulation of VEGF expression during bone development requires Cbfa1/Runx2. Mech. Dev. *106*, 97-106.

Zeng,C., McNeil,S., Pockwinse,S., Nickerson,J.A., Shopland,L., Lawrence,J.B., Penman,S., Hiebert,S.W., Lian,J.B., van Wijnen,A.J., Stein,J.L., and Stein,G.S. (1998). Intranuclear targeting of AML/CBFa regulatory factors to nuclear matrix-associated transcriptional domains. Proc. Natl. Acad. Sci. USA *95*, 1585-1589.

Zeng,C., van Wijnen,A.J., Stein,J.L., Meyers,S., Sun,W., Shopland,L., Lawrence,J.B., Penman,S., Lian,J.B., Stein,G.S., and Hiebert,S.W. (1997). Identification of a nuclear matrix targeting signal in the leukemia and bone-related AML/CBFa transcription factors. Proc. Natl. Acad. Sci. USA *94*, 6746-6751.

Zhang,Y.W., Yasui,N., Ito,K., Huang,G., Fujii,M., Hanai,J., Nogami,H., Ochi,T., Miyazono,K., and Ito,Y. (2000a). A RUNX2/PEBP2aA/CBFA1 mutation displaying impaired transactivation and Smad interaction in cleidocranial dysplasia. Proc. Natl. Acad. Sci. U. S. A *97*, 10549-10554.

Zhang,Y.W., Yasui,N., Kakazu,N., Abe,T., Takada,K., Imai,S., Sato,M., Nomura,S., Ochi,T., Okuzumi,S., Nogami,H., Nagai,T., Ohashi,H., and Ito,Y. (2000b). PEBP2alphaA/CBFA1 mutations in Japanese cleidocranial dysplasia patients. Gene *244*, 21-28.

Zhou,G., Chen,Y., Zhou,L., Thirunavukkarasu,K., Hecht,J., Chitayat,D., Gelb,B.D., Pirinen,S., Berry,S.A., Greenberg,C.R., Karsenty,G., and Lee,B. (1999). CBFA1 mutation analysis and functional correlation with phenotypic variability in cleidocranial dysplasia. Hum. Mol. Genet. *8*, 2311-2316.

Zink,D., Fischer,A.H., and Nickerson,J.A. (2004). Nuclear structure in cancer cells. Nat. Rev. Cancer *4*, 677-687.